REVIEW

Molecular imaging in living subjects: seeing fundamental biological processes in a new light

Tarik F. Massoud[1,3] and Sanjiv S. Gambhir[1,2,4,5]

[1]The Crump Institute for Molecular Imaging, [2]Department of Molecular & Medical Pharmacology, and Department of Biomathematics, David Geffen School of Medicine at University of California at Los Angeles, Los Angeles, California 90095, USA; [3]Departments of Radiology and Oncology, University of Cambridge School of Clinical Medicine, Cambridge CB2 2QQ, UK; [4]Stanford University School of Medicine, Stanford, California 94305, USA

Morphological observations have driven the course of biology ever since the first microscope was built in the late sixteenth century. Molecular imaging is a rapidly emerging biomedical research discipline that extends such observations in living subjects to a more meaningful dimension. It may be defined as the visual representation, characterization, and quantification of biological processes at the cellular and subcellular levels within intact living organisms. It is a novel multidisciplinary field, in which the images produced reflect cellular and molecular pathways and in vivo mechanisms of disease present within the context of physiologically authentic environments. The term "molecular imaging" implies the convergence of multiple image-capture techniques, basic cell/molecular biology, chemistry, medicine, pharmacology, medical physics, biomathematics, and bioinformatics into a new imaging paradigm.

Present imaging technologies rely mostly on nonspecific macroscopic physical, physiological, or metabolic changes that differentiate pathological from normal tissue rather than identifying specific molecular events (e.g., gene expression) responsible for disease. Molecular imaging usually exploits specific molecular probes as the source of image contrast. This change in emphasis from a nonspecific to a specific approach represents a significant paradigm shift, the impact of which is that imaging can now provide the potential for understanding of integrative biology, earlier detection and characterization of disease, and evaluation of treatment.

The emergence of molecular imaging strategies is largely due to recent unprecedented advances in molecular and cell biology techniques, the use of transgenic animal models, availability of newer imaging drugs and probes that are highly specific, and successful development of small-animal imaging instrumentation. These factors, along with continued expansion of scientific horizons in the current postgenomic era, have been pivotal in the drive toward a new standard that allows linking established in vitro and cell culture experimental assays to imaging studies within living subjects. This now creates the possibility of achieving several important goals in biomedical research, namely, (1) to develop noninvasive in vivo imaging methods that reflect specific cellular and molecular processes, for example, gene expression, or more complex molecular interactions such as protein–protein interactions; (2) to monitor multiple molecular events near-simultaneously; (3) to follow trafficking and targeting of cells; (4) to optimize drug and gene therapy; (5) to image drug effects at a molecular and cellular level; (6) to assess disease progression at a molecular pathological level; and (7) to create the possibility of achieving all of the above goals of imaging in a rapid, reproducible, and quantitative manner, so as to be able to monitor time-dependent experimental, developmental, environmental, and therapeutic influences on gene products in the same animal or patient.

Molecular imaging has its roots in nuclear medicine and in many ways is a direct extension of this existing discipline. Nuclear medicine is a discipline focused on the management of patients through the use of injected radiolabeled tracers in conjunction with imaging technologies. The underlying principles of molecular imaging can now be tailored to other imaging modalities such as optical imaging and magnetic resonance imaging (MRI). Molecular imaging probes can now also be developed by taking advantage of the rapidly increasing knowledge of available cellular/molecular targets. The merger of molecular biology and medical imaging is facilitating rapid growth of this new field by providing methods to monitor cellular/molecular events adapted from conventional molecular assays, for example, reporter gene assays. The present frenetic pace of advancements in biotechnology and functional genomics (Subramanian et al. 2001) is resulting in parallel progress in molecular imaging innovations and applications. The development, validation, and application of these novel imaging techniques in living subjects should further en-

[5]Corresponding author.
E-MAIL sgambhir@mednet.ucla.edu or sgambhir@stanford.edu; FAX (310) 209-4655.
Article and publication are at http://www.genesdev.org/cgi/doi/10.1101/gad.1047403.

hance our understanding of disease mechanisms and go hand in hand with the development of molecular medicine (Phelps 2002).

Advantages of molecular imaging strategies

Molecular imaging in living subjects offers distinct advantages when compared with conventional in vitro and cell culture research techniques in biology. Although in vitro studies in basic biological research have been, and remain, a mainstay for defining biochemical and gene expression pathways, the in vitro approach has been less successful in deciphering physiological whole-body contributions of proteins, in which redundancies and differences in regulation can alter the outcome from that initially predicted (Livingston 1999). In contrast to cell and tissue culture, in vivo animal models allow the assessment of phenomena such as tolerances, complementation, and redundancy in biological pathways (Gassmann and Hennet 1998). Molecular imaging permits both the temporal and the spatial biodistribution of a molecular probe and related biological processes to be determined in a more meaningful manner throughout an intact living subject. Visualization of functions and interactions of a particular gene becomes easier in a more realistic manner that respects the dynamics of complex biological networks and of complete and holistic biological systems in the entire living subject.

Molecular imaging of living subjects offers another important benefit: it is likely to prove useful as a tool or strategy for phenotype screening of transgenic and gene-targeted animal models (Hoit 2001). The large-scale application of random chemical mutagenesis and other more targeted genetic techniques is expected to substantially tax the ability of researchers to phenotype large numbers of mutant mice. Phenotypic changes can occasionally be detected on the basis of physical parameters; for example, tumor development or physiological abnormalities. In these instances, when mutations cause developmental abnormalities that are easily identified by external appearances, the problems involved in phenotypic screening are relatively straightforward. Difficulties arise when subtle phenotypes exist or in attempting to decipher phenotypes that may become apparent only in the presence of physiological or nutritional stress. For example, abnormalities that require molecular probes for analysis, or mutations that produce complex metabolic changes or affect immune cell populations and/or immune function, are most often not readily identifiable on gross examination. Present assays for evaluating responses to these induced complex changes are generally labor-intensive and time-consuming, often requiring the purification of individual cell populations, or analytical tests of metabolism that are difficult or technically challenging in tiny animals. In many instances, thorough phenotypic characterization would require volumes of blood, serum, or tissue that could be obtained only by killing genetically unique mice. As such, molecular imaging of living mice offers the following additional distinct advantages when investigating phenotypic abnormalities: (1) it eliminates the need to kill such mice as part of their phenotype determination; (2) by repetitive imaging it is possible to investigate mutants that are otherwise difficult to interpret with data taken at a single time point; (3) it allows concomitant visual and analytical biological phenotyping of animals; and (4) it allows the researcher to exercise options of multiple imaging strategies (e.g., by using different imaging reporter probes or modalities) in cases in which simple genetic manipulations could result in a very complex phenotype involving a large number of pathways and organs.

Molecular imaging assays in intact living animals could be of further benefit in resolving biological questions raised by pharmaceutical scientists. Transgenic animals are useful in guiding early drug discovery by "validating" the target protein, evaluating test compounds, determining whether the target is involved in any toxicological effects of test compounds, and testing the efficacy of compounds to ensure that the compounds will act as expected in man (Livingston 1999). The implementation of molecular imaging approaches in this drug discovery process offers the strong advantage of being able to meaningfully study a potential drug labeled for imaging in an animal model, often before phenotypic changes become obvious, and then quickly move into human studies. It is likely that preclinical trials can be accelerated to rule out drugs with unfavorable biodistribution and/or pharmacokinetics prior to human studies.

A further advantage over in vitro and cell culture experimentation may be achieved by repetitive study of the same animal model, using identical or alternative biological imaging assays at different time points. This reveals a dynamic and more meaningful picture of the progressive changes in biological parameters under scrutiny, as well as possible temporal assessment of therapeutic responses, all in the same animal without recourse to its death. This yields better quality results from far fewer experimental animals.

Despite their success, conventional microscopy methods (histopathological and cytological) suffer significant limitations when used in biological experimentation. They usually require chemical fixation of removed tissues, involve the observation of biological samples under nonphysiological conditions, can generally not resolve the dynamics of cellular processes, and most importantly, it has been very difficult to generate quantitative data using conventional microscopy (Phair and Misteli 2001). Although the use of genetically encoded fluorescent tags has revolutionized the way microscopy is used in biology and to some extent addresses these drawbacks, there nonetheless remains the problem of having to invasively obtain tissue samples for analysis and the inability to survey many/all tissues simultaneously. The impact of these relative drawbacks of microscopy may be lessened to some extent by the use of noninvasive molecular imaging techniques in intact living subjects. This feature also means that from a theoretical standpoint, once a molecular imaging experimental setup is fully established, functional, and efficient,

results of these imaging assays are potentially attainable quicker and less labor-intensively than with conventional in vitro or cell culture study of biological materials, perhaps facilitating achievement of a relatively higher-throughput facet to many biological laboratory investigations.

Another benefit of molecular imaging assays is their quantitative nature. The images obtained are usually not just subjective or qualitative, as is the case with standard use of several conventional medical imaging modalities, but instead, usually provide meaningful numerical measures of biological phenomena (exemplified below). Such quantitative data could even be considered more useful than similar data obtainable in vitro or ex vivo, on account of preserving the intactness and the physiology of the experimental subject. However, one exception to this can be made in cases in which general anesthesia of the living subject results in alteration of the biological function under investigation, as may occur; for example, in brain molecular imaging studies.

The combined ability to perform tomographic imaging assays in intact living subjects, followed by computational three-dimensional stacking/reconstruction of images after acquisition, and simultaneous quantification of these biological measures also permits the extraction of three-dimensional information regarding the spatial distribution of biological phenomena within a particular organ or throughout the entire body. Although ex vivo techniques, such as recently developed rapid sampling microscopy methods combined with the increased stability of fluorescent probes, now make it possible to routinely acquire three-dimensional microscopy data sets over time (a method commonly referred to as four-dimensional microscopy), these types of experiments generate large data sets that often cannot be intuitively and quantitatively interpreted (Phair and Misteli 2001). An alternative is the laborious and often crude three-dimensional reconstruction of information from many contiguous histological slides. Instead, and with continued developments in this field, molecular imaging should be capable of generating four-dimensional information (including temporal changes) of biological phenomena much quicker and easier than by more conventional invasive means of investigation.

A further incentive for use of molecular imaging strategies in basic biological research is the rising cost of laboratory mice and the relative scarcity of some genetically engineered mice. This has provided a major impetus for establishing in vivo mouse imaging as an alternative to killing many animals for histological processing at different time points. With each transgenic mouse valued in the $200–$300 range (and up to $30,000 for certain breeder pairs), the overall costs of conventional post mortem biological assays on many animals can mount substantially. The use of fewer animals in biological assays with molecular imaging would also be more appealing on ethical grounds. In theory, approval for research projects requiring large numbers or many separate cohorts of experimental animals could be obtained more easily.

Molecular imaging instrumentation and techniques

Biological discovery has moved at an accelerated pace in recent years, with considerable focus on the transition from in vitro to in vivo models. As such, there has been a greater need to adapt clinical imaging methods for noninvasive assays of biochemical processes. Considerable efforts have been directed in recent years toward the development of noninvasive, high-resolution, small animal in vivo imaging technologies (Fig. 1). The widespread availability and use of miniaturized imaging systems for rodents are not the fanciful and futuristic concepts that many researchers might imagine; these systems are generally cheaper than their clinical counterparts and can be housed in shared resources of basic science laboratories. Nonetheless, significant challenges remain to be overcome when attempting to image a 30-g mouse as compared with a 70-kg human, including the size of the subject, the total volume that must be evaluated, the spatial resolution necessary for obtaining meaningful anatomical and/or functional data, and the total time spent on acquiring a set of images (Weissleder and Mahmood 2001). In small animal research, the primary goal is to obtain as high a signal as possible and to localize the signal as accurately as possible with high temporal resolution and with minimal amount of molecular probe. The ultimate goal is to provide a single device that produces a final three-dimensional image of anatomical and biological information fused together, an objective that is likely to be achieved in the not too distant future.

The various existing imaging technologies differ in five main aspects: spatial and temporal resolution, depth penetration, energy expended for image generation (ionizing or nonionizing, depending on which component of the electromagnetic radiation spectrum is exploited for image generation), availability of injectable/biocompatible molecular probes, and the respective detection threshold of probes for a given technology. Collapsing the volume of an animal or tumor into a single image, known as planar imaging, is generally fast, the data sets generated are small, and imaging can be done in high throughput fashion, at the expense of internal resolution. Tomographic imaging allows a virtual slice of the subject to be obtained and is usually quantitative and capable of displaying internal anatomic structures and/or functional information, but generally requires longer acquisition times and higher energy expenditure. Volumetric image acquisition shows a volume of interest in all three dimensions and results in the highest spatial information content, although it can generate very large data sets. Further reviews of issues centered on molecular imaging techniques can be found elsewhere (Cherry and Gambhir 2001; Weissleder 2001, 2002; Weissleder and Mahmood 2001; Chatziioannou 2002). Moreover, a glossary of molecular imaging terminology has been published recently to enhance collaborative efforts between multiple disciplines (Wagenaar et al. 2001). Table 1 outlines some of the general characteristics of the imaging modalities available, and serves also as a simplified guide for biologists in choosing appropriate molecular imaging

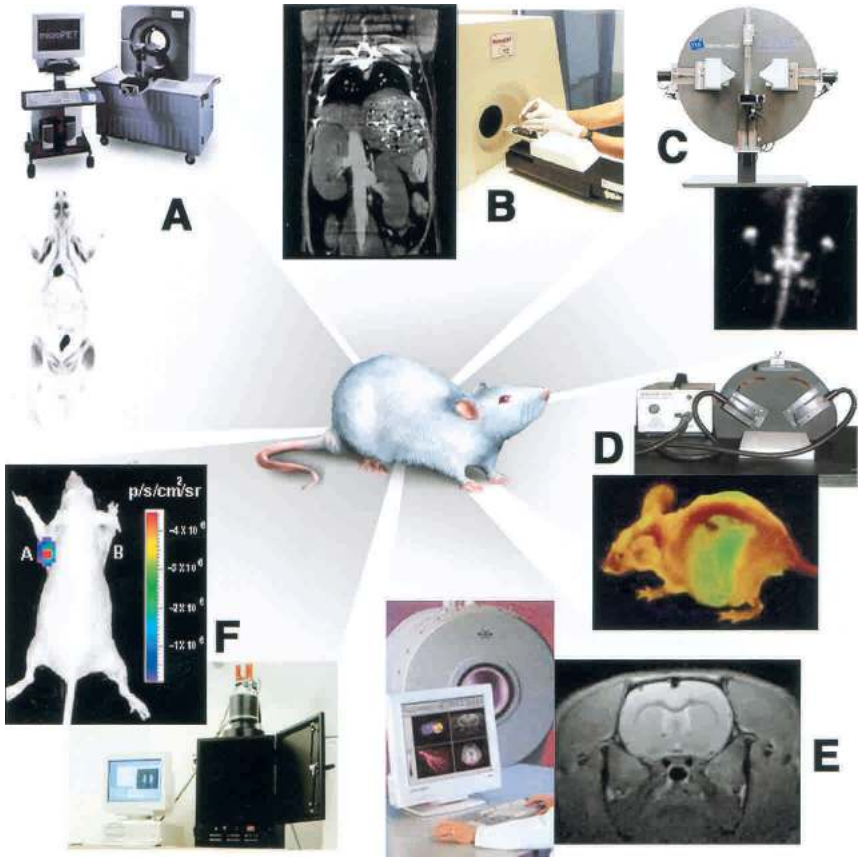

Figure 1. Multiple imaging modalities are available for small-animal molecular imaging. Shown are views of typical instruments available, and illustrative examples of the variety of images that can be obtained with these modalities. (*A*) microPET whole-body coronal image of a rat injected with ^{18}FDG, showing uptake of tracer in tissues including muscles, heart, brain, and accumulation in bladder owing to renal clearance. (*B*) microCT coronal image of a mouse abdomen after injection of intravenous iodinated contrast medium. (*C*) microSPECT coronal image of a mouse abdomen and pelvis regions after injection of ^{99m}Tc methylene diphosphonate, showing spine, pelvis, tail vertebrae, femurs, and knee joints owing to accumulation of tracer in bone. (*D*) Optical reflectance fluorescence image of a mouse showing GFP fluorescence from the liver, abdomen, spine, and brain. The mouse contains GFP-expressing tumor cells that have spread to various sites. Images are courtesy of Dr. Hoffman, Anticancer Inc. (*E*) microMRI coronal T2-weighted image of a mouse brain. (*F*) Optical bioluminescence image of a mouse with a subcutaneous xenograft expressing Renilla luciferase in the left shoulder region, after tail-vein injection of the substrate coelenterazine. Images were obtained using a cooled CCD camera. The color image of visible light is superimposed on a photographic image of the mouse with a scale in photons per second per square centimeter per steradian (sr).

modalities and approaches. Further information on molecular imaging instrumentation and their features, as well as commercial vendors, can be found at the Web site http://www.mi-central.org, which serves as a useful Internet resource for molecular imaging information. (Please see additional useful links listed at the end of this article.)

Radionuclide imaging

Positron emission tomography (PET) records high-energy γ-rays emitted from within the subject. Natural biological molecules can be labeled with a positron-emitting isotope that is capable of producing two γ-rays through emission of a positron from its nucleus, which eventually annihilates with a nearby electron to produce two 511,000-eV γ-rays at ~180° apart. Positron-emitting isotopes frequently used include ^{15}O, ^{13}N, ^{11}C, and ^{18}F, the latter used as a substitute for hydrogen. Other less commonly used positron emitters include ^{14}O, ^{64}Cu, ^{62}Cu, ^{124}I, ^{76}Br, ^{82}Rb, and ^{68}Ga. Most of these isotopes are produced in a cyclotron (Strijckmans 2001), but some can be produced using a generator (e.g., ^{68}Ga, ^{82}Rb). Labeled molecular probes (see below) or tracers can be introduced into the subject, and then PET imaging can follow the distribution and concentration of the injected molecules. Many of the positron-emitting isotopes used have relatively short half-lives (e.g., ^{18}F has $t_{1/2}$ = 110 min), so that the chemical reactions leading to incorporation of the isotope into the parent molecule and subsequent introduction into the subject must take place relatively quickly. PET radiopharmacies exist throughout the world and are capable of providing commonly used PET tracers on a daily basis (Gambhir 2002).

Isotopes that are β-emitters (e.g., ^{3}H, ^{14}C) are not useful for noninvasive imaging of living subjects because β-particles (electrons) do not travel significant distances; they are used instead in autoradiography (see below). γ-Emitting isotopes (e.g., ^{99m}Tc, ^{111}In, ^{123}I, ^{131}I) can also be used for imaging living subjects but require different types of scanners known as gamma cameras, which when rotated around the subject (then known as single photon emission computed tomography, SPECT), can result in production of tomographic images. A more detailed review of SPECT imaging can be found elsewhere (Rosenthal et al. 1995).

Detection of γ-rays is achieved through scintigraphic instrumentation, which consists of an array of scintillation crystals to convert γ-ray energy into visible light, suitable light sensors, readout electronics, and image processing units (for review, see Ziegler 2000). The coincidence detection of both γ-rays in PET within nanoseconds of each other defines the line of response in space and thus the direction of flight. In contrast to

SPECT, attenuation (quantifiable reduction in events present at the face of the detector due to absorption or scatter through tissues) of the emitted radiation in PET can be corrected precisely because the total length through the body determines the attenuation factor along a coincidence line. By doing so, quantitative information about the tracer distribution can be obtained. The reconstruction software then takes the coincidence events measured at all angular and linear positions to reconstruct an image that depicts the localization and concentration of the positron-emitting radioisotope within a plane of the organ that was scanned. If single photon emitters are used, the direction of flight has to be determined by geometric collimation. Because the emission of γ-rays from the subject is isotropic, such collimation is needed to restrict data to γ-rays of certain predefined directions. The main difference between SPECT and PET measurements is the necessity of lead collimators for the definition of the angle of incidence, compared with electronic collimation in the case of PET.

The sensitivity of PET is relatively high in the range of 10^{-11}–10^{-12} mole/L, and is independent of the location depth of the reporter probe of interest. Typically, several million cells accumulating reporter probe have to be in relative close proximity for a PET scanner to record them as a distinct entity relative to the background. In SPECT, collimator design is always a compromise between spatial resolution and sensitivity: reducing the size of the holes or using longer septae improves spatial resolution but reduces sensitivity at the same time. The use of collimators in SPECT results in a very low detection efficiency of ~10^{-4} times the emitted number of γ-rays. PET is therefore at least a log order more sensitive than SPECT. For example, even a triple-head SPECT system designed to image ^{99m}Tc-labeled tracers in the human brain is 15 times less sensitive than a PET if a 1-cm resolution is assumed in both systems (Budinger 1996). One alternative to PET that attempts to overcome sensitivity limitations, and that can also be adapted to available clinical systems, is "pinhole SPECT" for imaging small animals, with a reported spatial resolution as high as 1.7 mm. Even higher resolutions (200 μm) are possible with micropinhole apertures and ^{125}I SPECT imaging (Beekman et al. 2002).

Positron-emitting isotopes can usually be substituted readily for naturally occurring atoms, and therefore PET is a more robust technique than SPECT for imaging most molecular events. An important principle to note is that because all isotopes used result in two γ-rays of the same energy, if two molecular probes, each with a separate isotope, are injected simultaneously, it would not be possible for the PET detectors to distinguish them. Therefore, to investigate multiple molecular events, molecular probes are usually injected separately, allowing for the decay of one isotope prior to administration of the other. SPECT, on the other hand, does allow simultaneous detection of multiple events owing to the use of multiple isotopes, each with different-energy γ-rays. In practice, the concurrent use of several SPECT isotopes, without perturbation of the underlying parent molecules, would have to be possible before a clear advantage could be achieved for SPECT over PET in multiple-event imaging. The images from a PET scanner, although often shown in color, reflect identical-energy γ-ray events, and the color scale usually reflects the concentration of isotope in various locations of the body. The spatial resolution of most clinical PET scanners is ~$(6–8)^3$ mm^3, but higher-resolution clinical brain scanners have been developed approaching resolutions of ~3^3 mm^3.

In recent years, small animal micro-PET scanners have been developed. These systems typically have a spatial resolution of ~2^3 mm^3 (Cherry and Gambhir 2001), but newer generation systems in final stages of development will have a resolution of ~1^3 mm^3 (Chatziioannou et al. 2001). Development of molecular imaging assays with PET is particularly advantageous because of the ability to validate them in cell culture and small animal models prior to using the same reporter probe in established clinical PET centers around the world. The ability to perform translational research from a cell culture setting to preclinical animal models to clinical applications is one of the most unique and powerful features of PET technology. Further reviews of PET in small animals are to be found in Cherry and Gambhir (2001), Luker and Piwnica-Worms (2001), Price (2001), Reader and Zweit (2001), and Chatziioannou (2002).

Optical imaging

Optical imaging techniques have already been developed for in vitro and ex vivo applications in molecular and cellular biology (e.g., fluorescence microscopy and in benchtop luminometry using commercial substrate kits for bioluminescence). An extension of this concept toward noninvasive in vivo imaging with light photons represents an interesting avenue for extracting relevant biological information from living subjects. Progress in optical molecular imaging strategies has come from the recent development of targeted bioluminescence probes, near-infrared fluorochromes, activatable near-infrared fluorochromes, and red-shifted fluorescent proteins (Weissleder 2001). A notable theoretical advantage of optical techniques is the fact that multiple probes with different spectral characteristics could potentially be used for multichannel imaging, similar to in vivo karyotyping (Weissleder 1999). Optical imaging also allows for a relatively low-cost alternative to studying reporter gene expression in small animal models (see below).

A fundamental issue in optical imaging of living subjects is how to detect light emitted from the body, this being relevant to both bioluminescence and fluorescence imaging. In this regard, several technical advances for imaging very low levels of visible light have now emerged, allowing the use of highly sensitive detectors in living subjects, and not just restricted to cell cultures and small transparent animals. Charged coupled device (CCD) detectors are made of silicon crystals sliced into thin sheets for fabrication into integrated circuits using similar technologies to those used in making computer silicon chips. For a detailed overview of CCD technol-

Table 1. *Characteristics of imaging modalities available and guide to finding the appropriate molecular imaging approach*

Imaging technique	Portion of EM radiation spectrum used in image generation	Spatial resolution[a]	Depth	Temporal resolution[b]	Sensitivity[c]	Type of molecular probe[d]	Amount of molecular probe used
Positron emission tomography (PET)	high-energy γ rays	1–2 mm	no limit	10 sec to minutes	10^{-11}–10^{-12} mole/L	Radiolabeled, direct or indirect	nanograms
Single photon emission computed tomography (SPECT)	lower-energy γ rays	1–2 mm	no limit	minutes	10^{-10}–10^{-11} mole/L	radiolabeled direct or indirect	nanograms
Optical bioluminescence imaging	visible light	3–5 mm[f]	1–2 cm	seconds to minutes	not well-characterized possibly 10^{-15}–10^{-17} mole/L	activatable indirect[i]	micrograms to milligrams
Optical fluorescence imaging	visible light or near-infrared	2–3 mm[g]	<1 cm[h]	seconds to minutes	not well characterized, likely 10^{-9}–10^{-12} mole/L	activatable, direct or indirect	micrograms to milligrams
Magnetic resonance imaging (MRI)	radiowaves	25–100 μm	no limit	minutes to hours	10^{-3}–10^{-5} mole/L	activatable, direct or indirect	micrograms to milligrams
Computed tomography (CT)	X-rays	50–200 μm	no limit	minutes	not well characterized	may be possible (see text)	not applicable
Ultrasound	high-frequency sound	50–500 μm	millimeters to centimeters	seconds to minutes	not well characterized	limited activatable, direct	micrograms to milligrams

ogy, please refer to Spibey et al. (2001). One of the properties of silicon-based detectors is their high sensitivity to light, allowing them to detect light in the visible to near-infrared range. CCD cameras operate by converting light photons at wavelengths between 400 and 1000 nm that strike a CCD pixel with an energy of just 2–3 eV (as opposed to high-energy γ-rays of 511 keV in PET that would easily traverse a CCD chip) into electrons. A CCD contains semiconductors that are connected so that the output of one serves as the input of the next. In this way, an electrical charge pattern, corresponding to the intensity of incoming photons, is read out of the CCD into an output register and amplifier at the edge of the CCD for digitization. Older intensified CCD cameras had much lower sensitivities than newer-generation cooled CCD cameras. This is because thermal noise (termed "dark current") from thermal energy within the silicon lattice of a CCD chip resulted in constant release of electrons. Thermal noise is dramatically reduced if the chip is cooled; dark current falls by a factor of 10 for every 20°C decrease in temperature (Spibey et al. 2001). For bioluminescence imaging, CCD cameras are usually mounted in a light-tight specimen chamber, and are attached to a cryogenic refrigeration unit (for camera cooling to −120°C to −150°C). A camera controller, linked to a computer system, is used for data acquisition and analysis. A bioluminescence image is often shown as a color image that is superimposed on a gray-scale photographic image of the small animal using overlay and image analysis software. Usually a region of interest is manually selected over an area of signal intensity, and the maximum or average intensity is recorded as photons per second per

Table 1. *Continued*

Quantitative degree	Ability to scale to human imaging	Perturbation of biological system	Principal use	Advantages	Disadvantages	Cost[e]
+++	yes	no	metabolic, reporter/gene expression, receptor/ligand, enzyme targeting	high sensitivity, isotopes can substitute naturally occurring atoms, quantitative translational research	PET cyclotron or generator needed, relatively low spatial resolution, radiation to subject	$$$$
++	yes	no	reporter/gene expression, receptor/ligand	many molecular probes available, can image multiple probes simultaneously, may be adapted to clinical imaging systems	relatively low spatial resolution because of sensitivity, collimation, radiation	$$$
+ to ++	yes but limited	yes if necessary to give mass quantity of molecular probe	reporter/gene expression, cell trafficking	highest sensitivity, quick, easy, low-cost, relative high-throughput	low spatial resolution, current 2D imaging only, relatively surface-weighted, limited translational research	$$
+ to ++	yes but limited	yes if necessary to give mass quantity of molecular probe	reporter/gene expression, cell trafficking	high sensitivity, detects fluorochrome in live and dead cells	relatively low spatial resolution, surface-weighted[j]	$–$$
++	yes	yes if necessary to give mass quantity of molecular probe	morphological reporter/gene expression, receptor/ligand if many receptors	highest spatial resolution, combines morphological and functional imaging	relatively low sensitivity, long scan and postprocessing time, mass quantity of probe may be needed	$$$$
not applicable	yes	as MRI, and also if excessive radiation dose	morphological	bone and tumor imaging, anatomical imaging	limited "molecular" applications, limited soft tissue resolution, radiation	$$
+	yes	no	morphological	real-time, low cost	limited spatial resolution, mostly morphological	$$

[a]Spatial resolution is a measure of the accuracy or detail of graphic display in the images expressed in millimeters. It is the minimum distance between two independently measured objects that can be distinguished separately. It is a measure of how fine the image is.
[b]Temporal resolution is the frequency at which the final interpretable version of images can be recorded/captured from the subject once the imaging process is initiated. This relates to the time required to collect enough events to form an image, and to the responsiveness of the imaging system to rates of any change induced by the operator or in the biological system at hand.
[c]Sensitivity, the ability to detect a molecular probe when it is present, relative to the background, measured in moles per liter.
[d]Type of molecular probe. See text.
[e]This includes cost of equipment and cost per study. For details of instrumentation vendors, visit Web site www.mi-central.org.
[f]Spatial resolution of bioluminescence and reflectance fluorescence is depth-dependent. For bioluminescence, the resolution is slightly worse or equal to the depth of the object, that is, an object 3–5 mm deep has an ~3–5-mm spatial resolution.
[g]Use of fluorescence tomography is likely to result in better spatial resolution.
[h]This depth applies to reflectance fluorescence. Fluorescence tomography can likely image objects at greater depths (2–6 cm).
[i]Bioluminescence may also offer direct means of imaging through the use of the Renilla luciferase protein. Feasibility studies are underway.
[j]Except for fluorescence tomography, which has better spatial resolution and can image at greater depths.

centimeter squared per steradian (a steradian is a unit of solid angle; Wu et al. 2001). Whenever the exposure conditions (including time, f/stop, height of sample shelf, binning ratio, and time after injection with optical substrate) are kept identical, the measurements are highly reproducible (in our laboratory to within 6%).

The main advantage of optical bioluminescence imaging is that it can be used to detect very low levels of

signal because the light emitted is virtually background-free (see below). It is quick and easy to perform and allows rapid testing of biological hypotheses and proofs of principle in living experimental models. It is also uniquely suited for high-throughput imaging because of its ease of operation, short acquisition times (typically 10–60 sec), and the possibility of simultaneous measurement of six or more anesthetized living mice (Vooijs et al. 2002). However, the cooled CCD camera has three main drawbacks (Wu et al. 2001): Firstly, the efficiency of light transmission through an opaque animal can be somewhat limited and depends on tissue type and tissue scattering. Skin and muscle have the highest transmission and are fairly wavelength-dependent, whereas organs with a high vascular content such as liver and spleen have the lowest transmission because of absorption of light by oxyhemoglobin and deoxyhemoglobin. Estimates from in vitro studies show that the net reduction of bioluminescence signal is ~10-fold for every centimeter of tissue depth, varying with the exact tissue type (Contag et al. 1995). Secondly, images obtained from the cooled CCD camera are two-dimensional and lack depth information. However, it is expected that future bioluminescence image acquisition using rotating CCD cameras or multiple views of the same animal with a single CCD camera may allow volumetric imaging, especially when combined with novel red-shifted luciferases that have better tissue penetration. A third limitation is the lack of an equivalent imaging modality applicable for human studies, thus preventing direct translation of developed methods for clinical use.

In fluorescence imaging, an excitation light of one wavelength (in the visible light range of 395–600 nm) illuminates the living subject, and a CCD camera (usually a less-sensitive version than the cooled CCD required in bioluminescence detection, for technical reasons discussed in Golden and Ligler 2002) collects an emission light of shifted wavelength. Cells tagged with fluorescently labeled antibodies or those in which expression of the green fluorescent protein (*GFP*) gene (or its variants; Lippincott-Schwartz et al. 2001; Remington 2002) is introduced can be followed by this technique. GFP is a protein from the jellyfish *Aequorea victoria* that has become very popular over the last decade as a reporter in fixed and cultured cells and tissues. Wild-type GFP emits green (509-nm) light when excited by violet (395-nm) light. The variant EGFP has a shifted excitation spectrum to longer wavelengths and has increased (35-fold) brightness. Between 1000 and 10,000 fluorescently-labeled cells in the peritoneal cavity of a mouse can be imaged on its external surface (Kaneko et al. 2001). It may be necessary to expose internal organs surgically prior to their imaging (Bouvet et al. 2002; Yang et al. 2002), although this is true of bioluminescence imaging as well. The two main advantages of fluorescence imaging are that it can be used as a reporter in both live and fixed cells/tissues and no substrate is required for its visualization (Spergel et al. 2001). This simple, reflectance type of fluorescence imaging has been used extensively in studies of feasibility and development of these approaches (Kamiyama et al. 2002; X. Li et al. 2002). However, these systems are not quantitative, and the image information is surface-weighted (anything closer to the surface will appear brighter compared with deeper structures; Weissleder 2001). Direct comparisons of bioluminescence and fluorescence imaging have not been published to date, although these are presently underway in our laboratory. One clear difference between the two modalities is the observation of significantly more background signal owing to autofluorescence of tissues in fluorescence imaging as compared with bioluminescence imaging.

In contrast to fluorescence imaging in the visible light range, the use of the near-infrared (NIR) spectrum in the 700–900-nm range maximizes tissue penetration and minimizes autofluorescence from nontarget tissue (Weissleder 2002). This is because hemoglobin and water, the major absorbers of visible and infrared light, respectively, have their lowest absorption coefficients in the NIR region. Several NIR fluorochromes have recently become available (Lin et al. 2002) that can be coupled to affinity molecules (peptides, antibodies) or that are activatable. This type of NIR fluorescence reflectance imaging is still limited to targets that are fairly near the illuminated surface.

A newer approach to fluorescence imaging of deeper structures uses fluorescence-mediated tomography (Ntziachristos and Weissleder 2002; Ntziachristos et al. 2002). The subject is exposed to continuous wave or pulsed light from different sources, and detectors arranged in a spatially defined order in an imaging chamber capture the emitted light. Mathematical processing of this information results in a reconstructed tomographic image. Resulting images have a resolution of 1–2 mm, and the fluorochrome detection threshold is in the nanomolar range. Recent attempts at constructing a CCD-based scanner for tomography of fluorescent NIR probes have also yielded encouraging results. Prototype instruments attain better than 3-mm resolution, have linear detection within more than two orders of magnitude of fluorochrome concentration, and can detect fluorescent objects at femtomolar quantities in small animal-like geometries (Ntziachristos and Weissleder 2002). Fluorescence-mediated tomography is still in its infancy, requiring extensive mathematical validation prior to practical implementation.

Magnetic resonance imaging

The fundamental principle underlying MRI is that unpaired nuclear spins, called magnetic dipoles (such as hydrogen atoms in water and organic compounds), align themselves when placed into a magnetic field. In an MRI scanner, there is a strong magnet that produces a magnetic field surrounding the subject under investigation. There are also "coils" within the magnet to produce a gradient in this magnetic field in the X, Y, and Z directions. The magnet also contains a radiofrequency coil that can produce a temporary radiofrequency pulse to change the alignment of the spins. Following the pulse,

the magnetic dipoles return to their baseline orientation, which is detected (also by the radiofrequency coil) as a change in electromagnetic flux (radiofrequency waves in the range 1–100 MHz). An important function of the scanner is to determine the rate at which these dipoles relax to their baseline orientation; this measurement is translated into an MR signal. Dipoles in different physicochemical environments will have different relaxation times and, thus, generate different MR signals (Jacobs and Cherry 2001). For example, dipoles in a fat- or hydrocarbon-rich environment will have significantly shorter (up to 20×) relaxation times than dipoles in an aqueous environment (Hornack 2002). This is one of the main ways by which image contrast is achieved in MRI. The timing parameters of pulse excitation and recording can be altered by a central computer, resulting in images with different types of magnetic contrast. The two most frequently used timing parameters are known as T1 and T2 weighting. MRI is exquisitely sensitive to soft-tissue differences and abnormalities (Lewin et al. 1999; Shaharabany et al. 2001; Song et al. 2002). The addition of chemical agents that change the MR signal intensity near these abnormalities may also be used to enhance signal differences and to further highlight the abnormality. Specifically, paramagnetic metal cations such as chelated gadolinium or dysprosium, or superparamagnetic nanoparticles (Moore et al. 1997, 2000; Weissleder et al. 1997a; Turetschek et al. 2001), can be used as compartmental, targeted, or smart probes with this technique (see below). The development of novel contrast agents is an active area in both clinical and basic research. A more comprehensive account of the basic principles of MRI signal creation and detection can be found elsewhere (Jackson 2001; Hornack 2002), also with specific reference to animal research (Chatham and Blackband 2001).

MRI has two particular advantages over techniques that involve the use of radionuclides or optical probes: higher spatial resolution (micrometers rather than several millimeters) and the fact that physiological/molecular and anatomical information can be extracted simultaneously. Micro-MRI in particular is expected to have a substantial influence in developmental biology, in imaging of transgenic animals, and in cell trafficking.

However, MRI is several magnitudes less sensitive than radionuclide and optical techniques, which offer higher levels of sensitivity for imaging relatively low levels of reporter probe (see below): as low as 10^{-12} mole/L of radiolabeled substrate for PET (Phelps 1991), and probably in the femtomolar range for bioluminescence imaging. This implies that much larger amounts of molecular probe must be retained at the target site when using MRI in comparison to radionuclide approaches, and therefore, much larger amounts must be injected into the animal. The physical limitation to the total amount of probe that can be injected stems from the volume of the injectate. Typically, in an animal model, the total amount that can be safely injected intravenously is ~10% of the total blood volume; that is, ~0.25 mL in a mouse. This inherent low sensitivity of MRI arises because the percentage of hydrogen magnetic dipoles that preferentially align themselves within an applied external magnetic field is quite small: on the order of 10 in 1 million dipoles in an applied field of 1.5 T (teslas) at room temperature. The intrinsic poor signal-to-noise ratio of MRI is made worse by the small volumes of water contained in each voxel (volume pixel element) of a microscopic image, and the amount of time available to acquire the image (Jacobs and Cherry 2001). There are numerous ways of increasing the signal-to-noise ratio in micro-MRI when imaging small animals, and thus achieving near microscopic resolution (see below). These include working at relatively high magnetic fields (4.7–14 T), using hardware and software customized to the small size of animals of interest, and the relative flexibility of much longer acquisition times during imaging. Manufacturers of MR equipment are now offering dedicated animal imaging systems to meet expected demands for phenotyping mutant and transgenic mice.

An interesting new extension of MRI techniques to imaging mice is that of magnetic resonance microscopy. This will allow scientists to nondestructively image a whole perfusion-fixed killed mouse (the "Visible Mouse" atlas project; Johnson et al. 2002) with isotropic three-dimensional spatial resolution as small as 110 µm (1×10^{-3} mm^3) and spatial resolution in isolated organs as small as 25 µm (1.6×10^{-5} mm^3). It is anticipated that this atlas will provide a common morphological reference for the anatomy of the normal mouse and as a foundation for morphological phenotyping of a growing number of transgenic and knockout mice (Johnson et al. 2002).

Variations on standard MRI techniques for greater functional analysis include diffusion-weighted MRI, which exploits the translational mobility of water molecules to obtain information on the microscopic behavior of tissues (presence of macromolecules, presence and permeability of membranes, equilibrium of intracellular–extracellular water); and perfusion-weighted MRI, which makes use of endogenous and exogenous reporter probes for monitoring their hemodynamic status. In the clinical context, the combination of both techniques is extremely promising for the early detection and assessment of stroke, for tumor characterization, and for the evaluation of neurodegenerative diseases. There is likely to be a future transition of these same useful techniques into the molecular imaging arena for application to small-animal imaging. Luypaert et al. (2001) provide a review of the basic principles underlying these methodologies.

Another example of the use of magnetic resonance in imaging applies to magnetic resonance spectroscopy (MRS), in which characteristic imaging spectra, composed of specific resonance frequencies absorbed by a small volume of a sample or tissue, are obtained from the tissue subjected to magnetic resonance. These spectra depend on the chemical or "molecular" composition of the sample or tissue. The most useful nuclei for MRS are hydrogen, phosphorus, sodium, and, to a lesser extent, carbon. Hydrogen MR spectroscopy has a greater signal-to-noise ratio and better spatial resolution than phospho-

rus spectroscopy. The most interesting MR spectral components in living subjects are those of metabolites and amino acids; for example, choline, creatine, N-acetyl aspartate (NAA), lactate, myoinositol, glutamine and glutamate, lipids, leucine, and alanine (Castillo et al. 1996). The concentration of most metabolites is typically orders of magnitude less than that of the water or fat signal in tissues. Therefore, the ^{1}H MRI signals from water and fat must be suppressed when performing ^{1}H spectroscopy of metabolites. There are emerging applications for MRS in molecular imaging. For example, Stegman et al. (1999) have used MRS in mice to demonstrate the feasibility of monitoring expression of the cytosine deaminase transgene in tumors. Noninvasive measurement of gene expression in murine muscle using MRS has also been developed to monitor gene therapy in mouse models of neuromuscular diseases (Fraites et al. 2002).

Computed tomography imaging

Images in computed tomography (CT) are obtained when component tissues differentially absorb X-rays as they pass through the body (Dendy and Heaton 1999). A low-energy X-ray source of 30–50 kVp (i.e., of considerably lower energy than in clinical CT scanners) and a detector rotate around the animal, acquiring volumetric data. Most mouse CT images are collected with high-resolution phosphor screen/CCD detectors to optimize image quality. A scan of an entire mouse at 100-μm resolution takes ~15 min. Higher-resolution (50-μm) images are achievable with longer scanning times. The system spatial resolution is primarily limited by the pixel sampling rate, the X-ray source size, and blurring in the phosphor screen. The radiation dose, however, is not negligible (0.6 Gy per scan; 5% of the LD_{50} for mice), and this can limit repeated imaging of the same animal. Unlike MRI, CT has relatively poor soft-tissue contrast, often making it necessary to administer iodinated contrast media to delineate organs or tumors. In its present use, computed tomography is not a "molecular" imaging technique per se, but instead, dedicated high-resolution micro-CT scanners are available for anatomical imaging of small animals (Paulus et al. 2001; Berger et al. 2002; Holdsworth and Thornton 2002), thus complementing the functional information obtained by other modalities discussed above. In theory, several obstacles would have to be surmounted for CT to achieve "molecular" imaging capabilities. Importantly, specific CT-based "probes" to image biological processes would have to be iodinated (or tagged with another high-atomic-number atom that absorbs X-rays). Moreover, site-specific accumulation of large quantities of such probes would have to be possible in order to detect differential attenuation of X-rays that reflect the biological process in question. These approaches, along with development of small-animal CT using monochromatic X-rays (Dilmanian et al. 1997), are being evaluated at present.

Other imaging modalities

Ultrasonography is the most widely used clinical imaging modality because of its low cost, availability, and safety. Ultrasound images are obtained when high-frequency (>20-kHz) sound waves are emitted from a transducer placed against the skin and the ultrasound is reflected back from the internal organs under examination. Contrast in the images obtained depends on the imaging algorithm used, backscatter, attenuation of the sound, and sound speed. Ulrasound imaging using diagnostic ultrasound instrumentation operating in the 7.5–15-MHz frequency range has been successfully applied to a variety of mouse models (Turnbull and Foster 2002), yielding images with a spatial resolution of 300–500 μm. The role of ultrasonography in the spectrum of modalities available for mouse microimaging and phenotype analysis closely parallels its present role in clinical imaging. The strengths of ultrasound in cardiac, obstetric, vascular, and abdominal imaging appear most likely to extend to the mouse when the technology is scaled down to achieve high resolution and a level of practicality/functionality similar to that available with present clinical ultrasound systems. The real-time nature of ultrasound is also facilitating its application in image-guided injection procedures, enabling mouse embryos to be directly manipulated in utero when studying normal and diseased development. This visualization of small anatomical structures at the embryonic and early postnatal stages is possible using "ultrasound biomicroscopy": a high-frequency (20–100-MHz) pulse-echo ultrasound approach for imaging living biological tissues with near-microscopic resolution (50–100 μm; Turnbull and Foster 2002). This technique also allows color Doppler imaging for noninvasive blood velocity measurements and microcirculatory flow mapping.

Another recent emerging concept is that of using targeted ultrasonic contrast agents for molecular imaging of specific cell-surface receptors, especially within the vascular compartment (Lanza and Wickline 2001). For example, angioplasty-induced expression of tissue factor by smooth muscle cells within the carotid arteries of pigs can be identified with a ligand-targeted acoustic nanoparticle system. Tissue factor-targeted emulsions were found to bind to overstretched smooth muscle cells and increase their echogenicity and gray-scale levels (Lanza et al. 2000).

Although not used in living subjects, whole-body autoradiography is a type of small-animal imaging mentioned here because of its important complementary role to radionuclide tracer quantification and distribution studies in rodent models following their being killed. Autoradiography is the detection of radioactive isotopes on X-ray film or digital plates, where the specimen is the source of the radiation. The isotope emissions form a latent image on the film that produces a final image upon development. This is often performed at the end of microPET studies to provide a standard against which PET images and data can be compared (Gambhir et al. 1998). The killed animal is frozen in carboxymethyl cel-

lulose (CMC), and whole-body sections (20–45 μm) are obtained using a microtome. Sections are freeze-dried at –20°C and placed on X-ray film for exposure. Different radionuclides require different exposures because of varying exposure efficiencies. Autoradiography has a wide range of spatial resolutions; microautoradiography, with resolution down to 0.05 μm, is used to locate tracers within or between cells. Macroautoradiography (whole-body autoradiography), with a resolution of ~50 μm, is used to determine tracer concentration within tissues. Quantitative data can be obtained by densitometry using an isotope scale as a reference.

Multimodality imaging

By computer software, high-resolution anatomical images from CT or MRI can be registered mathematically onto physiologically/functionally informative PET images of the same subject to produce a bimodality image (Townsend 2001; Townsend and Cherry 2001). However, motion artifact and time-consuming and difficult realignment and computation for fusion of independent studies have until now limited the use of registration techniques (Israel et al. 2001). Ongoing research seeks to amalgamate two or more of the above-described powerful modalities. Future small-animal instrumentation will be integrated, thus housing different modalities in the same scanner, in the same mold as recently developed clinical CT/PET scanners (Townsend 2001), one of *Time* magazine's "Inventions of the Year 2000" (December 4, 2000). For example, combined radionuclide and magnetic probes should allow near-simultaneous MRI and PET imaging. Other combinations of optical, radionuclide, MRI, and CT techniques, and specifically designed dual-purpose probes (Bogdanov et al. 1998; Josephson et al. 2002) will be possible, producing truly multimodal images. Such multimodality systems may provide a number of unique opportunities, including improving the ability to quantify and locate biological processes and events, characterization of new imaging probes, and the ability to provide near perfectly registered images (with minimal or no motion artifact) to improve interpretation and quantification of data across many different experimental systems (Jacobs and Cherry 2001).

General requirements for performing molecular imaging in living subjects

The acquisition of ex vivo (i.e., in vitro, using test tubes containing cell extracts, or cell culture, using intact living cells) information in biomedical research has become relatively easy, because a myriad of specialty reagents, ligands, protocols, and devices have been commercially developed over the past two decades. On the other hand, molecular imaging in living subjects presents more theoretical and practical challenges than in vitro or cell culture detection, primarily because of the need for probes to be biocompatible, the presence of additional delivery barriers, and the necessity for developing special in vivo amplification strategies (Mahmood and Weissleder 2002). There are five general areas in which considerable research efforts are ongoing (Weissleder 1999; Weissleder and Mahmood 2001) and will also be necessary in the future to perform in vivo molecular imaging (by seeking answers to the questions in parenthesis): (1) selection of appropriate cellular and subcellular targets to image (what biological process is to be imaged?); (2) development of suitable in vivo affinity ligands, that is, molecular imaging probes (what biocompatible chemical/biochemical/molecular entity can be used in vivo to distinguish that particular biological process and help to generate specific images of that target?); (3) delivery of these probes in a manner that efficiently overcomes biological barriers (what are the pharmacokinetic attributes of these probes contributing to successful imaging?); (4) amplification strategies able to detect minimal target concentrations, usually in the pico- to nanomolar range (can the imaging signal be amplified?); and (5) development of imaging systems with high spatial/temporal resolution and sensitivity suitable for small laboratory animals, and that ultimately can be translated to the human patient (what are the imaging modalities and instrumentation available to achieve molecular imaging in living subjects?), as discussed above.

Molecular imaging probes

Molecular imaging probes provide the imaging signal (sometimes referred to as image contrast) in almost all molecular imaging assays. The notable exception is MRS, where the imaging signal often emanates from endogenous molecules. Molecular imaging probes can in many ways be compared with stains used in histological analysis of tissue samples, but are instead injected into living subjects to image specific biological/molecular events. Molecular imaging probes are referred to by many different names. These include but are not limited to: (1) molecular probes, (2) molecular beacons, (3) reporter probes, (4) tracers, (5) smart probes, (6) activatable probes, (7) nanoparticles, and (8) contrast agents. Molecular imaging probes typically are composed of an affinity component that interacts with the target and a signaling component that is useful for imaging. In radiolabeled approaches, the signaling component can be a small isotopic substitution (e.g., replacing ^{12}C for ^{11}C), a nonisotopic substitution (e.g., replacing ^{1}H with ^{18}F), or larger chelating approaches using larger isotopes (e.g., ^{64}Cu, ^{99m}Tc). In optical approaches, the signaling component can be a fluorochrome, and in MRI, it can be a paramagnetic atom (e.g., gadolinium). One of the advantages of PET is that drugs or existing molecules known to interact with a specific target can be modified with a radiolabel while minimally perturbing the parent molecule. For optical and MRI approaches, this is usually not possible, because the signaling portion is itself a large molecule (e.g., a fluorochrome) or a bulky atom (e.g., gadolinium).

Molecular probes can be categorized in many different ways. One particularly useful way of categorizing them

is either as radiolabeled or activatable probes (Fig. 2). Radiolabeled probes (for PET and SPECT imaging) produce signal constantly through the decay of the radioisotope, whereas activatable probes produce signal only when they interact with their target(s) (e.g., near-infrared fluorescent probes for optical imaging). Another way of categorizing molecular imaging probes is if they directly image a specific molecular process (e.g., a receptor target imaged with a ligand molecular imaging probe), as opposed to indirect imaging (e.g., expression of an imaging reporter gene indirectly measuring expression of an endogenous gene). Most radiolabeled molecular imaging probes are given in low doses (nonpharmacological nanogram levels) as compared with molecular imaging probes for MRI and optical techniques that are usually given in mass levels (typically micrograms to milligrams). A further useful classification of molecular imaging probes is whether they are nonspecific or specific. Nonspecific probes do not have a distinct set of targets, as do specific probes, but instead produce signal based on complex set(s) of biological events, many of which are not always fully known, such as ^{99m}Tc-sestamibi (Mariani 1996).

Molecular imaging probes can be small molecules, such as receptor ligands or enzyme substrates, or higher-molecular-weight affinity ligands, such as monoclonal antibodies or recombinant proteins. In addition to those probes discovered by chance, recent advances in the drug discovery process will aid in future selection and/or rational design of newer probes through combinatorial chemistry and high-throughput testing. It is anticipated that increasing multidisciplinary interactions between imaging research groups and the pharmaceutical industry will have a significant impact on the design and development of many more novel molecular imaging probes. This is because drug development shares many features in common with molecular imaging probe development, and the two fields likely will continue to influence each other (Gambhir 2002). In the next few paragraphs, various types of molecular imaging probes are briefly described to highlight some of their important features.

The simplest and commonest, but perhaps the least informative from a cell biology and molecular imaging standpoint, is the widely used class of nonspecific imaging probes with vascular distributions (e.g., circulating within blood vessels). These include most of the contrast media in conventional medical imaging (Dawson 1999), some nuclear medicine-based tracers (e.g., ^{15}O-H_2O for PET), and some fluorochrome reporters (e.g., indocyanine green). They can be used to image physiological processes such as changes in blood volume, flow, and perfusion, but cannot be targeted to specific biological processes at the cellular or subcellular level (Weissleder 2002). These probes serve quite a useful role in monitoring "downstream" changes in pathology, but do not generally serve to characterize changes early in a disease process.

Conversely, molecular imaging probes with greater specificity and targeting potential can be made by using antibodies, ligands, or substrates that can specifically interact with targets in particular cells or subcellular compartments. There are numerous examples in this category of probes, mainly including those for radionuclide imaging. Specific targeted probes include those used in most of the conventional radiotracer imaging methods, where the emphasis is on imaging the final products of gene expression with radiolabeled substrates that interact with a protein originating from a specific gene. These interactions are based on either receptor–radioligand binding (e.g., binding of ^{11}C-carfentanil to the mu opiate receptor; Frost et al. 1990) or enzyme-mediated trapping of a radiolabeled substrate (e.g., ^{18}F-2-fluoro-2-deoxyglucose [^{18}F-FDG] phosphorylation by hexokinase). The fundamental limitation of a majority of these conven-

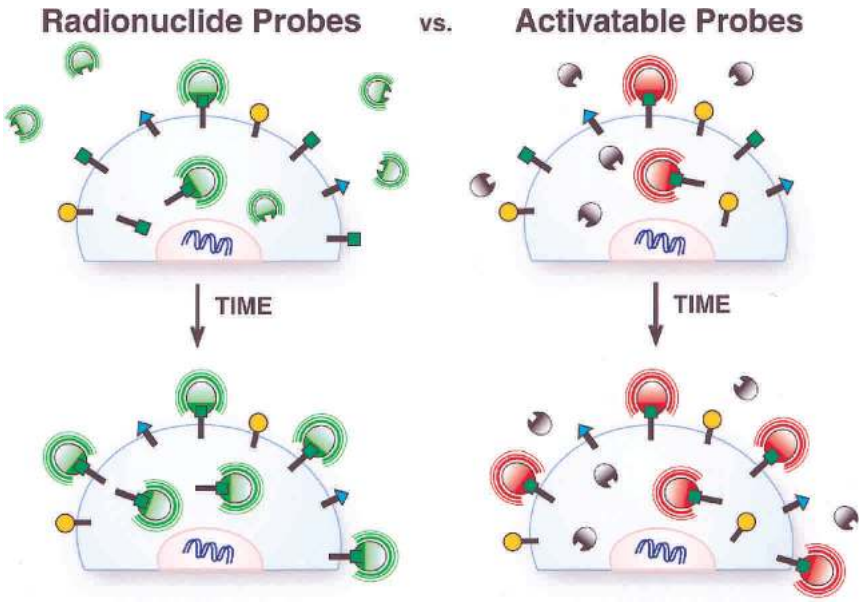

Figure 2. Two broad categories of molecular imaging probes. Radiolabeled probes (for PET and SPECT imaging and autoradiography) produce signal continuously, before and after interacting with their target(s), through the decay of the radioisotope. A time delay between injection of the probe and imaging helps to clear the untrapped probe. Activatable probes produce signal only when they interact with their target(s) (e.g., near-infrared fluorescent probes for optical imaging). A time delay between injection and imaging helps to achieve sufficient levels of activated probe at the target site.

tional approaches using these types of targeted probes is that a new substrate must be discovered and radiolabeled to yield a different probe for each new protein to be targeted (Gambhir 2000). Because of the difficulty, cost, and effort of radiolabeling new substrates, and the requirement for in vivo characterization of every such substrate under investigation, alternative methods would be desirable to develop new assays that are more generalizable; that is, that are able to image gene product targets arising from the expression of any gene of interest. Hence, there have been concerted efforts in recent years by several research groups to develop and validate molecular imaging reporter gene/reporter probe systems for use in living subjects (Gambhir et al. 1999a; Herschman et al. 2000; Adams et al. 2002; Iyer et al. 2002; Liang et al. 2002b). The underlying principles and ideal features of such reporter systems are discussed further in a section below.

Despite the specificity of the molecular probes exemplified above, background noise can be substantial with this approach. This is because the scanner cannot distinguish the parent tracer from the bound or metabolized tracer, and as such, time is required to allow the parent tracer to clear. To circumvent this relative drawback, another category of specific imaging probes consists of activatable or "smart" probes (also referred to as sensors or beacons). These can only be detected once they have interacted with their target, and have been developed mainly for optical and magnetic resonance imaging applications. They are relatively undetectable prior to interaction with their target (Weissleder 2002). Because they are only "switched on" at the target, they increase signal-to-noise ratio for imaging purposes. Molecular beacons are now reasonably well-accepted means of seeing nucleic acid hybridization in living cells under microscopy. They are also being used for in vitro studies, especially in PCR, and for nonspecific protein–DNA-binding studies (J.J. Li et al. 2002). They have been adapted recently as activatable smart probes for molecular imaging in living subjects. The conventional molecular beacon is a single DNA strand with a fluorophore covalently attached to one end and a quencher to the other. Unhybridized, the strand folds into a hairpin shape so that the quencher is in close proximity to the fluorophore and prevents it from fluorescing. When the probe hybridizes to DNA or RNA, its stem unwinds, separating the two ends and unquenching the fluorophore, thus allowing it to transfer energy by fluorescence resonance energy transfer (FRET) to an adjacent emitter (Mitchell 2001; Weissleder 2001). The beacon "lights up" only when the reaction of interest has occurred. A variation of these probes worthy of note includes quenched near-infrared fluorochromes that can be activated by proteases such as matrix metalloprotease 2 (MMP-2; Fig. 3; Bremer et al. 2001a,b). Such a molecular probe consists of three structural elements: A quenched NIR fluorochrome covalently coupled to a poly-L-lysine backbone sterically protected by methoxy polyethylene glycol (MPEG) side chains. Coupled to this backbone are specific synthetic peptide substrates containing motifs that can be cleaved by MMP-2. Owing to the proximity of the fluorochromes, quenching occurs so that almost no fluorescent signal can be detected in the nonactivated

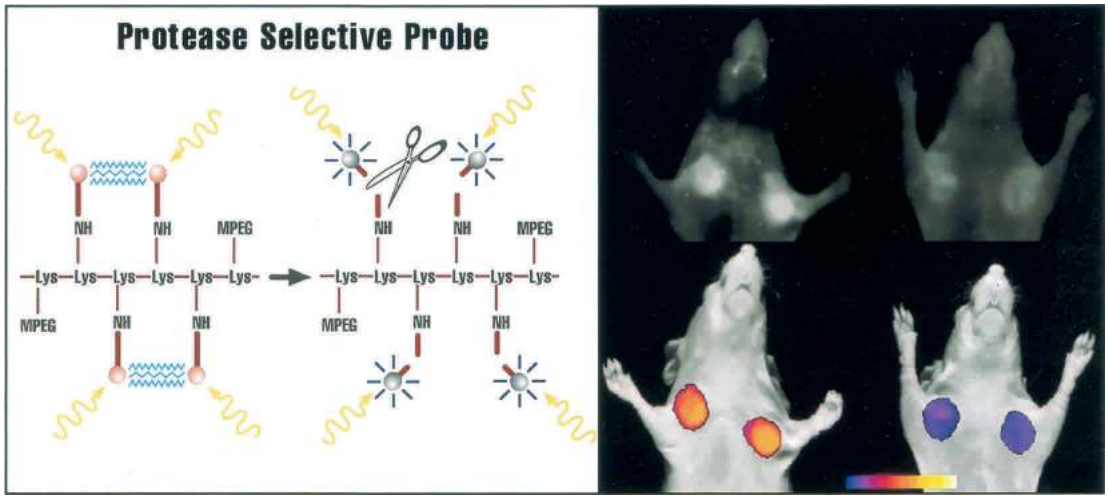

Figure 3. Imaging of matrix metalloprotease 2 (MMP-2) activity through the use of an activatable probe. Schematic shows design of the MMP-2-sensitive fluorescent probe for in vivo NIRF imaging. Fluorochromes with excitation and emission wavelengths in the NIR spectrum are covalently coupled to a poly-L-lysine backbone sterically protected by MPEG side chains by means of a synthetic MMP-2 peptide substrate (thick brown lines). Owing to the proximity of the fluorochromes, quenching (blue) occurs so that almost no fluorescent signal can be detected in the nonactivated state. After MMP-2 cleavage of the peptide spacer, fluorochromes are released from the carrier and become brightly fluorescent. Images show NIRF imaging of HT1080 tumor-bearing nude mice. The *top* row shows raw image acquisition obtained at 700-nm emission. Mouse on *left* was untreated, and on *right* was treated with an MMP-2 inhibitor (prinomastat). The *bottom* row shows color-coded tumoral maps of MMP-2 activity superimposed onto white-light images. Bright fluorescence is present in the absence of MMP-2 inhibitor. Color scale is an arbitrary one with yellow/white being the brightest fluorescence, and blue being the dimmest. Reproduced with permission from Bremer et al. (2001b).

state. After MMP-2 cleavage of the peptide spacer, fluorochromes are released from the carrier and become brightly fluorescent. The same principle can be applied to imaging the activities of other proteases, such as cathepsins (Bogdanov et al. 2002), caspases, or other enzymes (Weissleder et al. 1999). Other examples include magnetic nanosensors that can interact with DNA or RNA sequences, activatable paramagnetic chelators, and paramagnetic substrates that are polymerized by peroxidases or tyrosinases (Weissleder 2002).

Of related interest, the use of aptamers for in vitro specific protein-binding studies has drawn some attention recently. Aptamers are DNA or RNA oligonucleotides isolated to bind to various biomolecules with high specificity. These can be combined with the smart probes described above to produce probes called molecular aptamer beacons (MAB), likely also to be exploited in molecular imaging strategies in living subjects (J.J. Li et al. 2002).

Optical reporters, such as the substrate D-luciferin for the enzyme Firefly luciferase, are also examples of targeted activatable molecular imaging reporter gene/reporter probe systems (Contag et al. 1998, 2000; Zhang et al. 1999). The Firefly luciferase gene (*Fluc*) encodes Firefly luciferase, an enzyme that oxidizes its substrate D-luciferin to result in light emission (bioluminescence). This chemiluminescent reaction can only take place under physiological conditions within living cells expressing *Fluc*. Luciferases consist of a wide range of enzymes that catalyze the oxidation of substrate luciferins to yield nonreactive oxyluciferins and the release of photons of light that may be detected, collected, and quantified externally. Some luciferins require the presence of a cofactor to undergo oxidation, such as $FMNH_2^+$, Ca^{2+}, or ATP. Complexes that contain a luciferase, a luciferin, and generally requiring O_2 are also called photoproteins. The most common luciferin–luciferase system used in molecular imaging is that derived from the Firefly *Photinus*, although the sea pansy *Renilla* luciferase, which uses a different substrate (coelenterazine) and is not ATP-dependent, has also been validated recently for applications in living subjects (Bhaumik and Gambhir 2002). Both colorimetric (e.g., rhodamine red) and fluorescent (e.g., GFP) reporter proteins require an external source of light for excitation and emit light at a different wavelength for detection, thus making them more susceptible to background noise (autofluorescence). In contrast, the bioluminescence luciferase enzyme and substrate systems described above have several characteristics that make them useful reporter proteins (Wu et al. 2001). For example, Firefly luciferase does not need external light excitation and self-emits light from yellow to green wavelengths in the presence of D-luciferin, ATP, magnesium, and oxygen. Secondly, the fast rate of enzyme turnover ($T_{1/2}$ = 3 h) in the presence of substrate D-luciferin allows for real-time measurements because the enzyme does not accumulate intracellularly to the extent of other reporters. Thirdly, the relationship between the enzyme concentration and the peak height of emitted light in vitro is linear up to 7–8 orders of magnitude. Therefore, these properties potentially allow for sensitive noninvasive imaging of *Fluc* reporter gene expression in living subjects.

Overcoming biological barriers in molecular imaging

A specific molecular imaging probe must possess reasonable pharmacokinetic features such that it reaches its intended target at sufficient concentration and remains there sufficiently long to be detectable in living subjects. In this respect, the probe becomes subject to all the pharmacokinetic rules and constraints that govern the concentration of "drugs" in plasma, including absorption, distribution, metabolism, excretion, and other factors within the vascular compartment (e.g., plasma half-life, first- or zero-order pattern of elimination, volume of distribution, protein binding, relation of blood levels to any toxicity, and ultimately to the imaging signal itself; Fig. 4). Rapid excretion, nonspecific binding/trapping, metabolism, and delivery barriers all are important obstacles to be overcome (Huang and Phelps 1986; Weissleder and Mahmood 2001; Gambhir 2003).

Delivery barriers are typically the most challenging to deal with, particularly for larger probes. Even low-molecular-weight probes may not be easily internalized into cells, a requirement for imaging of intracellular targets. Several strategies have been developed to evade existing delivery barriers, and research is ongoing in this area. Examples include the use of peptide-mediated translocation signals (e.g., via the HIV-1 TAT peptide) that result in active shuttling of imaging probes across the cell lipid bilayer membrane into cells (Josephson et al. 1999; Bhorade et al. 2000; Lewin et al. 2000; Polyakov et al. 2000; Dodd et al. 2001; Wunderbaldinger et al. 2002), conjugating biomolecules with polyethylene glycol (PEG) to decrease both immunogenicity and rapid recognition (PEG is a polymer known to minimize molecular interactions and improve colloidal solubilities; Molineux 2002), use of long-circulating drugs to achieve a more homogeneous distribution (this applies to smart probes, not most other imaging probes, in which longer circulation times are undesirable), and/or local delivery combined with pharmacological or physical methods to improve targeting (Weissleder and Mahmood 2001).

An important consideration in using targeted probes is the fact that target-to-background ratios can be further limited by receptor density and/or availability, binding affinity, rapid efflux from cells, limited clearance kinetics from the interstitial space, and/or nonspecific cellular uptake or adhesion of probes. In particular, it may be difficult to differentiate specifically bound from unbound ligands. This frequent inability to eliminate unbound affinity ligands can be problematic, and at times may markedly contribute to background noise. In in vitro assays, this predicament is easily dealt with by washing off unbound ligands and then recording specific signals, with resultant high target-to-background ratios. Unfortunately, in a living subject, options are limited to optimization of pharmacokinetics, that is, waiting for nonspecific circulating surplus probe to be eliminated.

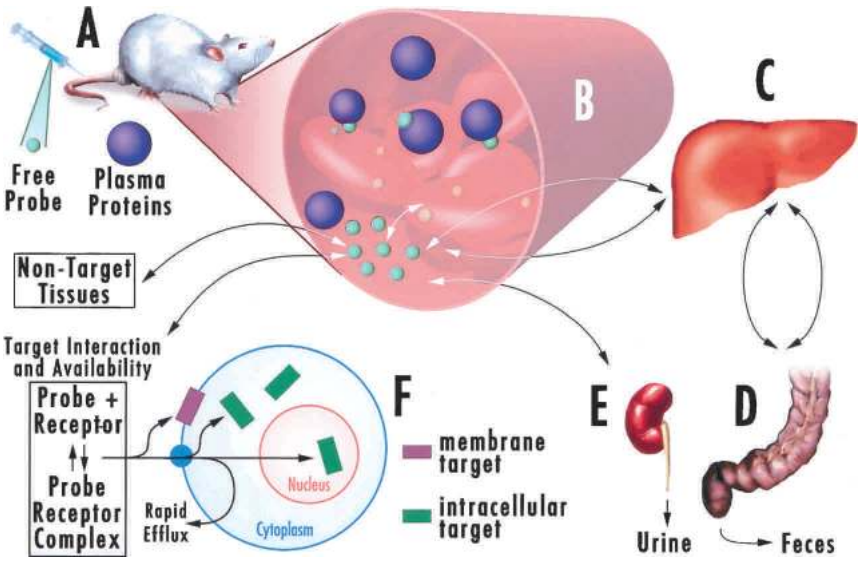

Figure 4. Pharmacokinetics of molecular imaging probes. Molecular imaging probes need to overcome many biological barriers when administered to living subjects. These probes are subject to all the pharmacokinetic rules and constraints that govern the concentration of "drugs" in plasma, including absorption/delivery (*A*), distribution (*B*), metabolism (*C*), excretion/reabsorption in the enterohepatic circulation (*D*), urinary excretion (*E*), and other factors within the vascular compartment (*B*; e.g., plasma half-life, protein binding). Rapid excretion, nonspecific binding/trapping in nontarget tissues, metabolism, and delivery barriers are all important obstacles to be overcome before availability to target(s) for interaction (*F*).

This may be aided by removing some of the ligand from the circulation (into the reticuloendothelial system) by means of the addition of specific "chase" compounds shortly before imaging (Weissleder and Mahmood 2001), and by use of smart probes that produce minimal signal until they interact with targets.

Strategies for signal amplification

Signal amplification is a key issue for molecular imaging strategies. Higher levels of imaging signal per unit level of target and probe interaction lead to higher sensitivity for any particular imaging assay. Unfortunately, the numbers of DNA and mRNA targets per cell (1–2, and about 10–1000, respectively) are limited, thus requiring extreme levels of signal amplification for adequate image visualization. The antisense imaging approach mentioned below therefore has the lowest concentration of the target (mRNA) and is the most challenging of the present molecular imaging methods under investigation. On the other hand, imaging of proteins and/or protein function is much more feasible, a process referred to as downstream imaging because of the much larger number of targets available, between 100 and 1 million per cell. In particular, the strategy entailing interaction of an imaging probe with a receptor shows relatively greater inherent signal amplification, owing to the presence of many receptors available for accepting these ligands. Better still is when each enzyme molecule in turn traps a large number of substrate probes, leading to the greatest degree of signal amplification. These differences must be borne in mind, depending on the biological process under investigation and when optimizing the decision to select a particular imaging assay over another.

The selection of an appropriate downstream target of gene expression may be sufficient to produce signal amplification for imaging purposes. There are some further strategies that can facilitate this process of protein imaging, such as improving target concentration by avidin–biotin amplification (Rosebrough 1996) or improved kinetics, trapping of converted ligands (as in the ^{18}F-FPCV/HSV1-TK reporter system outlined below), and the ability of probes to change their physical nature after target interaction (e.g., fluorescence dequenching; Bremer et al. 2001a), all of which serve to increase the sensitivity of the imaging assay.

Specific applications of molecular imaging in living subjects

The myriad of biological processes that could be targeted for molecular imaging and the associated approaches for developing technologies and reagents to make this possible may be conveniently grouped into two different strategies, direct and indirect. This is an important principle, mentioned above with regard to the types of imaging probes available, and bears further reiteration here. The first strategy is a direct one that uses de novo synthesis of unique molecular probes targeted to a specific molecular marker(s)/target(s), such as a receptor, transporter, or enzyme. For each novel target, iterative modifications in the structure of existing compounds are made, or new compounds are obtained, to develop a molecular probe specific to that target. Additionally, for each such target, the sensitivity of detection and specificity of interaction, pharmacokinetics of delivery, and signal-to-noise ratio for its molecular probe must be characterized by appropriate in vitro and in vivo assays. The development and validation of these specific imaging agents is time-consuming and requires significant effort. It is therefore important to select carefully a molecular marker for which a novel specific imaging agent may require conception and creation.

The second general strategy to image specific molecular and cellular events is an indirect one entailing the use of a pretargeting molecule that is subsequently activated

upon occurrence of a specific molecular event. Following this, a molecular probe specific for the activated pretargeting molecule is used to image its activation. Reporter genes fall into this category and are described in greater detail below. Although initial development of a reporter system has similarities to the more direct de novo synthesis paradigm described above, the final result of this approach is to engineer a generalizable system that may be used to image many different biological processes with the same reporter probe and different pretargeting molecules. This is an attractive means of indirectly visualizing transcriptional and posttranscriptional regulation of gene expression, protein–protein interactions, or trafficking of proteins or cells in living subjects. The downside, however, is the necessity to introduce one or more foreign proteins/genes into a cell, and the delivery of the reporter gene may be a limitation of this strategy in intact animals. Conceptually, the latter is less of an issue in the context of gene therapy approaches or for molecular imaging of transgenic animals expressing the reporter gene. When adopting this strategy it is important to determine how accurately the reporter protein reproduces regulation and function of the corresponding endogenous pathway, thus proving that the reporter does not perturb the underlying biological process being examined (Luker 2002).

Having set the scene for how molecular and cellular functions can be interrogated in living subjects using molecular imaging strategies, what follows are some examples of specific applications in this field. This information (other than the subject of reporter gene imaging discussed in greater detail below) is presented in Table 2 and Figures 5–8, and although comprehensive, is by no means exhaustive because of space limitations. For ease of display and comprehension, these examples of imaging biological processes presented in Table 2 are considered in a spatially represented manner with respect to a cell, extending from those present outside the cell, to those on the cell surface, those in the cytosol, to those events taking place within the nucleus.

Reporter gene imaging

Intense exploration is taking place in the biological sciences to determine the patterns of gene expression that encode normal biological processes. There is also a growing belief that diseases result from alterations in normal regulation of gene expression that transition cells to phenotypes of disease (Phelps 2000b). These alterations in gene expression can result from interactions with the environment, hereditary deficits, developmental errors, and the aging process (Phelps 2000a). Imaging of gene expression in living subjects can be directed either at genes externally transferred into cells of organ systems (transgenes) or at endogenous genes. Most present applications of reporter gene imaging are of the former variety. By adopting state-of-the-art molecular biology techniques, it is now possible to better image cellular/molecular events. One can also engineer cells that will accumulate imaging probes of choice, either to act as generic gene "markers" for localizing and tracking these cells, or to target a specific biological process or pathway. In the last few years, there has been a veritable explosion in the field of reporter gene imaging, with the aim of determining location, duration, and extent of gene expression within living subjects (Bogdanov and Weissleder 1998; Gambhir et al. 1999b,c; Bremer and Weissleder 2001; Hogemann and Basilion 2002; Jacobs and Heiss 2002).

General features of reporter imaging systems

Reporter genes are used to study promoter/enhancer elements involved in gene expression, inducible promoters to look at the induction of gene expression, and endogenous gene expression through the use of transgenes containing endogenous promoters fused to the reporter (Gambhir 2000). In all these cases, transcription of the reporter gene can be tracked, and therefore gene expression can be studied. Unlike most conventional reporter gene methods (e.g., chloramphenicol acetyl transferase, LacZ/β-galactosidase, alkaline phosphatase, Bla/β-lactamase, etc.; Spergel et al. 2001), molecular imaging techniques offer the possibility of monitoring the location, magnitude, and persistence of reporter gene expression in intact living animals or humans. The reporter gene driven by a promoter of choice must first be introduced into the cells of interest. This is a common feature for all delivery vectors in a reporter gene-imaging paradigm; that is, a complementary DNA expression cassette (an imaging cassette) containing the reporter gene of interest must be used. The promoter can be constitutive or inducible; it can also be cell-specific. If the reporter gene is transcribed, an enzyme or receptor product is made, thus trapping the imaging reporter probe, which may be a substrate for an enzyme or a ligand for a receptor. The trapping of the probe leads to an imaging signal, be it from a radioisotope, a photochemical reaction, or a magnetic resonance metal cation, depending on the exact nature of the probe itself.

The ideal reporter gene/probe would have the following characteristics (Gambhir 2000): (1) To prevent an immune response, the reporter gene should be present in mammalian cells, but not expressed. (2) Specific reporter probe should accumulate only where reporter gene is expressed. (3) No reporter probe should accumulate when the reporter gene is not expressed. (4) The product of the reporter gene should also be nonimmunogenic. (5) The reporter probe should be stable in vivo and not be metabolized before reaching its target. (6) The reporter probe should rapidly clear from the circulation and not interfere with detection of specific signal. (7) The reporter probe or its metabolites should not be cytotoxic. (8) The size of the reporter gene and its driving promoter should be small enough to fit into a delivery vehicle (plasmids, viruses), except for transgenic applications. (9) Natural biological barriers must not prevent the reporter probe from reaching its destination. (10) The image signal should correlate well with levels of reporter gene mRNA and protein in vivo. No single reporter gene/re-

Table 2. *Examples of specific applications of molecular imaging in living subjects*

Molecular imaging application	Imaging modality used	Type of molecular probe used	Category of imaging strategy[a]	Reference[b]
Extracellular protease imaging				
Cathepsin B in artherosclerosis	fluorescence	smart NIR fluorochrome	indirect	Chen et al. 2002
Cathepsin B in breast cancer	fluorescence	smart NIR fluorochrome	indirect	Bremer et al. 2002
Cathepsin B in dysplastic intestinal adenomata	fluorescence	smart NIR fluorochrome	indirect	Marten et al. 2002
Cathepsin B and H in breast cancer	fluorescence	smart NIR fluorochrome	indirect	Mahmood et al. 1999
Cathepsin D in cancer	fluorescence	smart NIR fluorochrome	indirect	Tung et al. 1999
Cathepsin D in cancer	fluorescence	smart NIR fluorochrome	indirect	Tung et al. 2000
Thrombin	fluorescence	smart NIR fluorochrome	indirect	Tung et al. 2002
Matrix metalloproteinase-2 in cancer	fluorescence	smart NIR fluorochrome	indirect	Bremer et al. 2001b
Receptor/ligand imaging				
Neurotransmitters and neuroreceptors				
Dopaminergic system				
^{18}F-fluoro-DOPA	PET	radiolabeled ligand	direct	Cumming and Gjedde 1998
^{11}C-nomifensine	PET	radiolabeled ligand	direct	*Lucignani and Frost 2000
^{18}F-GBR13,119	PET	radiolabeled ligand	direct	*Lucignani and Frost 2000
^{11}C-cocaine	PET	radiolabeled ligand	direct	*Lucignani and Frost 2000
^{11}C-CFT	PET	radiolabeled ligand	direct	*Lucignani and Frost 2000
^{11}C-WIN35,428	PET	radiolabeled ligand	direct	*Lucignani and Frost 2000
^{123}I-β-CIT.WIN35,428	SPECT	radiolabeled ligand	direct	*Lucignani and Frost 2000
^{123}-I-β-CIT	SPECT	radiolabeled ligand	direct	*Lucignani and Frost 2000
^{11}C-*N*-methyl-spiperone	PET	radiolabeled ligand	direct	Wagner et al. 1983
^{11}C-raclopride	PET	radiolabeled ligand	direct	Volkow et al. 1993
^{18}F-haloperidol	PET	radiolabeled ligand	direct	Zanzonico et al. 1983
^{18}F-fluoro-ethyl-spiperone	PET	radiolabeled ligand	direct	Coenen et al. 1987
^{123}I-iodobenzamide	SPECT	radiolabeled ligand	direct	Kung et al. 1990
^{11}C-SCH 23,390	PET	radiolabeled ligand	direct	Halldin et al. 1991
^{11}C-SCH 39,166	PET	radiolabeled ligand	direct	Halldin et al. 1991
Serotoninergic system				
^{11}C-ketanserin	PET	radiolabeled ligand	direct	Berridge et al. 1983
^{18}F-setoperone	PET	radiolabeled ligand	direct	Crouzel et al. 1988
Central benzodiazepine binding sites				
^{11}C-flumazenil	PET	radiolabeled ligand	direct	Shinotoh et al. 1986
^{123}I-iomazenil	SPECT	radiolabeled ligand	direct	Dey et al. 1994
Cholinergic presynaptic function				
^{11}C-*N*-methyl-piperydinil-proprionate	PET	radiolabeled ligand	direct	Kuhl et al. 1996
Nicotinic receptor function				
^{11}C-labeled nicotine	PET	radiolabeled ligand	direct	Lucignani and Frost 2000
Muscarinic receptor function				
^{123}I-quinuclinidylbenzilate	SPECT	radiolabeled ligand	direct	Eckelman et al. 1984
^{11}C-tropanylbenzilate	PET	radiolabeled ligand	direct	Mulholland et al. 1995
^{11}C-Nmethyl-piperydil-benzilate	PET	radiolabeled ligand	direct	Mulholland et al. 1995
Opiate receptor function				
^{11}C-carfentanil	PET	radiolabeled ligand	direct	Frost et al. 1990
^{11}C-diprenorphine	PET	radiolabeled ligand	direct	Jones et al. 1988
^{11}C-methyl-naltrindole	PET	radiolabeled ligand	direct	Madar et al. 1996
Histamine receptor function				
^{11}C-pyrilamine	PET	radiolabeled ligand	direct	Villemagne et al. 1991
Mitochondrial enzyme monoamine oxidase B				
^{11}C-L-deprenyl	PET	radiolabeled ligand	direct	Fowler et al. 1993
Tumor receptors				
Somatostatin receptors				
^{111}In-octreotide	SPECT	radiolabeled ligand	direct	*Virgolini 2000
^{111}In-lanreotide	SPECT	radiolabeled ligand	direct	*Virgolini 2000
^{99m}Tc-vapreotide	SPECT	radiolabeled ligand	direct	*Virgolini 2000
Vasointestinal peptide receptors				
^{123}I-VIP	SPECT	radiolabeled ligand	direct	*Virgolini 2000
^{99m}Tc-VIP	SPECT	radiolabeled ligand	direct	*Virgolini 2000

Table 2 continued on next page

Table 2. *Continued*

Molecular imaging application	Imaging modality used	Type of molecular probe used	Category of imaging strategy[a]	Reference[b]
Antibody/antigen imaging				
Cancer antigens				
^{131}I-labeled anticarcinoembryonic (CEA) monoclonal antibodies	SPECT	radiolabeled antibody	direct	Oriuchi and Yang 2001
^{86}Y-labeled anti-Lewis Y monoclonal antibodies	SPECT	radiolabeled antibody	direct	Lovqvist et al. 2001
^{111}In-satumomab pendetide antiglycoprotein-72 (TAG-72) monoclonal antibodies	SPECT	radiolabeled antibody	direct	*Kim 2001
^{99m}Tc-labeled anti-CEA murine FAB′ fragment monoclonal antibodies	SPECT	radiolabeled antibody	direct	*Kim 2001
^{111}In-labeled capromab pendetide anticytoplasmic membrane-rich fraction of LNCaP (prostate cancer) cells monoclonal antibodies	SPECT	radiolabeled antibody	direct	*Kim 2001
^{99m}Tc-labeled nofetumomab merpentan anti-cell surface antigen murine Fab′ fragment of the pancarcinoma monoclonal antibodies	SPECT	radiolabeled antibody	direct	*Kim 2001
^{64}Cu, or ^{124}I-labeled anti-CEA monoclonal antibody fragments (diabodies/ minibodies see Fig. 5)	PET	radiolabeled antibody	direct	Wu et al. 2000
Monocrystalline iron oxide nanoparticles conjugated to L6 anticarcinoma monoclonal antibodies	MRI	MIONs + antibody	direct	Remsen et al. 1996
Neovascular antigens				
^{111}In-labeled anti-endoglin antibodies	SPECT	radiolabeled antibody	direct	Bredow et al. 2000
Endothelial proinflammatory antigens				
Monocrystalline iron oxide nanoparticles conjugated to anti-human E-selectin F(ab′)$_2$ fragments	MRI	MIONs + antibody	direct	Kang et al. 2002
Fibrin (thrombus antigens)				
Gadolinium-DTPA nanoparticles conjugated to MRI anti-fibrin F(ab′) fragments	MRI	Gd-DTPA + antibody	direct	Flacke et al. 2001
Imaging other cell membrane components				
Multidrug resistance transporters				
^{99m}Tc-tetrofosmin targeting multiple members of the ATP-binding-cassette superfamily of membrane transporters	SPECT	radiolabeled substrate	direct	Chen et al. 2000
^{67}Ga complexes targeting MDR1 P-glycoprotein	PET	radiolabeled substrate	direct	Sharma et al. 2000
^{99m}Tc-MIBI (sestamibi) targeting P-glycoprotein	SPECT	radiolabeled substrate	direct	Del Vecchio et al. 2000
Membrane phospholipids				
^{99m}Tc-labeled annexin V, which binds to phosphatidylserine in apoptosis	SPECT	radiolabeled protein	direct	Blankenberg et al. 1998
Monocrystalline iron oxide nanoparticles conjugated to the first C_2 domain of synaptotagmin I, which binds to phosphatidylserine in apoptosis	MRI	MION + protein	direct	Zhao et al. 2001
Imaging intracellular proteins and receptors				
Intracellular enzymes or enzyme inhibitors				
^{18}F-2-fluoro-2-deoxyglucose [^{18}F-FDG] phosphorylation by hexokinase	PET	radiolabeled substrate	direct	Gambhir 2002
^{11}C-*N,N*-dimethylphenylethylamine (^{11}C-DMPEA) deamination by monoamine oxidase	PET	radiolabeled substrate	direct	Shinotoh et al. 1987
^{18}F-fluorothymidine targeting mammalian thymidine kinase and DNA replication	PET	radiolabeled thymidine analog	direct	Shields et al. 1998
^{18}F-SC63217 and ^{18}F-SC58125 inhibition of cyclo-oxygenases COX-1 and COX-2	PET	radiolabeled enzyme inhibitors	direct	McCarthy et al. 2002

Table 2 continued on next page

Table 2. *Continued*

Molecular imaging application	Imaging modality used	Type of molecular probe used	Category of imaging strategy[a]	Reference[b]
Intracellular receptors				
^{18}F-labeled estrogen analogs and androgen receptors	PET	radiolabeled hormone analogs	direct	Downer et al. 2001
Imaging reporter genes				
See text				
Imaging messenger RNA				
^{111}In-labeled oligodeoxynucleotides antisense to the amplified c-*myc* oncogene	SPECT	radiolabeled oligodeoxynucleotides	direct	Dewanjee et al. 1994

[a]For definition of category of imaging strategy, please see text.
[b]References marked with an asterisk are review articles with reference to this subject.

porter probe system meets all these criteria at present. Therefore, the development of multiple systems provides a choice based on the application of interest. The availability of multiple reporter gene/reporter probes also allows monitoring the expression of more than one reporter gene in the same living animal. Ray et al. (2001) have reviewed the many examples of these imaging reporter systems.

Categories of reporter imaging systems

A broad classification of reporter systems consists of those in which the gene product is intracellular (Fig. 6A,B), or is associated with the cell membrane (Fig. 6C,D). Examples of intracellular reporters include thymidine kinase, GFP, luciferase (Benaron et al. 1997; Contag et al. 1997), cytosine deaminase, and tyrosinase (Weissleder et al. 1997b), to name a few. Examples of reporters on or in the cell surface in the form of receptors include the dopamine 2 receptor (D2R) and receptors for somatostatin, transferrin (Moore et al. 1998; Hogemann et al. 2000), or the sodium iodide symporter (Boland et al. 2000; Haberkorn et al. 2001; Shen et al. 2001; Cho et al. 2002). Bogdanov et al. (2000) have also constructed fusion proteins that act as "artificial receptors," consisting of a binding domain such as a peptide-based chelator that binds ^{99m}Tc oxotechnetate and a membrane-anchoring domain. A variety of fusion proteins have been tested, and this approach may evolve into a useful strategy to "tag" transfected cells with ^{99m}Tc, thus assessing efficiency of gene delivery and expression. The major advantages of intracellular protein expression are the relatively uncomplicated expression strategy and lack of recognition of the expression product by the immune system. The major advantages of surface-expressed receptors and acceptors are favorable kinetics (sometimes avoiding the need for the tracer to penetrate into a cell) and the fact that synthetic reporters can be engineered to recognize already approved imaging drugs (Weissleder and Mahmood 2001).

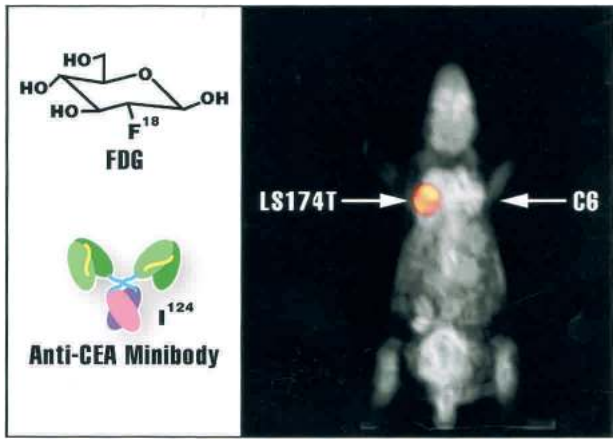

Figure 5. Direct imaging of carcinoembryonic antigen (CEA) in a living mouse using FDG and anti-CEA ^{124}I minibody. MicroPET imaging of a mouse 1 h after tail-vein injection of FDG (gray scale) superimposed on microPET imaging of the same mouse imaged 18 h after injection of an ^{124}I-labeled minibody (color scale) targeted against CEA. The mouse carries two tumor xenografts: a C6 rat glioma as a negative control and an LS174T line that expresses CEA. The minibody signal is seen almost exclusively from the LS174T tumor only, because most background activity has already cleared 18 h after tracer injection. Reproduced with permission from Gambhir (2002). Note the actual size of the FDG molecule is much smaller than anti-CEA minibody.

A well-studied isotope-based imaging reporter gene/reporter probe system is the reporter probe ^{18}F-fluoropenciclovir (^{18}F-FPCV) for the herpes simplex virus type 1 thymidine kinase (HSV1-TK) enzyme, adapted for PET imaging (Iyer et al. 2001a), and first developed in 1996 using ^{131}I-labeled 2′fluoro-2′-deoxy-1-β-D-arabinofuranosyl-5-iodo-uracil (FIAU) for SPECT imaging (Tjuvajev et al. 1996). Two main categories of substrates, uracil nucleoside derivatives labeled with radioactive iodine (e.g., FIAU; Tjuvajev et al. 1995) and acycloguanosine derivatives labeled with radioactive ^{18}F-fluorine (e.g., ^{18}F-FPCV, ^{18}F-FHBG), have been investigated in the last few years as reporter probes for imaging *HSV1-tk* reporter gene expression (Namavari et al. 2000). These radiolabeled reporter probes are transported into cells, and

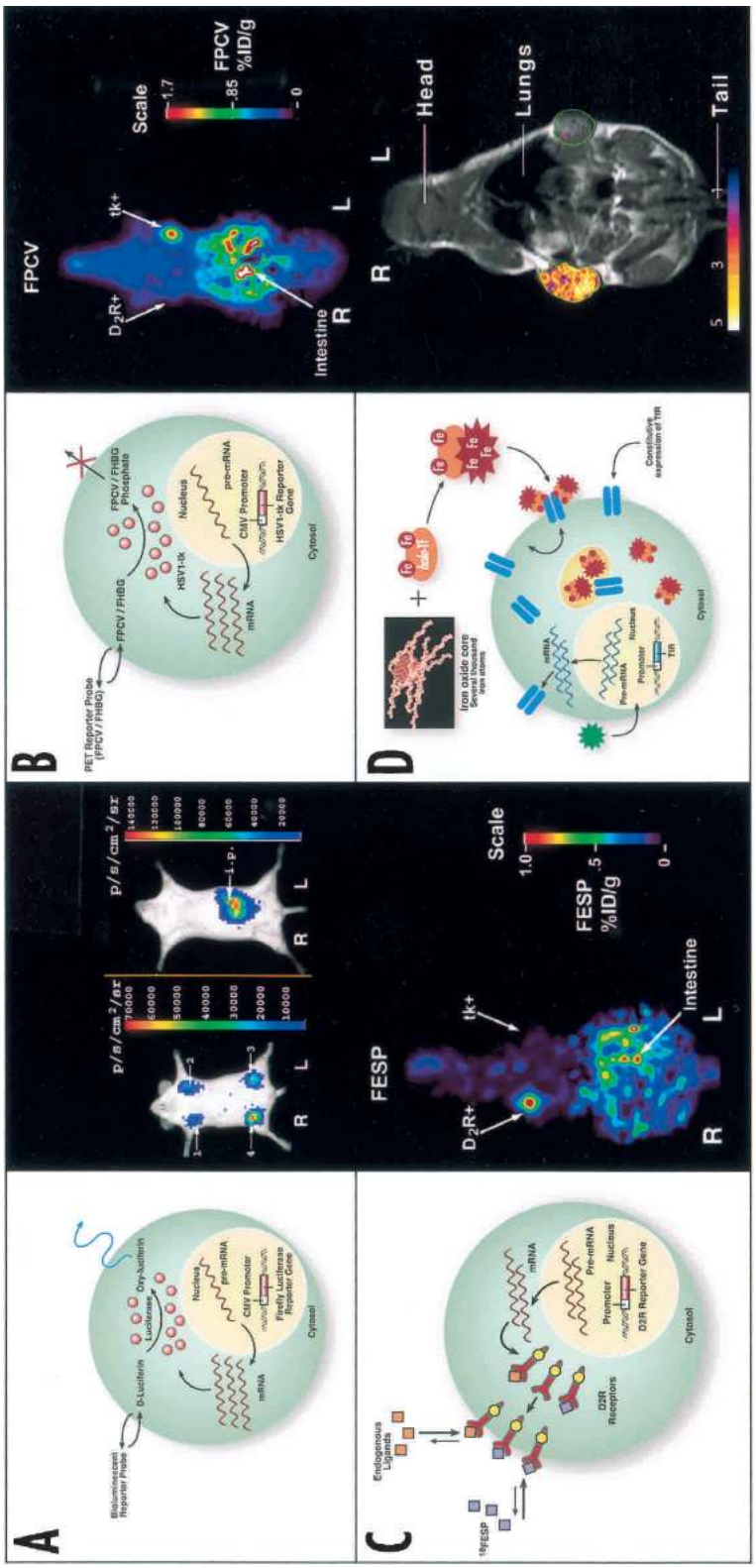

Figure 6. Four different types of imaging reporter gene/probe strategies. (*A*) Enzyme-based bioluminescence imaging. D-Luciferin is a substrate molecular probe that is acted upon by the enzyme Firefly luciferase to result in bioluminescence via a chemiluminescent reaction under physiological conditions only within living cells expressing the *Fluc* gene. Light photons may be detected, collected, and quantified externally. Images show examples of mice implanted with subcutaneous xenograft tumors expressing *Fluc* (*left* mouse) or intraperitoneal tumor cells expressing *Fluc* (*right* mouse) after administration of D-luciferin (either IV or IP). Color images of visible light are superimposed on photographic images of mice with a scale in photons per second per square centimeter per steradian (sr). (*B*) Enzyme-based PET imaging. ^{18}F-Fluoropenciclovir (^{18}F-FPCV) or other acycloguanosines are substrate molecular probes phosphorylated by the herpes simplex virus type 1 thymidine kinase (HSV1-TK) enzyme to result in intracellular trapping of the probe in cells expressing the *HSV1-tk* gene. Images of the same mouse are shown in *B* and *C*. The images show two reporter genes (*HSV1-tk* and *D2R*) in the same mouse and imaged with two different reporter probes (^{18}F-FPCV for HSV1-TK and ^{18}F-FESP for D2R). These images show specific accumulation of probes in a mouse carrying a tumor stably expressing *HSV1-tk* on the left shoulder and a separate tumor stably expressing *D2R* on the right shoulder. The accumulation of ^{18}F-FPCV and ^{18}F-FESP in each tumor reflects trapping caused by *HSV1-tk* and *D2R* expression, respectively. The color scale (%ID/g) indicates the percentage of injected dose that accumulates per gram of tumor. Nonspecific activity in the intestines is caused by hepato-biliary excretion of each molecular probe. Reproduced with permission from Iyer et al. (2001a). (*C*) Receptor-based PET imaging. ^{18}F-FESP is a ligand molecular probe interacting with the dopamine-2-receptor (D2R) to result in trapping of the probe on/in cells expressing the *D2R* gene. Images of the same mouse are shown in *B* and *C*. This image was taken a day after that shown in *B* to allow for decay of ^{18}F. The color scale (%ID/g) indicates the percentage of injected dose that accumulates per gram of tumor. Nonspecific activity in the intestines is caused by hepato-biliary excretion of molecular probes. (*D*) Receptor-based MRI imaging. Overexpression of engineered transferrin receptors (TfR) results in ~500% more cell uptake of the transferrin-monocrystalline iron oxide nanparticle (Tf-MION) probes per hour than would occur otherwise. During each internalization event, several thousand iron atoms (rather than just 2 atoms in holo-transferrin, holo-Tf) accumulate in the cytosol and within endosomes. Also, the cellular internalization of iron does not down-regulate the level of receptor overexpression. These changes result in a detectable contrast change on MRI. The image shows coronal MRI in a living mouse with a right TfR$^+$ flank tumor and a left TfR$^-$ flank tumor. The image is a coregistered color-mapped one of a T1-weighted spin echo image obtained for anatomical detail with superimposed gradient-echo image after Tf-MION administration, showing the increased uptake of iron in the right TfR$^+$ tumor. The color scale is an arbitrary one with relative units, in which white/yellow indicates the highest uptake and blue the lowest. Reproduced with permission from Weissleder et al. (2000).

are trapped as a result of phosphorylation by HSV1-TK. When used in nonpharmacological tracer doses, these substrates can serve as PET or SPECT targeted reporter probes by their accumulation in just the cells expressing the *HSV1-tk* gene. More recently, a mutant version of this gene, *HSV1-sr39tk*, was derived using site-directed mutagenesis to obtain an enzyme more effective at phosphorylating ganciclovir (and also less efficient at phosphorylating thymidine) with consequent gain in imaging signal (Gambhir et al. 2000a).

The *D2R* reporter gene has also been validated for PET imaging of reporter gene expression while using ^{18}F-fluoroethylspiperone (FESP) as the reporter probe ligand (MacLaren et al. 1999). More recently, a mutant D2R that uncouples signal transduction while maintaining affinity for FESP has also been reported (Liang et al. 2001).

Two general types of reporter systems are applicable to MRI-based molecular imaging, and have been reviewed by Louie et al. (2002). One imaging system relies on molecular probes that are sensitive to the activity of β-galactosidase, the product of the classic marker gene *LacZ*. The synthesis of a molecular probe in which gadolinium is protected by a carbohydrate "cap" that is β-galactosidase-cleavable would result in a probe with variable water access. This would provide a molecular probe of variable relaxivity because the interaction between water protons and paramagnetic metal centers of probes results in signal enhancement on T1-weighted images. If an external physiological process regulates water access, then the probe would be a reporter of the physiological process itself. Using the *Xenopus* embryo, Louie et al. (2000) have demonstrated the ability of these probes and MRI to detect gene expression in living subjects. Unfortunately, present enzyme-cleavable probes do not freely cross cell membranes (thus requiring direct intracellular injection), and the kinetics of cleavage are quite slow. However, these probes are useful for specific applications in tissues that are amenable to direct injection, for example, in developmental biology research.

An alternative to this conditional reporter probe is to couple MRI probes to targeting moieties. Weissleder et al. (2000) have highlighted the use of the transferrin receptor as a potential intracellular transporter of iron oxide nanoparticles (Fig. 6D). The transferrin receptor is found in most cells and is part of the iron regulatory system. The receptor binds to transferrin, an iron-carrying protein, and transports it into the cell. Normal expression of the receptor is under feedback regulation to prevent excessive cellular iron uptake. However, cells can be engineered to overexpress transferrin and, therefore, accumulate monocrystalline iron oxide nanoparticles intracellulary. This increased iron content results in differential MRI signal from these cells on a type of T2-weighted images called gradient-echo images, which are particularly sensitive to the presence of paramagnetic ions. Additional studies are required to assess this system further, including measurement of the effect of overexpressing the receptor on normal cellular function, and how well normal systems tolerate increased levels of freely circulating and intracellular iron.

Four broad categories of applications for reporter gene imaging are as follows: gene marking of cells with imaging genes, imaging of gene therapies, imaging of transgenic animals, and imaging of molecular interactions such as protein–protein interactions (Figs. 7, 8).

Applications of reporter gene imaging: gene marking of cells

Gene marking may be used to track the in vivo behavior of almost any tissue (Brenner 1996). It is necessary to stably transfect cells with the imaging marker gene if they and their progeny are to be followed for their entire lifespan within the living subject. In practice, however, transient transfection of cells suffices if these marked cells are to be imaged in a living subject for no more than ~7–10 d, depending on the cells in question and other parameters as well. In principle, gene marker studies may be used to follow the behavior of almost any cell type in living subjects. In clinical practice, this has been mostly used with hematopoietic cells (Brenner 1996). However, in molecular imaging research, a variety of cells have been engineered to incorporate reporter genes. Usually, gene marking of cells that are static in one location, for example, subcutaneous tumor xenografts, is used for first assessment and continued validation of reporter genes and their probes, or for studying the behavior of the cells themselves within living subjects. This can be accomplished in two ways: one is ex vivo transfection of the cells in question with a vector containing an imaging cassette, followed by placement of these cells in a living subject as a xenograft or an orthotopic transplant. The second approach entails direct in vivo placement, usually via injection, of the vectors carrying the reporter gene as part of the recombinant genome of viruses, into the cells of interest within the body.

There are numerous examples of molecular imaging of cells that are mostly destined to remain static in the body, after their ex vivo gene marking with imaging reporters and subsequent placement in living rodents (Fig. 7A,B). Examples of radionuclide applications include the assessment by Iyer et al. (2001a) of the *HSV1-tk* reporter gene system, which showed ^{18}F-fluoropenciclovir to be an improved probe over ^{18}F-fluoroganciclovir for microPET imaging in C6 cell mouse xenografts, and other studies of the human somatostatin receptor subtype 2 in ovarian cancer cell xenografts of immunodeficient mice (Hemminki et al. 2002; Zinn and Chaudhuri 2002). Weissleder et al. (2000) and Moore et al. (2001) have also assessed the transferrin receptor as an MRI reporter in rat gliosarcoma 9L cell xenografts (Fig. 6D). Other studies in which gene-marked xenografts were used in evaluation of optical imaging reporters include those of Bhaumik and Gambhir (2002) for Renilla luciferase, and those of Edinger et al. (1999) and Sweeney et al. (1999) for Firefly luciferase. Orthotopic mouse brain implants of rat 9L gliosarcoma cells gene-marked with *Fluc* have also been attempted (Rehemtulla et al. 2000), as well as orthotopic implantation of *Fluc*-marked human prostate cells into the prostate glands of mice (Honigman et al. 2001). Ex-

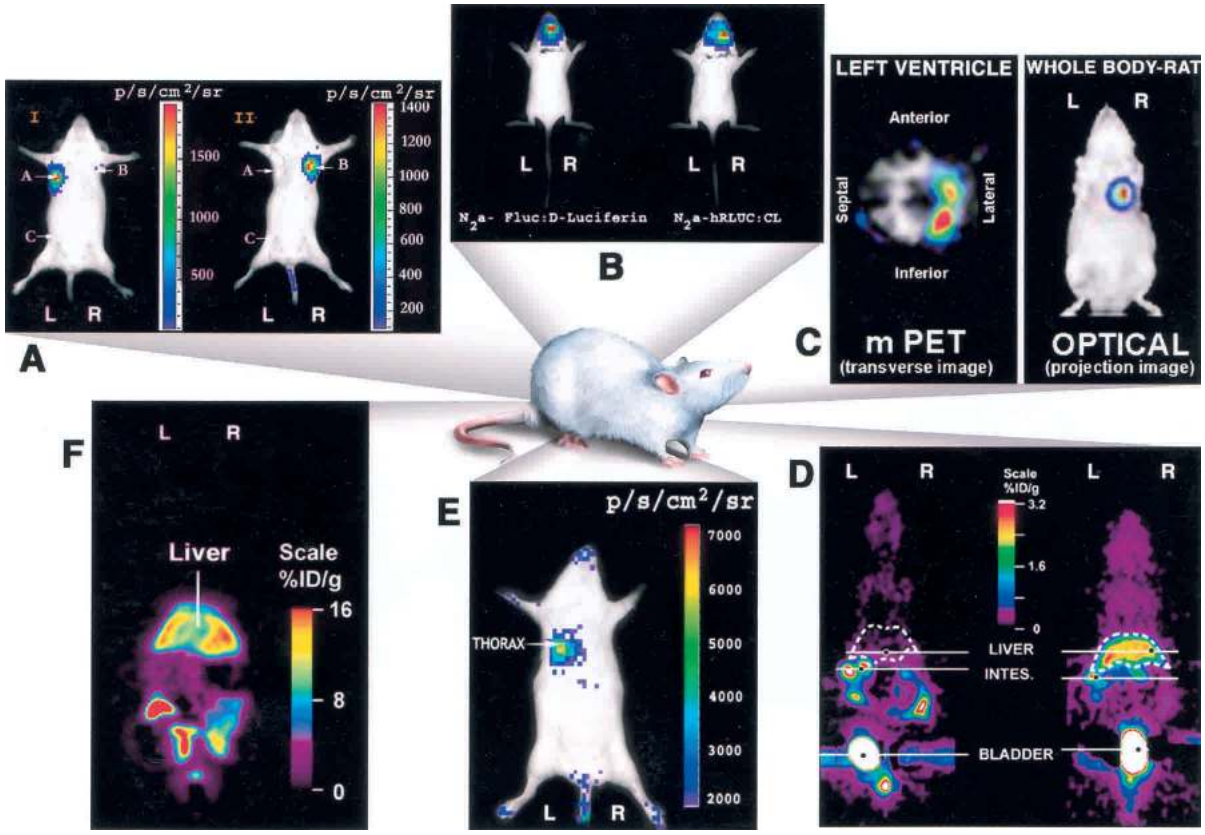

Figure 7. Different applications of imaging reporter gene/probe systems in small animals. (*A*) Bioluminescence imaging of subcutaneous tumor xenografts (in both shoulder regions). C6 cells expressing Firefly luciferase (A), C6 cells expressing Renilla luciferase (B), and control C6 cells (C). Injection of D-luciferin via tail-vein in the *left* mouse shows bioluminescence from site A and minimal signal from B and C. Injection of coelenterazine via tail-vein in the *right* mouse produces bioluminescence from site B but minimal signal from sites A or C. Reproduced with permission from Bhaumik and Gambhir (2002). (*B*) Bioluminescence imaging of N2a cells expressing Firefly luciferase or Renilla luciferase orthotopically implanted in brains of living mice. Images were obtained after tail-vein injection of the substrates D-luciferin and coelenterazine, respectively. (*C*) PET and bioluminescence imaging after direct intramyocardial injection of adenoviral vectors carrying the *HSV1-tk* or *Fluc* genes. The figure on the *right* shows a projection bioluminescence image of the mouse with light emanating from the heart. The figure on the *left* shows microPET transverse cross-sectional imaging through the heart after tail-vein injection of ^{13}N-ammonia (gray scale) superimposed on microPET imaging of the same mouse imaged later after injection ^{18}F-FHBG for *HSV1-tk* (color scale; see Wu et al. 2002a,b). (*D*) Trafficking of adenovirus carrying the *HSV1-tk* gene to the liver. Swiss-Webster mice were injected via the tail vein with 1.5×10^9 PFU of control virus (*left* mouse) or 1.5×10^9 PFU of AdCMV-HSV1-TK virus (*right* mouse). For each mouse, a whole-body mean coronal projection image of the fluorine-18 activity distribution is displayed. The liver outline is in white. The color scale represents the FGCV %ID/g. Reproduced with permission from Gambhir et al. (1999c). (*E*) Trafficking to the lungs of C6 rat glioma cells transiently expressing Renilla luciferase. Reproduced with permission from Bhaumik and Gambhir (2002). (*F*) Imaging endogenous albumin gene expression in the liver of transgenic mice with the *HSV1-tk* reporter gene driven by the albumin promoter. Nonspecific activity in the intestines is caused by hepato-biliary excretion of molecular probes. Reproduced with permission from Green et al. (2002).

amples of nonneoplastic cells that have been used in this way include myoblasts gene-marked with *Fluc* and injected directly into rat myocardium (Koransky et al. 2001), and several *Fluc*-gene-marked bacterial strains used for evaluation of mouse infection models (Francis et al. 2000, 2001; Burns et al. 2001; Rocchetta et al. 2001; Hamblin et al. 2002). Examples in which viral vectors containing the imaging reporter gene were placed directly into the living subject include *HSV1-tk* or *HSV1-sr39tk* vector injected into subcutaneous tumor xenografts (Tjuvajev et al. 1996, 1998, 1999a; Blasberg and Tjuvajev 1999; Bennett et al. 2001) or into the myocardium (Fig. 7C; Wu et al. 2002b) and *Fluc* vectors injected directly into thigh muscles of mice (Wu et al. 2001) or into the myocardium of rats (Fig. 7C; Wu et al. 2002a).

In vivo imaging of cell trafficking is presently performed in clinical practice (e.g., using ^{111}In-oxine for SPECT imaging of infection and inflammation; Becker and Meller 2001) and is the objective of many immunological and oncological studies. Several cell-trafficking approaches have been developed for MRI (Dodd et al. 2001) and PET imaging, including the ex vivo labeling of cells with ^{18}F-FDG, $^{11}CH_3I$, and recently studied ^{64}Cu-pyruvaldehyde-bis(N^4-methylthiosemicarbazone) (^{64}Cu-PTSM; Adonai et al. 2002). Gene marking may also be used to study trafficking of cells (Fig. 7E) or viral vectors

(Fig. 7D) in living subjects. For instance, Le et al. (2002) assessed the role of the BCR-ABL oncogene in lymphoid leukemogenesis using bone marrow cells gene-marked with *HSV1-tk*. $CD4^+$ T cells marked with *Fluc* have been used in an adoptive immunotherapy protocol whereby lymphocytes deliver a cytokine antagonist to the brains of mice with experimental autoimmune encephalomyelitis (Costa et al. 2001; Hardy et al. 2001). $CD4^+$ T cells marked with *Fluc* were also used as vehicles to deliver an immunoregulatory protein for treatment of collagen-induced arthritis in a mouse model of rheumatoid arthritis (Nakajima et al. 2001). Tjuvajev et al. (2001) used engineered nonvirulent *Salmonella* bacteria marked with *HSV1-tk* when studying their role as tumor-specific agents for tumor therapy; and found that these genetically engineered bacteria accumulated 30-fold higher in tumors than in muscle. *Salmonella* marked with *Fluc* has also been used to understand the systemic spread of pathogens and to monitor their antibiotic therapy (Contag et al. 1995). Recently, cancer cells marked with *Fluc* and injected into the left ventricle have helped in the study of micrometastatic spread to bone marrow (Wetterwald et al. 2002).

The trafficking of a viral vector itself carrying the imaging cassette can also be monitored to some extent after intravenous injection. In these approaches, it is usually only possible to image sites of viral infectivity and delivery of the imaging gene, although studies are underway at present in which labeling the virus itself provides information on its true trafficking after delivery. When replication-deficient adenovirus expressing the *HSV1-tk* or the *D2R* PET reporter genes is injected into mice, the great majority (>95%) home to and infect the liver owing to the presence of the coxsackie-adenovirus receptors on hepatocytes (Gambhir et al. 1998, 1999c, 2000a; MacLaren et al. 1998). Administration of radiolabeled reporter probes for these genes shows accumulation of PET signal only in the livers expressing *HSV1-tk* or *D2R*. Honigman et al. (2001) have performed similar systemic tracking of viral particles carrying the *Fluc* gene in BALB/c mice. In a different application, recombinant adeno-associated viruses carrying the *Fluc* gene were delivered in utero to the peritoneum of mouse fetuses. Tracking of the reporter gene expression in the neonates was shown to provide a sensitive whole-body assay useful for marking tissues for subsequent analysis when considering in utero gene transfer therapies to ameliorate genetic diseases with perinatal morbidity (Lipshutz et al. 2001).

Applications of reporter gene imaging: imaging of gene therapies

Although various methods of gene therapy have met with limited success, it is probable that eventually many diseases will be successfully treated with the delivery of one or more transgenes to target tissue(s). A concern in applying gene therapy is achievement of controlled and effective delivery of genes to target cells and avoidance of ectopic expression. Molecular imaging of reporters on particular therapeutic genes could be critical in optimizing gene therapy. The aim of these approaches is to quantitatively image reporter gene expression, and from this to infer levels, location, and duration of therapeutic gene expression (Gambhir et al. 2000b; MacLaren et al. 2000; Weissleder et al. 2000; Wunderbaldinger et al. 2000; Allport and Weissleder 2001; Berger and Gambhir 2001; Nichol and Kim 2001; Vries et al. 2002). There are several strategies to achieve linkage of expression of the therapeutic transgene and the imaging reporter gene (Ray et al. 2001; Sundaresan and Gambhir 2002). A fusion approach can be used in which two or more different genes are joined in such a way that their coding sequences are in the same reading frame, and thus a single protein with properties of both the original proteins is produced. This approach has been validated with fusion reporters such as HSV1TK-GFP (Jacobs et al. 1999; Doubrovin et al. 2001; Ponomarev et al. 2001), DHFR- HSV1TK (Banerjee et al. 2002; Mayer-Kuckuk et al. 2002), HSV1TK-LacZ (Jacobs et al. 2001), and DHFR-GFP (Banerjee et al. 2002). Another approach is to insert an internal ribosomal entry site (IRES) sequence between the two genes so that they are transcribed into a single mRNA from the same promoter but translated into two separate proteins. Yu et al. (2000) and Liang et al. (2002a) have recently reported on such a bicistronic vector, in which both *D2R* and *HSV1-sr39tk* genes were coexpressed from a common promoter with the aid of an encephalomyocarditis virus IRES and were imaged by microPET in multiple, stably transfected tumors in living mice. Similarly, *LacZ* and *HSV1-tk* genes were coexpressed in mice and imaged with SPECT (Tjuvajev et al. 1999b). A third approach uses two different genes expressed from distinct promoters within a single vector. A fourth approach entails coadministering both genes cloned in two different vectors but driven by the same promoter type (Yaghoubi et al. 2001).

Examples in which the molecular imaging approach was used in experimental gene therapy protocols include a recent study investigating the effect of HSV1-TK enzyme active-site variants on suicide gene therapy of prostate cancer cell xenografts (gene marked with *GFP*) in SCID mice (Pantuck et al. 2002). Another study by Weng et al. (2000) aimed at somatic cell gene transfer of the heme oxygenase-1 (*HO-1*) gene to the lung alveoli of neonatal mice via transpulmonary injection. The transgene was linked to *Fluc* for real-time monitoring of its gene expression. It was found that the transpulmonary approach might prove useful in targeting gene expression to cells of the alveolar epithelium or to circumscribed areas of the lung. Hemminki et al. (2002) have also used the somatostatin receptor subtype 2 reporter gene to image gene therapy in a mouse model of ovarian cancer, in which cancer cells were engineered to bypass their dependence on coxsackie-adenovirus receptors for infectivity, and thus, improve their transduction efficiency by adenoviral vectors. A recent study used the *HSV1-tk* gene marker to monitor for the first time the replication and spread of replication-conditional HSV-1 vector in tumor xenografts (Jacobs et al. 2001). Tumor areas of ^{124}I-FIAU-derived radioactivity identified viable parts of infected tumor tissue. In addition to providing further in-

sights into cancer biology, potential clinical applications of this include the ability to image the location, spread, and persistence of the viral vector in patients undergoing gene therapy.

Applications of reporter gene imaging: imaging of transgenic animals

The merits of molecular imaging of transgenic animals have been outlined above. To date, several research groups have used this in their assessment of transgenic mice. Green at al. (2002) have repetitively imaged endogenous albumin gene expression in transgenic mice with the *HSV1-tk* reporter gene driven by the albumin promoter (Fig. 7F). This demonstrated that the *HSV1-tk* gene could be used to monitor the modulated expression of transgenes in living animals. Most other examples to date have used bioluminescence imaging to monitor transgenic mice. To identify regions of the lactase gene involved in mediating its spatiotemporal expression pattern in the proximal and middle small intestine of developing transgenic mice, different fragments of this gene were cloned upstream of the *Fluc* reporter gene (Lee et al. 2002). It was found that a distinct 5′-region of the lactase promoter directed intestine-specific expression of the lactase gene and that bioluminescence imaging can be used for assessment of this intestinal expression. Two other examples by the same group (Zhang et al. 2001) consisted of transgenic approaches to study the mechanisms controlling bone morphogenetic protein 4 (Bmp4) expression during primordial and mature tissue development (Zhang et al. 2002a), and to study the effects of metalloporphyrins on the transcription of the *HO-1* gene in an attempt to target production of neonatal bilirubin. Carlsen et al. (2002) have developed transgenic mice that express *Fluc* under the control of the nuclear factor κB (NF-κB) promoter, enabling real-time imaging of NF-κB activity and its modulation in living mice. Another recent example by Vooijs et al. (2002) involved the use of a conditional mouse model for retinoblastoma suppressor gene-dependent pituitary cancer development with co-expression of the *Fluc* gene, enabling long-term bioluminescence imaging, quantification of tumor burden, and assessment of chemotherapeutic response.

The potential to monitor/image the pharmacologic induction of gene expression in transgenic animals and to image time-dependent variation of gene expression from vectors with inducible promoters has been established by Sun et al. (2001). They described a bidirectional, tetracycline-inducible system that can be used to pharmacologically induce target gene expression and to quantitatively image induced expression by using a PET reporter gene. They demonstrated the potential of this system in transient and stable cell transfection assays by repetitive and quantitative imaging of tetracycline and tetracycline-analog induction of gene expression in living animals. They used the *D2R* and the *HSV1-sr39tk* reporter genes to validate this system and found a high correlation ($r^2 = 0.98$) between "target" and reporter gene expression. Weng et al. (2000) have used a similar approach for modulating expression of the *HO-1* and *Fluc* genes in a gene therapy model targeting the alveolar epithelium.

Applications of reporter gene imaging: imaging of molecular interactions

Some interesting variations on standard reporter gene assays described above have also been adapted recently for imaging of molecular interactions in living subjects. A two-step transcriptional amplification (TSTA) method for imaging gene expression using weak promoters (i.e., most tissue-specific ones) has been described by Iyer et al. (2001b) and in a follow-up study by Zhang et al. (2002b). The TSTA system was used to amplify expression of *Fluc* and *HSV1-sr39tk* in a prostate cancer cell line using a duplicated variant of the prostate specific antigen gene enhancer to express GAL4 derivatives fused to one, two, or four VP16 activation domains. The resulting activators were targeted to cells with reporter templates bearing one, two, or five GAL4-binding sites upstream of the reporter gene. It was found, for example, that the expression of *Fluc* could be varied over an 800-fold range. A similar approach for tumor-specific transcriptional targeting of suicide gene therapy by Qiao et al. (2002) used a recombinant adenovirus containing a binary promoter system with a tumor-specific promoter (CEA) driving a transcription transactivator, which then activates a minimal promoter to express an *HSV1-tk* suicide gene. It remains to be determined when these approaches are adapted for amplifying endogenous promoters in transgenic models if use of the TSTA system could have any undesirable toxicity.

To image protein–protein interactions in living mice, Ray et al. (2002) have used the well-studied yeast two-hybrid system adapted for mammalian cells and modified it to be inducible (Fig. 8A). They used the *NF-κB* promoter to drive expression of two fusion proteins (VP16-MyoD and GAL4-Id), and modulated the *NF-κB* promoter through TNF-α. *Fluc* reporter gene expression was driven by the interaction of MyoD and Id through a transcriptional activation strategy. They demonstrated the ability to detect this induced protein–protein interaction in cell culture and image it in living mice by using transiently transfected cells. A similar strategy by Luker et al. (2002) involved interactions between the p53 tumor suppressor and the large T antigen of simian virus 40. This initiated the visualization of tumor xenografts of HeLa cells stably transfected with the imaging constructs. More recently, Paulmurugan et al. (2002) have also validated the use of split reporter technology to show that both complementation and intein-mediated reconstitution of Firefly luciferase can be used to also image protein–protein interactions in living mice (Fig. 9). This approach has the advantage of potentially imaging interactions anywhere in the cell, whereas the yeast two-hybrid approaches are limited to interactions in the nucleus. Imaging interacting protein partners in living subjects could pave the way to functional proteomics in whole animals and provide a tool for evaluation of new

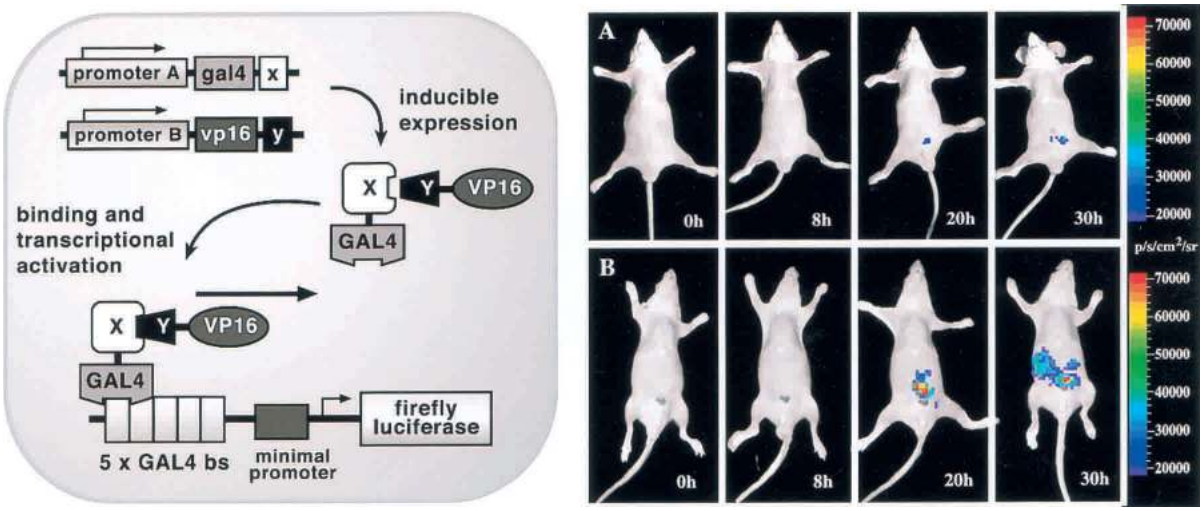

Figure 8. Imaging protein–protein interactions in living mice. (*Left*) Schematic diagram of the system for imaging the interaction of proteins X and Y. The first step involves the vectors pA-gal4-x and pB-vp16-y, which are used to drive transcription of *gal4-x* and *vp16-y* through use of promoters A and B. In the second step, the two fusion proteins GAL4-X and VP16-Y interact because of the specificity of protein X for protein Y. Subsequently, GAL4-X-Y-VP16 binds to GAL4-binding sites [five GAL4-binding sites (bs) are available] on a reporter template. This leads to VP16-mediated transactivation of Firefly luciferase reporter gene expression under the control of GAL4 response elements in a minimal promoter. Transcription of the Firefly luciferase reporter gene leads to Firefly luciferase protein, which, in turn, leads to a detectable visible light signal in the presence of the appropriate substrate (D-luciferin), ATP, Mg^{2+}, and oxygen. The NF-κB promoter was used for either pA or pB and TNF-α-mediated induction. (*Right*) In vivo optical CCD imaging of mice carrying transiently transfected 293T cells for induction of the yeast two-hybrid system. All images shown are the visible light image superimposed on the optical CCD bioluminescence image with a scale in photons per second per square centimeter per steradian. The mice in the *top* row (*A*) were imaged after injection of D-luciferin but with no TNF-α-mediated induction. The mice in the *bottom* row (*B*) were imaged after injection of D-luciferin after TNF-α-mediated induction, showing a marked gain in signal from the peritoneum over 30 h. For further details, please see Ray et al. (2002). Reproduced with permission from Ray et al. (2002).

pharmaceuticals targeted to modulate protein–protein interactions.

Several recent studies have successfully validated methods to indirectly monitor endogenous gene expression by reporter gene imaging in living subjects. Green et al. (2002) have measured correlated changes in the albumin gene (*alb*) and *HSV1-tk* expression in transgenic mice with the reporter gene driven by the *alb* promoter. A reduced protein diet was used to down-regulate *alb* expression. It was found that endogenous gene expression of albumin could be indirectly imaged using this approach. Doubrovin et al. (2001) developed and assessed a similar method for monitoring the transcriptional activation of endogenous genes. The *HSV1-tk/GFP (TKGFP)* dual reporter gene was used to monitor transcriptional activation of p53-dependent genes. They demonstrated that DNA-damage-induced up-regulation of *p53* transcriptional activity correlated with the expression of p53-dependent downstream genes, such as *p21*. PET imaging was sufficiently sensitive to image the transcriptional regulation of genes in the p53 signal transduction pathway. Ponomarev et al. (2001) used the same fusion reporter in the development and assessment of a novel method for monitoring the T-cell receptor (TCR)-dependent nuclear factor of activated T cells (NFAT)-mediated activation of T cells. The fusion reporter was used to monitor NFAT-mediated transcriptional activation in human Jurkat cells, and the NFAT-TKGFP reporter system was sufficiently sensitive to detect T-cell activation in vivo. PET imaging of TCR-induced NFAT-dependent transcriptional activity could be useful in the assessment of T-cell responses, T-cell-based adoptive therapies, vaccination strategies, and immunosuppressive drugs.

An important likely future possibility is the ability to image multiple molecular events in one population of cells. This may be attainable by combining two or more of the above-described strategies for gene marking and imaging the trafficking of cells with those entailing linked expression of an imaging gene to an endogenous promoter, or to an exogenous therapeutic gene. As such, in these experiments it is foreseeable that one reporter may reveal the spatial distribution of cells and whether they have reached a specific target, and another reporter may indicate whether a certain gene becomes up-regulated at this site or if a more complex interaction occurs. Efforts are underway to demonstrate the feasibility of this concept of simultaneous multiplexing of molecular imaging strategies, with a view to a better understanding the complexities of molecular pathways and networks.

Future outlook

Present advancements in molecular imaging appear analogous to recent development of methods to visualize gene expression by hybridization to arrays of DNA car-

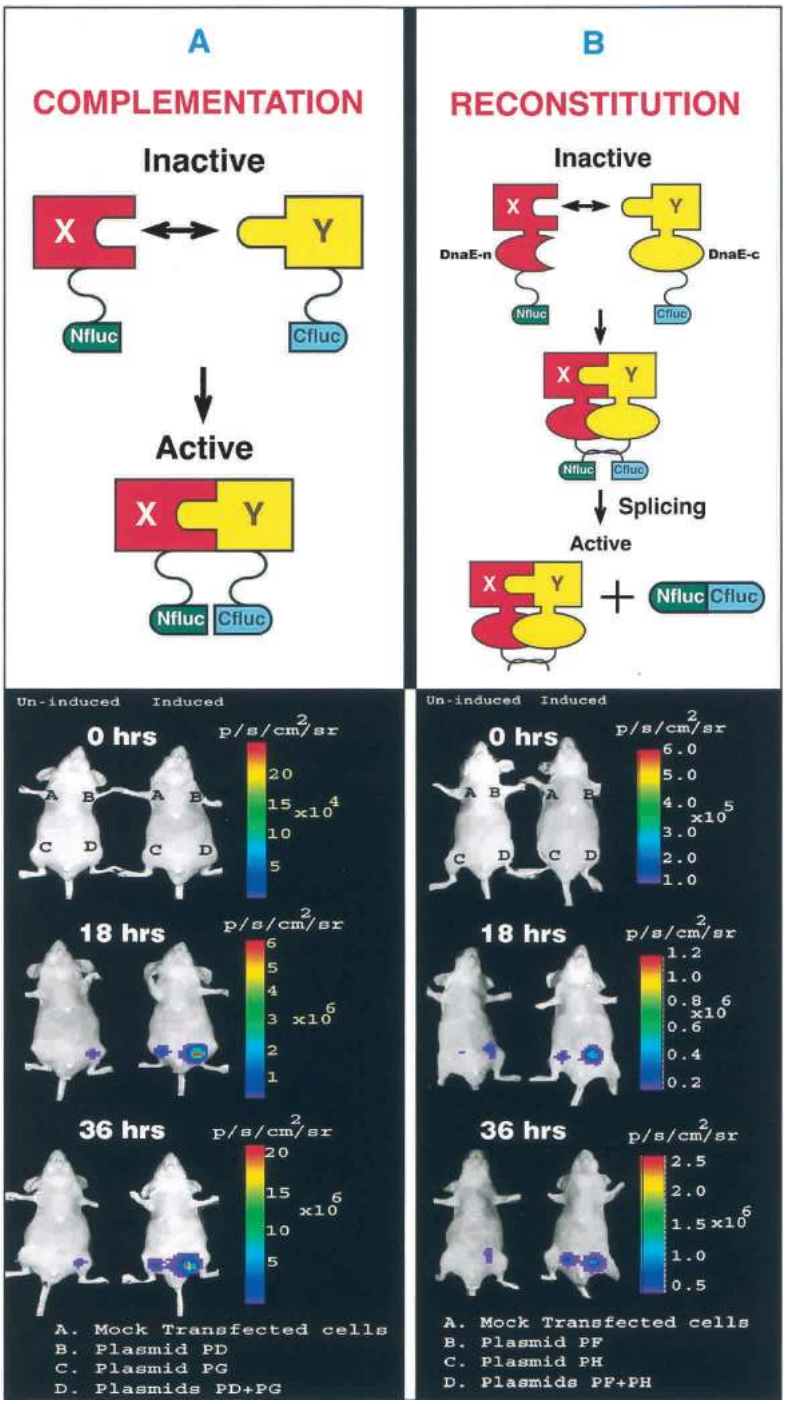

Figure 9. Schematic diagram of two strategies for using split reporters to monitor protein–protein interactions. (*A*, *top* panel) Complementation-mediated restoration of Firefly luciferase activity. The N-terminal half of Firefly luciferase is attached to protein X through a short peptide FFAGYC, and the C-terminal half of Firefly luciferase is connected to protein Y through the peptide CLKS. Interaction of proteins X and Y recovers *Fluc* activity through protein complementation. (*B*, *top* panel) Split Intein (DnaE)-mediated protein splicing leads to Firefly luciferase reconstitution. The N-terminal half of Firefly luciferase is connected to the N-terminal half of DnaE (DnaE-n) with peptide FFAGYC. The N-terminal half of DnaE, in turn, is connected to protein X. Similarly, the C-terminal half of Firefly luciferase is connected to the C-terminal half of DnaE (DnaE-c) with peptide CLKS, and the C-terminal half of intein is, in turn, connected to protein Y. The interaction of proteins X and Y mediates reconstitution through splicing of the N and C halves of DnaE. In vivo optical CCD imaging of mice carrying transiently transfected 293T cells for induction of the complementation-based (*A*) and intein-mediated reconstitution (*B*) of split luciferase system. All images shown are the visible light image superimposed on the optical CCD bioluminescence image with a scale in photons per second per square centimeter per steradian. Mice were imaged in a supine position after IP injection of D-luciferin. (*A*, *lower* panel) A set of nude mice was repetitively imaged after SC implantation of 293T cells transiently transfected with various plasmids as described in Paulmurugan et al. (2002). One group of mice was induced with TNF-α, and the other group was not induced. The images are from one representative mouse from each group immediately after implanting cells (0 h) and 18 and 36 h after TNF-α induction. The induced mouse showed higher *Fluc* signal at site D (where interacting proteins result in reporter complementation) when compared with the mouse not receiving TNF-α. The *Fluc* signal significantly increases after receiving TNF-α. (*B*, *lower* panel) A set of nude mice was repetitively imaged after subcutaneous implantation of 293T cells transiently transfected with various plasmids as described in Paulmurugan et al. (2002) to test the reconstitution-based split-luciferase system. One group of mice was induced with TNF-α, and the other group was not induced. The images are from one representative mouse from each group immediately after implanting cells (0 h) and 18 h and 36 h after TNF-α induction. The induced mouse showed significantly higher *Fluc* signal at site D (where interacting proteins result in intein-mediated reconstitution of the reporter) when compared with the mouse not receiving TNF-α. Reproduced with permission from Paulmurugan et al. (2002).

ried on chips; both promise to enable observation of the previously unobservable. Just as development of the telescope and microscope was followed by periods during which science was mostly done by observation rather than experiment, it is possible that the development of molecular imaging methods of gene expression monitoring along with other functional genomic methods may portend a new phase in which biology once again becomes, in part, observational (Brent 1999). This "not so hypothesis-driven" approach constitutes something of a departure from the mainstream biology that has developed during the past 30 years, but it has sound roots. After all, biology started with individuals looking, seeing, describing, and making simple inferences from what they saw (Brent 1999). We can expect this process to speed up and progress to be made in many aspects of

molecular imaging so that it integrates further with functional genomic and proteomic endeavors. The initial methodological/technological descriptions and validations are being made in molecular imaging, and soon it is anticipated that the second generation of experiments will face the interesting task of applying these techniques to help answer specific hypothesis-driven questions in many areas of biological study.

Innovation and accurate validation of biotechnologies are a critical necessity when bringing together and fully integrating molecular and cellular biology concepts with imaging in living subjects. Many developments in molecular imaging are anticipated over the next decade. Starting in the near future, many high-resolution, fast-imaging systems for mice will become commercially available, and miniaturized imaging technologies will begin to appear in core facilities of basic science laboratories. This trend will likely expand significantly in the future as more research groups acquire these technologies. Improved instrumentation will make use of advances in detector technology, including the exploitation of solid-state detector technology and better image-reconstruction techniques. This should help to produce newer generations of scanners with better resolution, sensitivity, and significantly higher-throughput time, which will aid substantially in the screening of mice (Kudo et al. 2002). Given the inherent advantages of optical imaging, these approaches are likely to be used increasingly in bridging imaging studies from small animals to larger ones and humans. For limited applications (e.g., in endoscopic or breast imaging), optical imaging may even have the potential to be directly translated to human investigations in the future, assuming that the mass amounts of substrate that have to be given to patients are proven to be safe. In addition, newer multimodality imaging systems for small animals will provide anatomical and functional image registration. Several microPET/CT scanners are in development at present, as are attempts at building instruments that combine MRI or optical imaging with PET.

Linked to the development of better reporter probes (Hadjantonakis and Nagy 2001; Remington 2002) is the need to develop tomographic three-dimensional imaging systems that can accurately quantify fluorescence and bioluminescence in deep heterogeneous media in vivo (Weissleder 2001; Ntziachristos et al. 2002). Ultimately, scanner performance, overall cost, access to multiple imaging probes, and simplicity of operation will dictate the extent of small-animal imaging participation in the era of postgenomic biology (Chatziioannou 2002). Rapid progress is being made to advance and refine the technologies to maximize their use and value.

For microPET imaging, small radiopharmacies with cyclotrons should continue to grow, providing for the routine availability of various more commonly used reporter probes. At present, no comprehensive databases exist of all the available molecular imaging probes, but such a database (MOLI) for all of the major imaging modalities is being compiled by the National Cancer Institute. Many existing reporter probes should eventually give way to newer generations of probes that are more sensitive and specific. PET assays will need to move toward generalized reporter probes where the chemistry behind radioisotope labeling remains relatively similar, but the underlying molecular structure can be easily modified to image a new molecular target. These generalizable reporter probes will facilitate the easier use of customized imaging approaches. To this aim, a greater investment in chemistry research and the development of a larger number of smart molecular imaging probes will be necessary. It is also anticipated that closer ties between molecular biologists and imaging researchers will produce imaging assays that are more sensitive to low-level biological events. This need for enhancing the sensitivity of imaging will dictate to some extent a future greater exploitation and use of optical imaging, which at present has the highest inherent sensitivity for target detection at limited depths. As optical technologies have changed biotechnology, they could also change in vivo imaging and provide more sophisticated methods for imaging molecular events (Weissleder 2002).

Adoption of molecular imaging approaches and establishment of a molecular imaging facility within a basic biological research setup is likely to be cost-effective in the long term. Although substantial start-up expenses are necessary to lay the foundation for this research methodology, it is anticipated that the cost of small-animal imaging instrumentation and the required core facilities will continue to fall with continued future developments and demands. Ongoing proliferation of small radiopharmacies with cyclotrons will also facilitate the spread of cheaper PET-based molecular imaging technologies to the biological research communities. Moreover, the costs of present optical and some small-animal magnetic resonance and computed tomography imaging technologies are not prohibitive, and will likely continue to drop in the future.

An intriguing future prospect is the integration of living cells with microdevices to provide a foundation for the development of new microassays of biological processes (LaVan et al. 2002). This could enable hybrid living/electronic systems to be developed for imaging in living subjects. Nanoparticles are among the most promising emerging fluorescent labels for cellular imaging in vivo (Mitchell 2001; Akerman et al. 2002; Chan et al. 2002). Nanocrystals (also called quantum dots or nanodots) are crystalline clumps as few as several dozen atoms and <10 nm in diameter. They absorb light at a wide range of wavelengths, but emit almost monochromatic light of a specific wavelength (and therefore color) that depends on the size of the crystal only. It may be possible to conjugate larger peptides or proteins to quantum dots to confer specificity as a molecular probe. Multiplexing with differently colored quantum dots could allow simultaneous imaging of many molecular targets (Chan et al. 2002). However, many challenges still exist in implementing these approaches, for example, developments are required in the chemical processes necessary to link these dots to biological molecules without altering tar-

geting affinity and pharmacological properties of the biological molecule of interest.

How will the practice of molecular imaging in the laboratory link with other developing disciplines in biological research? It is likely that the present budding endeavors in functional genomics will increasingly assimilate and make use of molecular imaging methodologies in the future. Functional genomics is a systematic effort to understand the function of genes and gene products by high-throughput analysis of gene products (transcripts, proteins) and biological systems (cell, tissue, organism) using automated procedures allowing us to scale up experiments classically performed for single genes (e.g., generation of mutants, analysis of transcript and protein expression on a genome-wide basis, analysis of protein structure and protein–protein interactions; Yaspo 2001). In many respects, the most interesting aspect of the function of a gene is its function in the organism as a whole, requiring the mutations of specific genes followed by the analysis of the complex molecular pathways resulting in the phenotype of the organism carrying this mutation (gene-driven paradigm), as opposed to identification of organisms with an interesting phenotype followed by the mapping of mutated genes (phenotype-driven paradigm; Yaspo 2001). The analysis of gene expression patterns using molecular imaging approaches—hitherto performed mainly by in-frame fusions of open reading frames of interest and their promoters to the coding sequence of reporters, for example, GFP or β-galactosidase, and subsequent in vitro localization of the reporter (Walhout and Vidal 2001)—is likely to contribute to a greater extent and more meaningfully to the understanding of such complex molecular pathways.

Comparative genomics allows us to integrate different types of information derived from various animal models to generate a synergistic platform for understanding complex disease mechanisms (Jacob and Kwitek 2002). In this way, information gained from each organism can guide the study of human disease phenotypes. We are entering an era in which comparative genomic data can be used to develop animal models that better recapitulate human disease at both the phenotypic and the genomic levels. The contribution of molecular imaging approaches to studying small animal models and to integrative mammalian biology will undoubtedly trickle onto the field of comparative mapping. A more significant contribution to comparative genomic endeavors will critically depend on future availability of higher-throughput molecular imaging assays (and the ability to multiplex them) that can be implemented on a practical level. Through molecular imaging of intact living subjects in this manner, it will be possible to accelerate the conversion of comparative genomics to sequence-based biology—the ability to assign variation in function to particular alleles. Such comparative genomics studies are likely to provide data for annotating the human genome sequence, for building better animal models, for assisting in the development of new therapeutic agents, and for understanding gene regulation (Jacob and Kwitek 2002).

Another discipline that is likely to cross paths in the future with molecular imaging is that of computational cell biology. Just as the ability to visualize protein dynamics and biological processes by in vivo microscopy is revolutionizing many areas of biology, so will the case be as well for molecular imaging techniques in intact living subjects. Although the general aim of molecular imaging researchers would be to continue to enhance the user-friendly aspect of imaging small animal models, nevertheless, with future greater capabilities and sophistication in noninvasive imaging of biological processes in living subjects, these methods may generate large, kinetically complex data sets that may not be possible to interpret in an intuitive manner. The combination of dynamic imaging and computational modeling will emerge as a powerful tool for the quantification of biophysical properties of molecules and processes (Phair and Misteli 2001). A fruitful interchange between molecular imaging and the emerging new discipline of computational cell biology will be essential in uncovering the pathways, mechanisms, and controls of biological processes and systems as they occur in vivo.

We predict that greater implementation of molecular imaging techniques in the study of living experimental animal models is likely to contribute significantly to research in many facets of biology. Approaches that relate gene expression to phenotyping outcome will also be well served by molecular imaging strategies. There is a marked increase in interest in these approaches, and several technologies are being developed to achieve this end, namely, genomics, transcriptomics, proteomics, metabolomics (which investigates metabolic regulation and fluxes in individual cells or cell types), and metabonomics (the determination of systemic biochemical profiles and regulation of function in whole organisms by analyzing biofluids and tissues; Nicholson et al. 2002). Ultimately, we foresee innovative molecular imaging tools helping to some extent to satisfy the postgenomic era need for display of entire biological pathway systems and accelerating significantly the achievement of a "systems biology" understanding of biological complexity (Kitano 2002). Even though molecular imaging is in its formative years, recent studies clearly reflect the first fruits of powerful, and possibly ultimately transformative, technologies. With luck and perseverance, insights made from these methods may be as useful as those made from telescopes turned on the skies and microscopes focused on cells and tissues. This potential power of molecular imaging to see fundamental biological processes in a new light will not only help to enhance our knowledge and understanding but should also accelerate considerably the rate of discovery in the biological sciences.

Additional useful Internet links

In addition to http://www.mi-central.org: The Crump Institute for Molecular Imaging at University of California at Los Angeles: http://www.crump.ucla.edu. The Academy of Molecular Imaging: http://www.ami-imaging.org. The Society for Molecular Imaging: http://www.molecularimaging.org. Society of Nuclear Medicine: http://www.snm.org.

Acknowledgments

T.F.M. and S.S.G. are supported in part by NIH grants P50 CA86306. T.F.M. is also generously supported by a Mid-Career Award for Established Practitioners from The PPP Foundation, General Electric Medical Systems, the Palgrave Brown Foundation, the Cancer Prevention Research Trust, a Royal College of Radiologists *X*-Appeal pump priming grant, the Steel Charitable Trust, and the Sir Samuel Scott of Yews Trust, all in the UK. S.S.G. is also generously supported by R01 CA82214, SAIRP R24 CA92865, Department of Energy Contract DE-FC03-87ER60615, and CaP Cure. S.S.G. thanks H. Herschman, M.E. Phelps, M. Carey, L. Wu, A. Wu, H. Wu, C. Sawyers, O. Witte, J. Barrio, N. Satyamurthy, D. Kaufman, S. Chow, A. Chatziioannou, S. Cherry, M. Dhalbom, J. Czernin, M. Iyer, and many postdoctoral fellows and graduate students who continue to help build the new field of molecular imaging. We also thank S. Biswal, J. Park, P. Dubey, and J. Schwimmer for helping to improve this manuscript.

References

Adams, J.Y., Johnson, M., Sato, M., Berger, F., Gambhir, S.S., Carey, M., Iruela-Arispe, M.L., and Wu, L. 2002. Visualization of advanced human prostate cancer lesions in living mice by a targeted gene transfer vector and optical imaging. *Nat. Med.* **8:** 891–897.

Adonai, N., Nguyen, K.N., Walsh, J., Iyer, M., Toyokuni, T., Phelps, M.E., McCarthy, T., McCarthy, D.W., and Gambhir, S.S. 2002. Ex vivo cell labeling with ^{64}Cu-pyruvaldehyde-bis(N^4-methylthiosemicarbazone) for imaging cell trafficking in mice with positron-emission tomography. *Proc. Natl. Acad. Sci.* **99:** 3030–3035.

Akerman, M.E., Chan, W.C., Laakkonen, P., Bhatia, S.N., and Ruoslahti, E. 2002. Nanocrystal targeting in vivo. *Proc. Natl. Acad. Sci.* **99:** 12617–12621.

Allport, J.R. and Weissleder, R. 2001. In vivo imaging of gene and cell therapies. *Exp. Hemal.* **29:** 1237–1246.

Banerjee, D., Mayer-Kuckuk, P., Capiaux, G., Budak-Alpdogan, T., Gorlick, R., and Bertino, J.R. 2002. Novel aspects of resistance to drugs targeted to dihydrofolate reductase and thymidylate synthase. *Biochim. Biophys. Acta* **1587:** 164–173.

Becker, W. and Meller, J. 2001. The role of nuclear medicine in infection and inflammation. *Lancet Infect. Dis.* **1:** 326–333.

Beekman, F.J., McElroy, D.P., Berger, F., Gambhir, S.S., Hoffman, E.J., and Cherry, S.R. 2002. Towards in vivo nuclear microscopy: Iodine-125 imaging in mice using micro-pinholes. *Eur. J. Nucl. Med. Mol. Imaging* **29:** 933–938.

Benaron, D.A., Contag, P.R., and Contag, C.H. 1997. Imaging brain structure and function, infection and gene expression in the body using light. *Philos. Trans. R. Soc. Lond. B Biol. Sci.* **352:** 755–761.

Bennett, J.J., Tjuvajev, J., Johnson, P., Doubrovin, M., Akhurst, T., Malholtra, S., Hackman, T., Balatoni, J., Finn, R., Larson, S.M., et al. 2001. Positron emission tomography imaging for herpes virus infection: Implications for oncolytic viral treatments of cancer. *Nat. Med.* **7:** 859–863.

Berger, F. and Gambhir, S.S. 2001. Recent advances in imaging endogenous or transferred gene expression utilizing radionuclide technologies in living subjects: Applications to breast cancer. *Breast Cancer. Res.* **3:** 28–35.

Berger, F., Lee, Y.-P., Loening, A.M., Chatziioannou, A., Freedland, S.J., Leahy, R., Lieberman, J.R., Belldegrun, A.S., Sawyers, C.L., and Gambhir, S.S. 2002. Whole-body skeletal imaging in mice utilizing microPET: Optimization of reproducibility and applications in animal models of bone disease. *Eur. J. Nucl. Med. Mol. Imaging* **29:** 1225–1236.

Berridge, M., Comar, D., Crouzel, C., and Baron, J.C. 1983. ^{11}C-Labeled ketanserin: A selective serotonin S2 anatagonist. *J. Label. Compounds Radiopharmacol.* **20:** 73.

Bhaumik, S. and Gambhir, S.S. 2002. Optical imaging of Renilla luciferase reporter gene expression in living mice. *Proc. Natl. Acad. Sci.* **99:** 377–382.

Bhorade, R., Weissleder, R., Nakakoshi, T., Moore, A., and Tung, C.H. 2000. Macrocyclic chelators with paramagnetic cations are internalized into mammalian cells via a HIV-tat derived membrane translocation peptide. *Bioconjug. Chem.* **11:** 301–305.

Blankenberg, F.G., Katsikis, P.D., Tait, J.F., Davis, R.E., Naumovski, L., Ohtsuki, K., Kopiwoda, S., Abrams, M.J., Darkes, M., Robbins, R.C., et al. 1998. In vivo detection and imaging of phosphatidylserine expression during programmed cell death. *Proc. Natl. Acad. Sci.* **95:** 6349–6354.

Blasberg, R.G. and Tjuvajev, J.G. 1999. Herpes simplex virus thymidine kinase as a marker/reporter gene for PET imaging of gene therapy. *Quart. J. Nucl. Med.* **43:** 163–169.

Bogdanov Jr., A. and Weissleder, R. 1998. The development of in vivo imaging systems to study gene expression. *Trends Biotechnol.* **16:** 5–10.

Bogdanov Jr., A., Simonova, M., and Weissleder, R. 1998. Design of metal-binding green fluorescent protein variants. *Biochim. Biophys. Acta* **1397:** 56–64.

———. 2000. Engineering membrane proteins for nuclear medicine: Applications for gene therapy and cell tracking. *Quart. J. Nucl. Med.* **44:** 224–235.

Bogdanov Jr., A.A., Lin, C.P., Simonova, M., Matuszewski, L., and Weissleder, R. 2002. Cellular activation of the self-quenched fluorescent reporter probe in tumor microenvironment. *Neoplasia* **4:** 228–236.

Boland, A., Ricard, M., Opolon, P., Bidart, J.M., Yeh, P., Filetti, S., Schlumberger, M., and Perricaudet, M. 2000. Adenovirus-mediated transfer of the thyroid sodium/iodide symporter gene into tumors for a targeted radiotherapy. *Cancer Res.* **60:** 3484–3492.

Bouvet, M., Wang, J., Nardin, S.R., Nassirpour, R., Yang, M., Baranov, E., Jiang, P., Moossa, A.R., and Hoffman, R.M. 2002. Real-time optical imaging of primary tumor growth and multiple metastatic events in a pancreatic cancer orthotopic model. *Cancer Res.* **62:** 1534–1540.

Bredow, S., Lewin, M., Hofmann, B., Marecos, E., and Weissleder, R. 2000. Imaging of tumour neovasculature by targeting the TGF-β binding receptor endoglin. *Eur. J. Cancer* **36:** 675–681.

Bremer, C. and Weissleder, R. 2001. In vivo imaging of gene expression. *Acad. Radiol.* **8:** 15–23.

Bremer, C., Bredow, S., Mahmood, U., Weissleder, R., and Tung, C.H. 2001a. Optical imaging of matrix metalloproteinase-2 activity in tumors: Feasibility study in a mouse model. *Radiology* **221:** 523–529.

Bremer, C., Tung, C.H., and Weissleder, R. 2001b. In vivo molecular target assessment of matrix metalloproteinase inhibition. *Nat. Med.* **7:** 743–748.

Bremer, C., Tung, C.H., Bogdanov Jr., A., and Weissleder, R. 2002. Imaging of differential protease expression in breast cancers for detection of aggressive tumor phenotypes. *Radiology* **222:** 814–818.

Brenner, M. 1996. Gene marking. *Hum. Gene. Ther.* **7:** 1927–1936.

Brent, R. 1999. Functional genomics: Learning to think about gene expression data. *Curr. Biol.* **9:** R338–R341.

Budinger, T. 1996. Single photon emission computed tomogra-

phy. In *Diagnostic nuclear medicine* (eds. M. Sandler et al.), pp. 121–138. Williams and Wilkins, Baltimore, MD.

Burns, S.M., Joh, D., Francis, K.P., Shortliffe, L.D., Gruber, C.A., Contag, P.R., and Contag, C.H. 2001. Revealing the spatiotemporal patterns of bacterial infectious diseases using bioluminescent pathogens and whole body imaging. *Contrib. Microbiol.* **9:** 71–88.

Carlsen, H., Moskaug, J.O., Fromm, S.H., and Blomhoff, R. 2002. In vivo imaging of NF-κB activity. *J. Immunol.* **168:** 1441–1446.

Castillo, M., Kwock, L., and Mukherji, S.K. 1996. Clinical applications of proton MR spectroscopy. *Am. J. Neuroradiol.* **17:** 1–15.

Chan, W.C., Maxwell, D.J., Gao, X., Bailey, R.E., Han, M., and Nie, S. 2002. Luminescent quantum dots for multiplexed biological detection and imaging. *Curr. Opin. Biotechnol.* **13:** 40–46.

Chatham, J.C. and Blackband, S.J. 2001. Nuclear magnetic resonance spectroscopy and imaging in animal research. *Ilar. J.* **42:** 189–208.

Chatziioannou, A.F. 2002. Molecular imaging of small animals with dedicated PET tomographs. *Eur. J. Nucl. Med.* **29:** 98–114.

Chatziioannou, A., Tai, Y.C., Doshi, N., and Cherry, S.R. 2001. Detector development for microPET II: A 1 microl resolution PET scanner for small animal imaging. *Phys. Med. Biol.* **46:** 2899–2910.

Chen, J., Tung, C.H., Mahmood, U., Ntziachristos, V., Gyurko, R., Fishman, M.C., Huang, P.L., and Weissleder, R. 2002. In vivo imaging of proteolytic activity in atherosclerosis. *Circulation* **105:** 2766–2771.

Chen, W.S., Luker, K.E., Dahlheimer, J.L., Pica, C.M., Luker, G.D., and Piwnica-Worms, D. 2000. Effects of MDR1 and MDR3 P-glycoproteins, MRP1, and BCRP/MXR/ABCP on the transport of ^{99m}Tc-tetrofosmin. *Biochem. Pharmacol.* **60:** 413–426.

Cherry, S.R. and Gambhir, S.S. 2001. Use of positron emission tomography in animal research. *Ilar. J.* **42:** 219–232.

Cho, J.Y., Shen, D.H., Yang, W., Williams, B., Buckwalter, T.L., La Perle, K.M., Hinkle, G., Pozderac, R., Kloos, R., Nagaraja, H.N., et al. 2002. In vivo imaging and radioiodine therapy following sodium iodide symporter gene transfer in animal model of intracerebral gliomas. *Gene Ther.* **9:** 1139–1145.

Coenen, H.H., Laufer, P., Stöcklin, G., Wienhard, K., Pawlik, G., Böcher-Schwarz, H.G., and Heiss, W.D. 1987. 3-N-(2-[^{18}F]-fluoroethyl)-spiperone: A novel ligand for cerebral dopamine receptor studies with PET. *Life Sci.* **40:** 81–88.

Contag, C.H., Contag, P.R., Mullins, J.I., Spilman, S.D., Stevenson, D.K., and Benaron, D.A. 1995. Photonic detection of bacterial pathogens in living hosts. *Mol. Microbiol.* **18:** 593–603.

Contag, C.H., Spilman, S.D., Contag, P.R., Oshiro, M., Eames, B., Dennery, P., Stevenson, D.K., and Benaron, D.A. 1997. Visualizing gene expression in living mammals using a bioluminescent reporter. *Photochem. Photobiol.* **66:** 523–531.

Contag, C.H., Jenkins, D., Contag, P.R., and Negrin, R.S. 2000. Use of reporter genes for optical measurements of neoplastic disease in vivo. *Neoplasia* **2:** 41–52.

Contag, P.R., Olomu, I.N., Stevenson, D.K., and Contag, C.H. 1998. Bioluminescent indicators in living mammals. *Nat. Med.* **4:** 245–247.

Costa, G.L., Sandora, M.R., Nakajima, A., Nguyen, E.V., Taylor-Edwards, C., Slavin, A.J., Contag, C.H., Fathman, C.G., and Benson, J.M. 2001. Adoptive immunotherapy of experimental autoimmune encephalomyelitis via T cell delivery of the IL-12 p40 subunit. *J. Immunol.* **167:** 2379–2387.

Crouzel, C., Venet, M., Irie, T., Sanz, G., and Boullais, C. 1988. Labeling of serotonergic ligand with ^{18}F: [^{18}F]Setoperone. *J. Label. Compd. Radiopharm.* **25:** 403.

Cumming, P. and Gjedde, A. 1998. Compartmental analysis of dopa decarboxylation in living brain from dynamic positron emission tomograms. *Synapse* **29:** 37–61.

Dawson, P. 1999. *Textbook of contrast media.* Isis Medical, Wigan, UK.

Del Vecchio, S., Ciarmiello, A., and Salvatore, M. 2000. Scintigraphic detection of multidrug resistance in cancer. *Cancer Biother. Radiopharm.* **15:** 327–337.

Dendy, P. and Heaton, B. 1999. Tomographic imaging. In *Physics for diagnostic radiology* (eds. P. Dendy and B. Heaton), pp. 249–278. Institute of Physics, Bristol, UK.

Dewanjee, M.K., Ghafouripour, A.K., Kapadvanjwala, M., Dewanjee, S., Seafini, A.N., Lopez, D.M., and Sfakianakis, G.N. 1994. Noninvasive imaging of c-myc oncogene messenger RNA with Indium-111-antisense probes in a mammary tumor-bearing mouse model. *J. Nucl. Med.* **35:** 1054–1063.

Dey, H.M., Seibyl, J.P., Stubbs, J.B., Zoghbi, S.S., Baldwin, R.M., Smith, E.O., Zubal, I.G., Zea-Ponce, Y., Olson, C., Charney, D.S., et al. 1994. Human biodistribution and dosimetry of the SPECT benzodiazepine receptor radioligand Iodine-123-iomazenil. *J. Nucl. Med.* **35:** 399–404.

Dilmanian, F.A., Wu, X.Y., Parsons, E.C., Ren, B., Kress, J., Button, T.M., Chapman, L.D., Coderre, J.A., Giron, F., Greenberg, D., et al. 1997. Single- and dual-energy CT with monochromatic synchrotron X-rays. *Phys. Med. Biol.* **42:** 371–387.

Dodd, C.H., Hsu, H.C., Chu, W.J., Yang, P., Zhang, H.G., Mountz Jr., J.D., Zinn, K., Forder, J., Josephson, L., Weissleder, R., et al. 2001. Normal T-cell response and in vivo magnetic resonance imaging of T cells loaded with HIV transactivator-peptide-derived superparamagnetic nanoparticles. *J. Immunol. Methods* **256:** 89–105.

Doubrovin, M., Ponomarev, V., Beresten, T., Balatoni, J., Bornmann, W., Finn, R., Humm, J., Larson, S., Sadelain, M., Blasberg, R., et al. 2001. Imaging transcriptional regulation of p53-dependent genes with positron emission tomography in vivo. *Proc. Natl. Acad. Sci.* **98:** 9300–9305.

Downer, J.B., Jones, L.A., Engelbach, J.A., Lich, L.L., Mao, W., Carlson, K.E., Katzenellenbogen, J.A., and Welch, M.J. 2001. Comparison of animal models for the evaluation of radiolabeled androgens. *Nucl. Med. Biol.* **28:** 613–626.

Eckelman, W.C., Reba, R.C., Rzeszotarski, W.J., Gibson, R.E., Hill, T., Holman, B.L., Budinger, T., Conklin, J.J., Eng, R., and Grissom, M.P. 1984. External imaging of cerebral muscarinic acetylcholine receptors. *Science* **223:** 291–293.

Edinger, M., Sweeney, T.J., Tucker, A.A., Olomu, A.B., Negrin, R.S., and Contag, C.H. 1999. Noninvasive assessment of tumor cell proliferation in animal models. *Neoplasia* **1:** 303–310.

Flacke, S., Fischer, S., Scott, M.J., Fuhrhop, R.J., Allen, J.S., McLean, M., Winter, P., Sicard, G.A., Gaffney, P.J., Wickline, S.A., et al. 2001. Novel MRI contrast agent for molecular imaging of fibrin: Implications for detecting vulnerable plaques. *Circulation* **104:** 1280–1285.

Fowler, J.S., Volkow, N.D., Logan, J., Schlyer, D.J., MacGregor, R.R., Wang, G.J., Wolf, A.P., Pappas, N., Alexoff, D., Shea, C., et al. 1993. Monoamine oxidase B (MAO B) inhibitor therapy in Parkinson's disease: The degree and reversibility of human brain MAO B inhibition by Ro 19 6327. *Neurology* **43:** 1984–1992.

Fraites Jr., T.J., Schleissing, M.R., Shanely, R.A., Walter, G.A., Cloutier, D.A., Zolotukhin, I., Pauly, D.F., Raben, N., Plotz,

P.H., Powers, S.K., et al. 2002. Correction of the enzymatic and functional deficits in a model of Pompe disease using adeno-associated virus vectors. *Mol. Ther.* **5:** 571–578.

Francis, K.P., Joh, D., Bellinger-Kawahara, C., Hawkinson, M.J., Purchio, T.F., and Contag, P.R. 2000. Monitoring bioluminescent *Staphylococcus aureus* infections in living mice using a novel luxABCDE construct. *Infect. Immun.* **68:** 3594–3600.

Francis, K.P., Yu, J., Bellinger-Kawahara, C., Joh, D., Hawkinson, M.J., Xiao, G., Purchio, T.F., Caparon, M.G., Lipsitch, M., and Contag, P.R. 2001. Visualizing pneumococcal infections in the lungs of live mice using bioluminescent *Streptococcus pneumoniae* transformed with a novel Gram-positive lux transposon. *Infect. Immun.* **69:** 3350–3358.

Frost, J.J., Mayberg, H.S., Sadzot, B., Dannals, R.F., Lever, J.R., Ravert, H.T., Wilson, A.A., Wagner Jr., H.N., and Links, J.M. 1990. Comparison of [^{11}C]diprenorphine and [^{11}C]carfentanil binding to opiate receptors in humans by positron emission tomography. *J. Cereb. Blood. Flow Metab.* **10:** 484–492.

Gambhir, S.S. 2000. Imaging gene expression: Concepts and future outlook. In *Diagnostic nuclear medicine* (ed. C. Schiepers), pp. 253–272. Springer-Verlag, Berlin.

———. 2002. Molecular imaging of cancer with positron emission tomography. *Nat. Rev. Cancer* **2:** 683–693.

———. 2003. Quantiative assay development for positron emission tomography. In *Molecular imaging with positron emission tomography* (ed. M.E. Phelps). Springer-Verlag, New York (In press).

Gambhir, S.S., Barrio, J.R., Wu, L., Iyer, M., Namavari, M., Satyamurthy, N., Bauer, E., Parrish, C., MacLaren, D.C., Borghei, A.R., et al. 1998. Imaging of adenoviral-directed herpes simplex virus type 1 thymidine kinase reporter gene expression in mice with radiolabeled ganciclovir. *J. Nucl. Med.* **39:** 2003–2011.

Gambhir, S.S., Barrio, J.R., Herschman, H.R., and Phelps, M.E. 1999a. Assays for noninvasive imaging of reporter gene expression. *Nucl. Med. Biol.* **26:** 481–490.

———. 1999b. Imaging gene expression: Principles and assays. *J. Nucl. Cardiol.* **6:** 219–233.

Gambhir, S.S., Barrio, J.R., Phelps, M.E., Iyer, M., Namavari, M., Satyamurthy, N., Wu, L., Green, L.A., Bauer, E., MacLaren, D.C., et al. 1999c. Imaging adenoviral-directed reporter gene expression in living animals with positron emission tomography. *Proc. Natl. Acad. Sci.* **96:** 2333–2338.

Gambhir, S.S., Bauer, E., Black, M.E., Liang, Q., Kokoris, M.S., Barrio, J.R., Iyer, M., Namavari, M., Phelps, M.E., and Herschman, H.R. 2000a. A mutant herpes simplex virus type 1 thymidine kinase reporter gene shows improved sensitivity for imaging reporter gene expression with positron emission tomography. *Proc. Natl. Acad. Sci.* **97:** 2785–2790.

Gambhir, S.S., Herschman, H.R., Cherry, S.R., Barrio, J.R., Satyamurthy, N., Toyokuni, T., Phelps, M.E., Larson, S.M., Balatoni, J., Finn, R., et al. 2000b. Imaging transgene expression with radionuclide imaging technologies. *Neoplasia* **2:** 118–138.

Gassmann, M. and Hennet, T. 1998. From genetically altered mice to integrative physiology. *News Physiol. Sci.* **13:** 53–57.

Golden, J. and Ligler, F. 2002. A comparison of imaging methods for use in an array biosensor. *Biosens. Bioelectron.* **17:** 719.

Green, L.A., Yap, C.S., Nguyen, K., Barrio, J.R., Namavari, M., Satyamurthy, N., Phelps, M.E., Sandgren, E.P., Herschman, H.R., and Gambhir, S.S. 2002. Indirect monitoring of endogenous gene expression by positron emission tomography (PET) imaging of reporter gene expression in transgenic mice. *Mol. Imag. Biol.* **4:** 71–81.

Haberkorn, U., Henze, M., Altmann, A., Jiang, S., Morr, I., Mahmut, M., Peschke, P., Kubler, W., Debus, J., and Eisenhut, M. 2001. Transfer of the human NaI symporter gene enhances iodide uptake in hepatoma cells. *J. Nucl. Med.* **42:** 317–325.

Hadjantonakis, A.K. and Nagy, A. 2001. The color of mice: In the light of GFP-variant reporters. *Histochem. Cell Biol.* **115:** 49–58.

Halldin, C., Farde, L., Barnett, A., and Sedvall, G. 1991. Synthesis of carbon-11 labelled SCH 39166, a new selective dopamine D-1 receptor ligand, and preliminary PET investigations. *Intl. J. Rad. Appl. Instrum. A* **42:** 451–455.

Hamblin, M.R., O'Donnell, D.A., Murthy, N., Contag, C.H., and Hasan, T. 2002. Rapid control of wound infections by targeted photodynamic therapy monitored by in vivo bioluminescence imaging. *Photochem. Photobiol.* **75:** 51–57.

Hardy, J., Edinger, M., Bachmann, M.H., Negrin, R.S., Fathman, C.G., and Contag, C.H. 2001. Bioluminescence imaging of lymphocyte trafficking in vivo. *Exp. Hematol.* **29:** 1353–1360.

Hemminki, A., Zinn, K.R., Liu, B., Chaudhuri, T.R., Desmond, R.A., Rogers, B.E., Barnes, M.N., Alvarez, R.D., and Curiel, D.T. 2002. In vivo molecular chemotherapy and noninvasive imaging with an infectivity-enhanced adenovirus. *J. Natl. Cancer Inst.* **94:** 741–749.

Herschman, H.R., MacLaren, D.C., Iyer, M., Namavari, M., Bobinski, K., Green, L.A., Wu, L., Berk, A.J., Toyokuni, T., Barrio, J.R., et al. 2000. Seeing is believing: Non-invasive, quantitative and repetitive imaging of reporter gene expression in living animals, using positron emission tomography. *J. Neurosci. Res.* **59:** 699–705.

Hogemann, D. and Basilion, J.P. 2002. "Seeing inside the body": MR imaging of gene expression. *Eur. J. Nucl. Med. Mol. Imaging* **29:** 400–408.

Hogemann, D., Josephson, L., Weissleder, R., and Basilion, J.P. 2000. Improvement of MRI probes to allow efficient detection of gene expression. *Bioconjug. Chem.* **11:** 941–946.

Hoit, B.D. 2001. New approaches to phenotypic analysis in adult mice. *J. Mol. Cell Cardiol.* **33:** 27–35.

Holdsworth, D.W. and Thornton, M.M. 2002. Micro-CT in small animal and specimen imaging. *Trends Biotechnol.* **20:** S34–S39.

Honigman, A., Zeira, E., Ohana, P., Abramovitz, R., Tavor, E., Bar, I., Zilberman, Y., Rabinovsky, R., Gazit, D., Joseph, A., et al. 2001. Imaging transgene expression in live animals. *Mol. Ther.* **4:** 239–249.

Hornack, J.P. 2002. *The basics of MRI.* http://www.cis.rit.edu/htbooks/mri.

Huang, S.C. and Phelps, M.E. 1986. Principles of tracer kinetic modeling in PET and autoradiography. In *Positron emission tomography and autoradiography, principles and applications for the brain and heart* (eds. M.E. Phelps et al.), pp. 287–346. Raven Press, New York.

Israel, O., Keidar, Z., Iosilevsky, G., Bettman, L., Sachs, J., and Frenkel, A. 2001. The fusion of anatomic and physiologic imaging in the management of patients with cancer. *Semin. Nucl. Med.* **31:** 191–205.

Iyer, M., Barrio, J.R., Namavari, M., Bauer, E., Satyamurthy, N., Nguyen, K., Toyokuni, T., Phelps, M.E., Herschman, H.R., and Gambhir, S.S. 2001a. 8-[F-18]fluoropenciclovir: An improved reporter probe for imaging HSV1-tk reporter gene expression in vivo using PET. *J. Nucl. Med.* **42:** 96–105.

Iyer, M., Wu, L., Carey, M., Wang, Y., Smallwood, A., and Gambhir, S.S. 2001b. Two-step transcriptional amplification as a method for imaging reporter gene expression using weak promoters. *Proc. Natl. Acad. Sci.* **98:** 14595–14600.

Iyer, M., Berenji, M., Templeton, N.S., and Gambhir, S.S. 2002. Noninvasive imaging of cationic lipid-mediated delivery of

optical and PET reporter genes in living mice. *Mol. Ther.* **6:** 555–562.

Jackson, E.F. 2001. Principles of magnetic resonance imaging and magnetic resonance spectroscopy. In *Targeted molecular imaging in oncology* (eds. E.E. Kim and D.J. Yang), pp. 30–61. Springer-Verlag, New York.

Jacob, H.J. and Kwitek, A.E. 2002. Rat genetics: Attaching physiology and pharmacology to the genome. *Nat. Rev. Genet.* **3:** 33–42.

Jacobs, A. and Heiss, W.D. 2002. Towards non-invasive imaging of HSV-1 vector-mediated gene expression by positron emission tomography. *Vet. Microbiol.* **86:** 27–36.

Jacobs, A., Dubrovin, M., Hewett, J., Sena-Esteves, M., Tan, C.W., Slack, M., Sadelain, M., Breakefield, X.O., and Tjuvajev, J.G. 1999. Functional coexpression of HSV-1 thymidine kinase and green fluorescent protein: Implications for noninvasive imaging of transgene expression. *Neoplasia* **1:** 154–161.

Jacobs, A., Tjuvajev, J.G., Dubrovin, M., Akhurst, T., Balatoni, J., Beattie, B., Joshi, R., Finn, R., Larson, S.M., Herrlinger, U., et al. 2001. Positron emission tomography-based imaging of transgene expression mediated by replication-conditional, oncolytic herpes simplex virus type 1 mutant vectors in vivo. *Cancer Res.* **61:** 2983–2995.

Jacobs, R.E. and Cherry, S.R. 2001. Complementary emerging techniques: High-resolution PET and MRI. *Curr. Opin. Neurobiol.* **11:** 621–629.

Johnson, G.A., Cofer, G.P., Gewalt, S.L., and Hedlund, L.W. 2002. Morphologic phenotyping with MR microscopy: The visible mouse. *Radiology* **222:** 789–793.

Jones, A.K., Luthra, S.K., Maziere, B., Pike, V.W., Loc'h, C., Crouzel, C., Syrota, A., and Jones, T. 1988. Regional cerebral opioid receptor studies with [^{11}C]diprenorphine in normal volunteers. *J. Neurosci. Methods* **23:** 121–129.

Josephson, L., Tung, C.H., Moore, A., and Weissleder, R. 1999. High-efficiency intracellular magnetic labeling with novel superparamagnetic-Tat peptide conjugates. *Bioconjug. Chem.* **10:** 186–191.

Josephson, L., Kircher, M.F., Mahmood, U., Tang, Y., and Weissleder, R. 2002. Near-infrared fluorescent nanoparticles as combined MR/optical imaging probes. *Bioconjug. Chem.* **13:** 554–560.

Kamiyama, M., Ichikawa, Y., Ishikawa, T., Chishima, T., Hasegawa, S., Hamaguchi, Y., Nagashima, Y., Miyagi, Y., Mitsuhashi, M., Hyndman, D., et al. 2002. VEGF receptor antisense therapy inhibits angiogenesis and peritoneal dissemination of human gastric cancer in nude mice. *Cancer Gene. Ther.* **9:** 197–201.

Kaneko, K., Yano, M., Yamano, T., Tsujinaka, T., Miki, H., Akiyama, Y., Taniguchi, M., Fujiwara, Y., Doki, Y., Inoue, M., et al. 2001. Detection of peritoneal micrometastases of gastric carcinoma with green fluorescent protein and carcinoembryonic antigen promoter. *Cancer Res.* **61:** 5570–5574.

Kang, H.W., Josephson, L., Petrovsky, A., Weissleder, R., and Bogdanov Jr., A., 2002. Magnetic resonance imaging of inducible E-selectin expression in human endothelial cell culture. *Bioconjug. Chem.* **13:** 122–127.

Kim, E.E. 2001. Radioimmunodetection of cancer. In *Targeted molecular imaging in oncology* (eds. E.E. Kim and D.J. Yang), pp. 88–101. Springer-Verlag, New York.

Kitano, H. 2002. Systems biology: A brief overview. *Science* **295:** 1662–1664.

Koransky, M.L., Ip, T.K., Wu, S., Cao, Y., Berry, G., Contag, C., Blau, H., and Robbins, R. 2001. In vivo monitoring of myoblast transplantation into rat myocardium. *J. Heart Lung Transplant.* **20:** 188–189.

Kudo, T., Fukuchi, K., Annala, A.J., Chatziioannou, A.F., Allada, V., Dahlbom, M., Tai, Y.C., Inubushi, M., Huang, S.C., Cherry, S.R., et al. 2002. Noninvasive measurement of myocardial activity concentrations and perfusion defect sizes in rats with a new small-animal positron emission tomograph. *Circulation* **106:** 118–123.

Kuhl, D.E., Minoshima, S., Fessler, J.A., Frey, K.A., Foster, N.L., Ficaro, E.P., Wieland, D.M., and Koeppe, R.A. 1996. In vivo mapping of cholinergic terminals in normal aging, Alzheimer's disease, and Parkinson's disease. *Ann. Neurol.* **40:** 399–410.

Kung, H.F., Alavi, A., Chang, W., Kung, M.P., Keyes Jr., J.W., Velchik, M.G., Billings, J., Pan, S., Noto, R., Rausch, et al. 1990. In vivo SPECT imaging of CNS D-2 dopamine receptors: Initial studies with iodine-123-IBZM in humans. *J. Nucl. Med.* **31:** 573–579.

Lanza, G.M. and Wickline, S.A. 2001. Targeted ultrasonic contrast agents for molecular imaging and therapy. *Prog. Cardiovasc. Dis.* **44:** 13–31.

Lanza, G.M., Abendschein, D.R., Hall, C.S., Marsh, J.N., Scott, M.J., Scherrer, D.E., and Wickline, S.A. 2000. Molecular imaging of stretch-induced tissue factor expression in carotid arteries with intravascular ultrasound. *Invest. Radiol.* **35:** 227–234.

LaVan, D.A., Lynn, D.M., and Langer, R. 2002. Moving smaller in drug discovery and delivery. *Nat. Rev. Drug. Discov.* **1:** 77–84.

Le, L.Q., Kabarowski, J.H., Wong, S., Nguyen, K., Gambhir, S.S., and Witte, O.N. 2002. Positron emission tomography imaging analysis of G2A as a negative modifier of lymphoid leukemogenesis initiated by the BCR-ABL oncogene. *Cancer Cell* **1:** 381–391.

Lee, S.Y., Wang, Z., Lin, C.K., Contag, C.H., Olds, L.C., Cooper, A.D., and Sibley, E. 2002. Regulation of intestine-specific spatiotemporal expression by the rat lactase promoter. *J. Biol. Chem.* **277:** 13099–13105.

Lewin, M., Bredow, S., Sergeyev, N., Marecos, E., Bogdanov Jr., A., and Weissleder, R. 1999. In vivo assessment of vascular endothelial growth factor-induced angiogenesis. *Intl. J. Cancer* **83:** 798–802.

Lewin, M., Carlesso, N., Tung, C.H., Tang, X.W., Cory, D., Scadden, D.T., and Weissleder, R. 2000. Tat peptide-derivatized magnetic nanoparticles allow in vivo tracking and recovery of progenitor cells. *Nat. Biotechnol.* **18:** 410–414.

Li, J.J., Fang, X., and Tan, W. 2002. Molecular aptamer beacons for real-time protein recognition. *Biochem. Biophys. Res. Commun.* **292:** 31–40.

Li, X., Wang, J., An, Z., Yang, M., Baranov, E., Jiang, P., Sun, F., Moossa, A.R., and Hoffman, R.M. 2002. Optically imageable metastatic model of human breast cancer. *Clin. Exp. Metastasis.* **19:** 347–350.

Liang, Q., Satyamurthy, N., Barrio, J.R., Toyokuni, T., Phelps, M.P., Gambhir, S.S., and Herschman, H.R. 2001. Noninvasive, quantitative imaging in living animals of a mutant dopamine D2 receptor reporter gene in which ligand binding is uncoupled from signal transduction. *Gene Ther.* **8:** 1490–1498.

Liang, Q., Gotts, J., Satyamurthy, N., Barrio, J., Phelps, M.E., Gambhir, S.S., and Herschman, H.R. 2002a. Noninvasive, repetitive, quantitative measurement of gene expression from a bicistronic message by positron emission tomography, following gene transfer with adenovirus. *Mol. Ther.* **6:** 73–82.

Liang, Q., Nguyen, K., Satyamurthy, N., Barrio, J.R., Phelps, M.E., Gambhir, S.S., and Herschman, H.R. 2002b. Monitor-

ing adenoviral DNA delivery, using a mutant herpes simplex virus type 1 thymidine kinase gene as a PET reporter gene. *Gene Ther.* **9:** 1659–1666.

Lin, Y., Weissleder, R., and Tung, C.H. 2002. Novel near-infrared cyanine fluorochromes: Synthesis, properties, and bioconjugation. *Bioconjug. Chem.* **13:** 605–610.

Lippincott-Schwartz, J., Snapp, E., and Kenworthy, A. 2001. Studying protein dynamics in living cells. *Nat. Rev. Mol. Cell Biol.* **2:** 444–456.

Lipshutz, G.S., Gruber, C.A., Cao, Y., Hardy, J., Contag, C.H., and Gaensler, K.M. 2001. In utero delivery of adeno-associated viral vectors: Intraperitoneal gene transfer produces long-term expression. *Mol. Ther.* **3:** 284–292.

Livingston, J.N. 1999. Genetically engineered mice in drug development. *J. Intern. Med.* **245:** 627–635.

Louie, A.Y., Huber, M.M., Ahrens, E.T., Rothbacher, U., Moats, R., Jacobs, R.E., Fraser, S.E., and Meade, T.J. 2000. In vivo visualization of gene expression using magnetic resonance imaging. *Nat. Biotechnol.* **18:** 321–325.

Louie, A.Y., Duimstra, J.A., and Meade, T.J. 2002. Mapping gene expression by MRI. In *Brain mapping: The methods* (eds. A.W. Toga and J.C. Mazziotta), pp. 819–828. Academic Press, San Diego, CA.

Lovqvist, A., Humm, J.L., Sheikh, A., Finn, R.D., Koziorowski, J., Ruan, S., Pentlow, K.S., Jungbluth, A., Welt, S., Lee, F.T., et al. 2001. PET imaging of ^{86}Y-labeled anti-Lewis Y monoclonal antibodies in a nude mouse model: Comparison between ^{86}Y and ^{111}In radiolabels. *J. Nucl. Med.* **42:** 1281–1287.

Lucignani, G. and Frost, H.H. 2000. Neurochemical imaging with emission tomography: Clinical applications. In *Diagnostic nuclear medicine* (ed. C. Schiepers), pp. 7–35. Springer-Verlag, Berlin.

Luker, G.D. 2002. Special conference of the American Association for Cancer Research on molecular imaging in cancer: Linking biology, function, and clinical applications in vivo. *Cancer Res.* **62:** 2195–2198.

Luker, G.D. and Piwnica-Worms, D. 2001. Molecular imaging in vivo with PET and SPECT. *Acad. Radiol.* **8:** 4–14.

Luker, G.D., Sharma, V., Pica, C.M., Dahlheimer, J.L., Li, W., Ochesky, J., Ryan, C.E., Piwnica-Worms, H., and Piwnica-Worms, D. 2002. Noninvasive imaging of protein–protein interactions in living animals. *Proc. Natl. Acad. Sci.* **99:** 6961–6966.

Luypaert, R., Boujraf, S., Sourbron, S., and Osteaux, M. 2001. Diffusion and perfusion MRI: Basic physics. *Eur. J. Radiol.* **38:** 19–27.

MacLaren, D.C., Gambhir, S.S., Cherry, S.R., Barrio, J.R., Satyamurthy, N., Toyokuni, T., Berk, A., Wu, L., Phelps, M.E., and Herschman, H.R. 1998. Repetitive and non-invasive in vivo imaging of reporter gene expression using andenovirus delivered dopamine D2 receptor as a PET reporter gene and FESP as a PET reporter probe. *J. Nucl. Med.* **39:** 35P.

MacLaren, D.C., Gambhir, S.S., Satyamurthy, N., Barrio, J.R., Sharfstein, S., Toyokuni, T., Wu, L., Berk, A.J., Cherry, S.R., Phelps, M.E., et al. 1999. Repetitive, non-invasive imaging of the dopamine D2 receptor as a reporter gene in living animals. *Gene Ther.* **6:** 785–791.

MacLaren, D.C., Toyokuni, T., Cherry, S.R., Barrio, J.R., Phelps, M.E., Herschman, H.R., and Gambhir, S.S. 2000. PET imaging of transgene expression. *Biol. Psychiatry* **48:** 337–348.

Madar, I., Lever, J.R., Kinter, C.M., Scheffel, U., Ravert, H.T., Musachio, J.L., Mathews, W.B., Dannals, R.F., and Frost, J.J. 1996. Imaging of delta opioid receptors in human brain by N$^{1'}$-([^{11}C]methyl)naltrindole and PET. *Synapse* **24:** 19–28.

Mahmood, U. and Weissleder, R. 2002. Some tools for molecular imaging. *Acad. Radiol.* **9:** 629–631.

Mahmood, U., Tung, C.H., Bogdanov Jr., A., and Weissleder, R. 1999. Near-infrared optical imaging of protease activity for tumor detection. *Radiology* **213:** 866–870.

Mariani, G. 1996. Unexpected keys in cell biochemistry imaging: Some lessons from technetium-99m-sestamibi. *J. Nucl. Med.* **37:** 536–538.

Marten, K., Bremer, C., Khazaie, K., Sameni, M., Sloane, B., Tung, C.H., and Weissleder, R. 2002. Detection of dysplastic intestinal adenomas using enzyme-sensing molecular beacons in mice. *Gastroenterology* **122:** 406–414.

Mayer-Kuckuk, P., Banerjee, D., Malhotra, S., Doubrovin, M., Iwamoto, M., Akhurst, T., Balatoni, J., Bornmann, W., Finn, R., Larson, S., et al. 2002. Cells exposed to antifolates show increased cellular levels of proteins fused to dihydrofolate reductase: A method to modulate gene expression. *Proc. Natl. Acad. Sci.* **99:** 3400–3405.

McCarthy, T.J., Sheriff, A.U., Graneto, M.J., Talley, J.J., and Welch, M.J. 2002. Radiosynthesis, in vitro validation, and in vivo evaluation of ^{18}F-labeled COX-1 and COX-2 inhibitors. *J. Nucl. Med.* **43:** 117–124.

Mitchell, P. 2001. Turning the spotlight on cellular imaging. *Nat. Biotechnol.* **19:** 1013–1017.

Molineux, G. 2002. Pegylation: Engineering improved pharmaceuticals for enhanced therapy. *Cancer Treat. Rev.* **28 Suppl A:** 13–16.

Moore, A., Weissleder, R., and Bogdanov Jr., A. 1997. Uptake of dextran-coated monocrystalline iron oxides in tumor cells and macrophages. *J. Magn. Reson. Imaging* **7:** 1140–1145.

Moore, A., Basilion, J.P., Chiocca, E.A., and Weissleder, R. 1998. Measuring transferrin receptor gene expression by NMR imaging. *Biochim. Biophys. Acta* **1402:** 239–249.

Moore, A., Marecos, E., Bogdanov Jr., A., and Weissleder, R. 2000. Tumoral distribution of long-circulating dextran-coated iron oxide nanoparticles in a rodent model. *Radiology* **214:** 568–574.

Moore, A., Josephson, L., Bhorade, R.M., Basilion, J.P., and Weissleder, R. 2001. Human transferrin receptor gene as a marker gene for MR imaging. *Radiology* **221:** 244–250.

Mulholland, G.K., Kilbourn, M.R., Sherman, P., Carey, J.E., Frey, K.A., Koeppe, R.A., and Kuhl, D.E. 1995. Synthesis, in vivo biodistribution and dosimetry of [^{11}C]N-methylpiperidyl benzilate ([^{11}C]NMPB), a muscarinic acetylcholine receptor antagonist. *Nucl. Med. Biol.* **22:** 13–17.

Nakajima, A., Seroogy, C.M., Sandora, M.R., Tarner, I.H., Costa, G.L., Taylor-Edwards, C., Bachmann, M.H., Contag, C.H., and Fathman, C.G. 2001. Antigen-specific T cell-mediated gene therapy in collagen-induced arthritis. *J. Clin. Invest.* **107:** 1293–1301.

Namavari, M., Barrio, J.R., Toyokuni, T., Gambir, S.S., Cherry, S.R., Herschman, H.R., Phelps, M.E., and Satyamurthy, N. 2000. Synthesis of 8-[^{18}F] fluoroguanine derivatives: In-vivo probes for imaging gene expression with PET. *Nucl. Med. Biol.* **27:** 157–162.

Nichol, C. and Kim, E.E. 2001. Molecular imaging and gene therapy. *J. Nucl. Med.* **42:** 1368–1374.

Nicholson, J.K., Connelly, J., Lindon, J.C., and Holmes, E. 2002. Metabonomics: A platform for studying drug toxicity and gene function. *Nat. Rev. Drug. Discov.* **1:** 153–161.

Ntziachristos, V. and Weissleder, R. 2002. Harge-coupled-device based scanner for tomography of fluorescent ear-infrared probes in turbid media. *Med. Phys.* **29:** 803–809.

Ntziachristos, V., Tung, C.H., Bremer, C., and Weissleder, R. 2002. Fluorescence molecular tomography resolves protease activity in vivo. *Nat. Med.* **8:** 757–760.

Oriuchi, N. and Yang, D.J. 2001. Antibodies for targeted imag-

ing: Properties and radiolabeling. In *Targeted molecular imaging in oncology* (eds. E.E. Kim and D.J. Yang), pp. 83–87. Springer-Verlag, New York.

Pantuck, A.J., Matherly, J., Zisman, A., Nguyen, D., Berger, F., Gambhir, S.S., Black, M.E., Belldegrun, A., and Wu, L. 2002. Optimizing prostate cancer suicide gene therapy using herpes simplex virus thymidine kinase active site variants. *Hum. Gene Ther.* **13:** 777–789.

Paulmurugan, R., Umezawa, Y., and Gambhir, S.S. 2002. Noninvasive imaging of protein–protein interactions in living subjects by using reporter protein complementation and reconstitution strategies. *Proc. Natl. Acad. Sci.* **99:** 15608–15613.

Paulus, M.J., Gleason, S.S., Easterly, M.E., and Foltz, C.J. 2001. A review of high-resolution X-ray computed tomography and other imaging modalities for small animal research. *Lab. Anim. (NY)* **30:** 36–45.

Phair, R.D. and Misteli, T. 2001. Kinetic modelling approaches to in vivo imaging. *Nat. Rev. Mol. Cell. Biol.* **2:** 898–907.

Phelps, M.E. 1991. PET: A biological imaging technique. *Neurochem. Res.* **16:** 929–940.

———. 2000a. Inaugural article: Positron emission tomography provides molecular imaging of biological processes. *Proc. Natl. Acad. Sci.* **97:** 9226–9233.

———. 2000b. PET: The merging of biology and imaging into molecular imaging. *J. Nucl. Med.* **41:** 661–681.

———. 2002. Nuclear medicine, molecular imaging, and molecular medicine. *J. Nucl. Med.* **43:** 13N–14N.

Polyakov, V., Sharma, V., Dahlheimer, J.L., Pica, C.M., Luker, G.D., and Piwnica-Worms, D. 2000. Novel Tat-peptide chelates for direct transduction of technetium-99m and rhenium into human cells for imaging and radiotherapy. *Bioconjug. Chem.* **11:** 762–771.

Ponomarev, V., Doubrovin, M., Lyddane, C., Beresten, T., Balatoni, J., Bornman, W., Finn, R., Akhurst, T., Larson, S., Blasberg, R., et al. 2001. Imaging TCR-dependent NFAT-mediated T-cell activation with positron emission tomography in vivo. *Neoplasia* **3:** 480–488.

Price, P. 2001. PET as a potential tool for imaging molecular mechanisms of oncology in man. *Trends Mol. Med.* **7:** 442–446.

Qiao, J., Doubrovin, M., Sauter, B.V., Huang, Y., Guo, Z.S., Balatoni, J., Akhurst, T., Blasberg, R.G., Tjuvajev, J.G., Chen, S.H., et al. 2002. Tumor-specific transcriptional targeting of suicide gene therapy. *Gene Ther.* **9:** 168–175.

Ray, P., Bauer, E., Iyer, M., Barrio, J.R., Satyamurthy, N., Phelps, M.E., Herschman, H.R., and Gambhir, S.S. 2001. Monitoring gene therapy with reporter gene imaging. *Semin. Nucl. Med.* **31:** 312–320.

Ray, P., Pimenta, H., Paulmurugan, R., Berger, F., Phelps, M.E., Iyer, M., and Gambhir, S.S. 2002. Noninvasive quantitative imaging of protein–protein interactions in living subjects. *Proc. Natl. Acad. Sci.* **99:** 3105–3110.

Reader, A.J. and Zweit, J. 2001. Developments in whole-body molecular imaging of live subjects. *Trends Pharmacol. Sci.* **22:** 604–607.

Rehemtulla, A., Stegman, L.D., Cardozo, S.J., Gupta, S., Hall, D.E., Contag, C.H., and Ross, B.D. 2000. Rapid and quantitative assessment of cancer treatment response using in vivo bioluminescence imaging. *Neoplasia* **2:** 491–495.

Remington, S.J. 2002. Negotiating the speed bumps to fluorescence. *Nat. Biotechnol.* **20:** 28–29.

Remsen, L.G., McCormick, C.I., Roman-Goldstein, S., Nilaver, G., Weissleder, R., Bogdanov, A., Hellstrom, I., Kroll, R.A., and Neuwelt, E.A. 1996. MR of carcinoma-specific monoclonal antibody conjugated to monocrystalline iron oxide nanoparticles: The potential for noninvasive diagnosis. *Am. J. Neuroradiol.* **17:** 411–418.

Rocchetta, H.L., Boylan, C.J., Foley, J.W., Iversen, P.W., LeTourneau, D.L., McMillian, C.L., Contag, P.R., Jenkins, D.E., and Parr Jr., T.R. 2001. Validation of a noninvasive, real-time imaging technology using bioluminescent *Escherichia coli* in the neutropenic mouse thigh model of infection. *Antimicrob. Agents Chemother.* **45:** 129–137.

Rosebrough, S.F. 1996. Two-step immunological approaches for imaging and therapy. *Quart. J. Nucl. Med.* **40:** 234–251.

Rosenthal, M.S., Cullom, J., Hawkins, W., Moore, S.C., Tsui, B.M., and Yester, M. 1995. Quantitative SPECT imaging: A review and recommendations by the Focus Committee of the Society of Nuclear Medicine Computer and Instrumentation Council. *J. Nucl. Med.* **36:** 1489–1513.

Shaharabany, M., Abramovitch, R., Kushnir, T., Tsarfaty, G., Ravid-Megido, M., Horev, J., Ron, R., Itzchak, Y., and Tsarfaty, I. 2001. In vivo molecular imaging of met tyrosine kinase growth factor receptor activity in normal organs and breast tumors. *Cancer Res.* **61:** 4873–4878.

Sharma, V., Beatty, A., Wey, S.P., Dahlheimer, J., Pica, C.M., Crankshaw, C.L., Bass, L., Green, M.A., Welch, M.J., and Piwnica-Worms, D. 2000. Novel gallium(III) complexes transported by MDR1 P-glycoprotein: Potential PET imaging agents for probing P-glycoprotein-mediated transport activity in vivo. *Chem. Biol.* **7:** 335–343.

Shen, D.H., Kloos, R.T., Mazzaferri, E.L., and Jhian, S.M. 2001. Sodium iodide symporter in health and disease. *Thyroid* **11:** 415–425.

Shields, A.F., Grierson, J.R., Dohmen, B.M., Machulla, H.J., Stayanoff, J.C., Lawhorn-Crews, J.M., Obradovich, J.E., Muzik, O., and Mangner, T.J. 1998. Imaging proliferation in vivo with [F-18]FLT and positron emission tomography. *Nat. Med.* **4:** 1334–1336.

Shinotoh, H., Yamasaki, T., Inoue, O., Itoh, T., Suzuki, K., Hashimoto, K., Tateno, Y., and Ikehira, H. 1986. Visualization of specific binding sites of benzodiazepine in human brain. *J. Nucl. Med.* **27:** 1593–1599.

Shinotoh, H., Inoue, O., Suzuki, K., Yamasaki, T., Iyo, M., Hashimoto, K., Tominaga, T., Itoh, T., Tateno, Y., and Ikehira, H. 1987. Kinetics of [^{11}C]N,N-dimethylphenylethylamine in mice and humans: Potential for measurement of brain MAO-B activity. *J. Nucl. Med.* **28:** 1006–1011.

Song, S.K., Qu, Z., Garabedian, E.M., Gordon, J.I., Milbrandt, J., and Ackerman, J.J. 2002. Improved magnetic resonance imaging detection of prostate cancer in a transgenic mouse model. *Cancer Res.* **62:** 1555–1558.

Spergel, D.J., Kruth, U., Shimshek, D.R., Sprengel, R., and Seeburg, P.H. 2001. Using reporter genes to label selected neuronal populations in transgenic mice for gene promoter, anatomical, and physiological studies. *Prog. Neurobiol.* **63:** 673–686.

Spibey, C.A., Jackson, P., and Herick, K. 2001. A unique charge-coupled device/xenon arc lamp based imaging system for the accurate detection and quantitation of multicolour fluorescence. *Electrophoresis* **22:** 829–836.

Stegman, L.D., Rehemtulla, A., Beattie, B., Kievit, E., Lawrence, T.S., Blasberg, R.G., Tjuvajev, J.G., and Ross, B.D. 1999. Noninvasive quantitation of cytosine deaminase transgene expression in human tumor xenografts with in vivo magnetic resonance spectroscopy. *Proc. Natl. Acad. Sci.* **96:** 9821–9826.

Strijckmans, K. 2001. The isochronous cyclotron: Principles and recent developments. *Comput. Med. Imaging Graph.* **25:** 69–78.

Subramanian, G., Adams, M.D., Venter, J.C., and Broder, S.

2001. Implications of the human genome for understanding human biology and medicine. *JAMA* **286:** 2296–2307.

Sun, X., Annala, A.J., Yaghoubi, S.S., Barrio, J.R., Nguyen, K.N., Toyokuni, T., Satyamurthy, N., Namavari, M., Phelps, M.E., Herschman, H.R., et al. 2001. Quantitative imaging of gene induction in living animals. *Gene Ther.* **8:** 1572–1579.

Sundaresan, G. and Gambhir, S.S. 2002. Radionuclide imaging of reporter gene expression. In *Brain mapping: The methods* (eds. A.W. Toga and J.C. Mazziotta), pp. 799–818. Academic Press, San Diego, CA.

Sweeney, T.J., Mailander, V., Tucker, A.A., Olomu, A.B., Zhang, W., Cao, Y., Negrin, R.S., and Contag, C.H. 1999. Visualizing the kinetics of tumor-cell clearance in living animals. *Proc. Natl. Acad. Sci.* **96:** 12044–12049.

Tjuvajev, J.G., Stockhammer, G., Desai, R., Uehara, H., Watanabe, K., Gansbacher, B., and Blasberg, R.G. 1995. Imaging the expression of transfected genes in vivo. *Cancer Res.* **55:** 6126–6132.

Tjuvajev, J.G., Finn, R., Watanabe, K., Joshi, R., Oku, T., Kennedy, J., Beattie, B., Koutcher, J., Larson, S., and Blasberg, R.G. 1996. Noninvasive imaging of herpes virus thymidine kinase gene transfer and expression: A potential method for monitoring clinical gene therapy. *Cancer Res.* **56:** 4087–4095.

Tjuvajev, J.G., Avril, N., Oku, T., Sasajima, T., Miyagawa, T., Joshi, R., Safer, M., Beattie, B., DiResta, G., Daghighian, F., et al. 1998. Imaging herpes virus thymidine kinase gene transfer and expression by positron emission tomography. *Cancer Res.* **58:** 4333–4341.

Tjuvajev, J.G., Chen, S.H., Joshi, A., Joshi, R., Guo, Z.S., Balatoni, J., Ballon, D., Koutcher, J., Finn, R., Woo, S.L., et al. 1999a. Imaging adenoviral-mediated herpes virus thymidine kinase gene transfer and expression in vivo. *Cancer Res.* **59:** 5186–5193.

Tjuvajev, J.G., Joshi, A., Callegari, J., Lindsley, L., Joshi, R., Balatoni, J., Finn, R., Larson, S.M., Sadelain, M., and Blasberg, R.G. 1999b. A general approach to the non-invasive imaging of transgenes using cis-linked herpes simplex virus thymidine kinase. *Neoplasia* **1:** 315–320.

Tjuvajev, J., Blasberg, R., Luo, X., Zheng, L.M., King, I., and Bermudes, D. 2001. *Salmonella*-based tumor-targeted cancer therapy: Tumor amplified protein expression therapy (TAPET) for diagnostic imaging. *J. Control. Release* **74:** 313–315.

Townsend, D.W. 2001. A combined PET/CT scanner: The choices. *J. Nucl. Med.* **42:** 533–534.

Townsend, D.W. and Cherry, S.R. 2001. Combining anatomy and function: The path to true image fusion. *Eur. Radiol.* **11:** 1968–1974.

Tung, C.H., Bredow, S., Mahmood, U., and Weissleder, R. 1999. A cathepsin D sensitive near infrared fluorescence probe for in vivo imaging of enzyme activity. *Bioconj. Chem.* **10:** 892–896.

Tung, C.H., Mahmood, U., Bredow, S., and Weissleder, R. 2000. In vivo imaging of proteolytic enzyme activity using a novel molecular reporter. *Cancer Res.* **60:** 4953–4958.

Tung, C.H., Gerszten, R.E., Jaffer, F.A., and Weissleder, R. 2002. A novel near-infrared fluorescence sensor for detection of thrombin activation in blood. *Chembiochem.* **3:** 207–211.

Turetschek, K., Roberts, T.P., Floyd, E., Preda, A., Novikov, V., Shames, D.M., Carter, W.O., and Brasch, R.C. 2001. Tumor microvascular characterization using ultrasmall superparamagnetic iron oxide particles (USPIO) in an experimental breast cancer model. *J. Magn. Reson. Imaging* **13:** 882–888.

Turnbull, D.H. and Foster, F.S. 2002. In vivo ultrasound biomicroscopy in developmental biology. *Trends Biotechnol.* **20:** S29–S33.

Villemagne, V.L., Dannals, R.F., Sanchez-Roa, P.M., Ravert, H.T., Vazquez, S., Wilson, A.A., Natarajan, T.K., Wong, D.F., Yanai, K., and Wagner Jr., H.N. 1991. Imaging histamine H1 receptors in the living human brain with carbon-11-pyrilamine. *J. Nucl. Med.* **32:** 308–311.

Virgolini, I. 2000. Peptide imaging. In *Diagnostic nuclear medicine* (ed. C. Schiepers), pp. 135–158. Springer-Verlag, Berlin.

Volkow, N.D., Fowler, J.S., Wang, G.J., Dewey, S.L., Schlyer, D., MacGregor, R., Logan, J., Alexoff, D., Shea, C., Hitzemann, R., et al. 1993. Reproducibility of repeated measures of carbon-11-raclopride binding in the human brain. *J. Nucl. Med.* **34:** 609–613.

Vooijs, M., Jonkers, J., Lyons, S., and Berns, A. 2002. Noninvasive imaging of spontaneous retinoblastoma pathway-dependent tumors in mice. *Cancer Res.* **62:** 1862–1867.

Vries, E.F., Buursma, A.R., Hospers, G.A., Mulder, N.H., and Vaalburg, W. 2002. Scintigraphic imaging of HSVtk gene therapy. *Curr. Pharm. Des.* **8:** 1435–1450.

Wagenaar, D.J., Weissleder, R., and Hengerer, A. 2001. Glossary of molecular imaging terminology. *Acad. Radiol.* **8:** 409–420.

Wagner Jr., H.N., Burns, H.D., Dannals, R.F., Wong, D.F., Langstrom, B., Duelfer, T., Frost, J.J., Ravert, H.T., Links, J.M., Rosenbloom, S.B., et al. 1983. Imaging dopamine receptors in the human brain by positron tomography. *Science* **221:** 1264–1266.

Walhout, A.J. and Vidal, M. 2001. Protein interaction maps for model organisms. *Nat. Rev. Mol. Cell Biol.* **2:** 55–62.

Weissleder, R. 1999. Molecular imaging: Exploring the next frontier. *Radiology* **212:** 609–614.

———. 2001. A clearer vision for in vivo imaging. *Nat. Biotechnol.* **19:** 316–317.

———. 2002. Scaling down imaging: Molecular mapping of cancer in mice. *Nat. Rev. Cancer* **2:** 11–18.

Weissleder, R. and Mahmood, U. 2001. Molecular imaging. *Radiology* **219:** 316–333.

Weissleder, R., Cheng, H.C., Bogdanova, A., and Bogdanov Jr., A. 1997a. Magnetically labeled cells can be detected by MR imaging. *J. Magn. Reson. Imaging* **7:** 258–263.

Weissleder, R., Simonova, M., Bogdanova, A., Bredow, S., Enochs, W.S., and Bogdanov Jr., A. 1997b. MR imaging and scintigraphy of gene expression through melanin induction. *Radiology* **204:** 425–429.

Weissleder, R., Tung, C.H., Mahmood, U., and Bogdanov, A. 1999. In vivo imaging of tumors with protease-activated near-infrared fluorescent probes. *Nat. Biotechnol.* **17:** 375–378.

Weissleder, R., Moore, A., Mahmood, U., Bhorade, R., Benveniste, H., Chiocca, E.A., and Basilion, J.P. 2000. In vivo magnetic resonance imaging of transgene expression. *Nat. Med.* **6:** 351–355.

Weng, Y.H., Tatarov, A., Bartos, B.P., Contag, C.H., and Dennery, P.A. 2000. HO-1 expression in type II pneumocytes after transpulmonary gene delivery. *Am. J. Physiol. Lung Cell. Mol. Physiol.* **278:** L1273–L1279.

Wetterwald, A., van der Pluijm, G., Que, I., Sijmons, B., Buijs, J., Karperien, M., Lowik, C.W., Gautschi, E., Thalmann, G.N., and Cecchini, M.G. 2002. Optical imaging of cancer metastasis to bone marrow: A mouse model of minimal residual disease. *Am. J. Pathol.* **160:** 1143–1153.

Wu, A.M., Yazaki, P.J., Tsai, S., Nguyen, K., Anderson, A.L., McCarthy, D.W., Welch, M.J., Shively, J.E., Williams, L.E., Raubitschek, A.A., et al. 2000. High-resolution microPET

imaging of carcinoembryonic antigen-positive xenografts by using a copper-64-labeled engineered antibody fragment. *Proc. Natl. Acad. Sci.* **97:** 8495–8500.

Wu, J.C., Sundaresan, G., Iyer, M., and Gambhir, S.S. 2001. Noninvasive optical imaging of firefly luciferase reporter gene expression in skeletal muscles of living mice. *Mol. Ther.* **4:** 297–306.

Wu, J.C., Inubushi, M., Sundaresan, G., Schelbert, H.R., and Gambhir, S.S. 2002a. Optical imaging of cardiac reporter gene expression in living rats. *Circulation* **105:** 1631–1634.

———. 2002b. Positron emission tomography imaging of cardiac reporter gene expression in living rats. *Circulation* **106:** 180–183.

Wunderbaldinger, P., Bogdanov, A., and Weissleder, R. 2000. New approaches for imaging in gene therapy. *Eur. J. Radiol.* **34:** 156–165.

Wunderbaldinger, P., Josephson, L., and Weissleder, R. 2002. Tat peptide directs enhanced clearance and hepatic permeability of magnetic nanoparticles. *Bioconjug. Chem.* **13:** 264–268.

Yaghoubi, S.S., Wu, L., Liang, Q., Toyokuni, T., Barrio, J.R., Namavari, M., Satyamurthy, N., Phelps, M.E., Herschman, H.R., and Gambhir, S.S. 2001. Direct correlation between positron emission tomographic images of two reporter genes delivered by two distinct adenoviral vectors. *Gene Ther.* **8:** 1072–1080.

Yang, M., Baranov, E., Wang, J.W., Jiang, P., Wang, X., Sun, F.X., Bouvet, M., Moossa, A.R., Penman, S., and Hoffman, R.M. 2002. Direct external imaging of nascent cancer, tumor progression, angiogenesis, and metastasis on internal organs in the fluorescent orthotopic model. *Proc. Natl. Acad. Sci.* **99:** 3824–3829.

Yaspo, M.L. 2001. Taking a functional genomics approach in molecular medicine. *Trends Mol. Med.* **7:** 494–501.

Yu, Y., Annala, A.J., Barrio, J.R., Toyokuni, T., Satyamurthy, N., Namavari, M., Cherry, S.R., Phelps, M.E., Herschman, H.R., and Gambhir, S.S. 2000. Quantification of target gene expression by imaging reporter gene expression in living animals. *Nat. Med.* **6:** 933–937.

Zanzonico, P.B., Bigler, R.E., and Schmall, B. 1983. Neuroleptic binding sites: Specific labeling in mice with [^{18}F]haloperidol, a potential tracer for positron emission tomography. *J. Nucl. Med.* **24:** 408–416.

Zhang, J., Tan, X., Contag, C.H., Lu, Y., Guo, D., Harris, S.E., and Feng, J.Q. 2002a. Dissection of promoter control modules that direct Bmp4 expression in the epithelium-derived components of hair follicles. *Biochem. Biophys. Res. Commun.* **293:** 1412–1419.

Zhang, L., Adams, J.Y., Billick, E., Ilagan, R., Iyer, M., Le, K., Smallwood, A., Gambhir, S.S., Carey, M., and Wu, L. 2002b. Molecular engineering of a two-step transcription amplification (TSTA) system for transgene delivery in prostate cancer. *Mol. Ther.* **5:** 223–232.

Zhang, W., Contag, P.R., Madan, A., Stevenson, D.K., and Contag, C.H. 1999. Bioluminescence for biological sensing in living mammals. *Adv. Exp. Med. Biol.* **471:** 775–784.

Zhang, W., Feng, J.Q., Harris, S.E., Contag, P.R., Stevenson, D.K., and Contag, C.H. 2001. Rapid in vivo functional analysis of transgenes in mice using whole body imaging of luciferase expression. *Transgenic. Res.* **10:** 423–434.

Zhao, M., Beauregard, D.A., Loizou, L., Davletov, B., and Brindle, K.M. 2001. Non-invasive detection of apoptosis using magnetic resonance imaging and a targeted contrast agent. *Nat. Med.* **7:** 1241–1244.

Ziegler, S.I. 2000. Instrumentation and data acquisition. In *Diagnostic nuclear medicine* (ed. C. Schiepers), pp. 221–236. Springer-Verlag, Berlin.

Zinn, K.R. and Chaudhuri, T.R. 2002. The type 2 human somatostatin receptor as a platform for reporter gene imaging. *Eur. J. Nucl. Med. Mol. Imaging* **29:** 388–399.

Molecular imaging in living subjects: seeing fundamental biological processes in a new light

Tarik F. Massoud and Sanjiv S. Gambhir

Genes Dev. 2003, **17:**
Access the most recent version at doi:10.1101/gad.1047403